Flexible multibody dynamics
Superelements using absolute interface coordinates
in the floating frame formulation

Jurnan Schilder

FLEXIBLE MULTIBODY DYNAMICS
SUPERELEMENTS USING ABSOLUTE INTERFACE COORDINATES
IN THE FLOATING FRAME FORMULATION

DISSERTATION

to obtain
the degree of doctor at the University of Twente,
on the authority of the rector magnificus,
prof. dr. T.T.M. Palstra,
on account of the decision of the graduation committee,
to be publicly defended
on Thursday the 1st of November 2018 at 14:45 hours

by

Jurnan Paul Schilder

born on the 9th of December 1990
in Almere, The Netherlands

This dissertation has been approved by:

Supervisor: prof. dr. ir. A. de Boer
Co-supervisor: dr. ir. M.H.M. Ellenbroek

Graduation committee

Chairman and Secretary
Prof. dr. G.P.M.R Dewulf   University of Twente

Supervisor
Prof. dr. ir. A. de Boer   University of Twente

Co-supervisor
Dr. ir. M.H.M. Ellenbroek   University of Twente

Members
Prof. dr. ir. W. Desmet   KU Leuven
Prof. dr. A. Cardona   Universidad Nacional del Litoral
Prof. dr. J.A.C. Ambrósio   University of Lisbon
Prof. dr. ir. D.M. Brouwer PDEng   University of Twente
Prof. dr. ir. H. van der Kooij   University of Twente
Em. prof. dr. ir. J.B. Jonker   University of Twente

Summary

The floating frame formulation is a well-established and widely used formulation in flexible multibody dynamics. In this formulation the rigid body motion of a flexible body is described by the absolute generalized coordinates of the body's floating frame with respect to the inertial frame. The body's flexible behavior is described locally, relative to the floating frame, by a set of deformation shapes. Because in many situations, the elastic deformations of a body remain small, these deformation shapes can be determined by applying powerful model order reduction techniques to a body's linear finite element model. This is an important advantage of the floating frame formulation in comparison with for instance nonlinear finite element formulations.

An important disadvantage of the floating frame formulation is that it requires Lagrange multipliers to satisfy the kinematic constraint equations. The constraint equations are typically formulated in terms of the generalized coordinates corresponding to the body's interface points, where it is connected to other bodies or the fixed world. As the interface coordinates are not part of the degrees of freedom of the formulation, the constraint equations are in general nonlinear equations in terms of the generalized coordinates, which cannot be solved analytically.

In this work, a new formulation is presented with which it is possible to eliminate the Lagrange multipliers from the constrained equations of motion, while still allowing the use of linear model order reduction techniques in the floating frame. This is done by reformulating a flexible body's kinematics in terms of its absolute interface coordinates. One could say that the new formulation creates a superelement for each flexible body. These superelements are created by establishing a coordinate transformation from the absolute floating frame coordinates and local interface coordinates to the absolute interface coordinates. In order to establish such a coordinate transformation, existing formulations commonly require the floating frame to be in an interface point. The new formulation does not require such strict demands and only requires that

there is zero elastic deformation at the location of the floating frame. In this way, the new formulation offers a more general and elegant solution to the traditional problem of creating superelements in the floating frame formulation.

The fact that the required coordinate transformation involves the interface coordinates, makes it natural to use the Craig-Bampton method for describing a body's local elastic deformation. After all, the local interface coordinates equal the generalized coordinates corresponding to the static Craig-Bampton modes. However, in this work it is shown that the new formulation can deal with any choice for the local deformation shapes. Also, it is shown how the method can be expanded to include geometrical nonlinearities within a body.

A full and complete mathematical derivation of the new formulation is presented. However, an extensive effort is made to give geometric interpretation to the transformation matrices involved. In this way the new method can be understood better from an intuitive engineering perspective. This perspective has led to the proposal of several additional approximations to simplify the formulation. Validation simulations of benchmark problems have shown the new formulation to be accurate and the proposed additional approximations to be appropriate indeed.

Samenvatting

In het vakgebied flexibele multibody dynamica wordt het dynamisch gedrag van flexibele lichamen vaak beschreven door de zogenaamde floating frame formulering. Hierin wordt de starre beweging van een lichaam beschreven door de absolute coördinaten van een assenstelsel dat meebeweegt (floats) met het lichaam. Flexibel gedrag wordt vervolgens ten opzichte van dit lokale assenstelsel beschreven door een set vervormingsfuncties. Omdat de elastische vervormingen van een lichaam vaak klein blijven, kunnen deze vervormingsfuncties worden bepaald met behulp van lineaire eindige-elementenmodellen. Om rekentijd te besparen kunnen efficiënte lineaire reductiemethoden worden toegepast. Dit is een belangrijk voordeel van de floating frame formulering ten opzichte van niet-lineaire eindige-elementenmethoden.

Een belangrijk nadeel van de floating frame formulering is dat Lagrange multiplicators nodig zijn om aan de kinematische randvoorwaarden te voldoen. Deze randvoorwaarden worden geïntroduceerd door de wijze waarop de interfacepunten van een lichaam zijn verbonden aan andere lichamen of aan de vaste wereld. De vergelijkingen die hierbij horen zijn typisch geformuleerd in termen van de coördinaten die toebehoren aan de interfacepunten. Omdat deze coördinaten geen onderdeel zijn van de vrijheidsgraden in de floating frame formulering, zijn de kinematische randvoorwaarden vaak niet-lineaire vergelijkingen waarvoor een analytische oplossing niet zonder meer bestaat.

In dit werk wordt een nieuwe formulering gepresenteerd waarmee het mogelijk is om de Lagrange multiplicators te elimineren uit de bewegingsvergelijkingen. In de nieuwe formulering blijft het mogelijk om lineaire reductiemethoden toe te passen op lokale eindige-elementen-modellen. Dit wordt gedaan door de kinematica van een flexibel lichaam volledig uit te drukken in termen van de absolute interfacecoördinaten. Het resultaat is dat elk lichaam kan worden beschreven als een superelement. Een superelement is gebaseerd op een speciale transformatie van de absolute floating-framecoördinaten en de lokale

interfacecoördinaten naar de absolute interfacecoördinaten. Om een dergelijke transformatie te bewerkstelligen, vereisen reeds beschikbare formuleringen dat het floating frame in een interfacepunt ligt. In de nieuwe formulering zijn zulke beperkende voorwaarden niet nodig. Het is voldoende om te eisen dat er geen elastische vervorming optreedt ter plekke van het floating frame – waar dat ook ligt. Op deze manier biedt de nieuwe formulering een meer algemene en zeer elegante manier om gekoppelde superelementen te beschrijven in de floating frame formulering.

Omdat de interfacecoördinaten een onmisbare rol spelen in de benodigde coördinatentransformatie, is het aantrekkelijk de Craig-Bamptonmethode te gebruiken voor de beschrijving van het flexibele gedrag van een lichaam. De gegeneraliseerde coördinaten die horen bij de statische Craig-Bamptonmodes zijn immers gelijk aan de lokale interfacecoördinaten. Echter, in deze thesis zal ook worden beschreven dat de nieuwe formulering geschikt is voor een willekeurige keuze voor de lokale vervormingsfuncties. Ook wordt toegelicht hoe de formulering zou kunnen worden uitgebreid naar een geometrisch niet-lineaire beschrijving binnen een lichaam.

De volledige wiskunde afleiding van de nieuwe formulering wordt gepresenteerd. Daarnaast is er ook aanzienlijk veel aandacht voor de geometrische interpretatie van de relevante transformatiematrices. Op deze manier wordt de nieuwe formulering voorzien van een meer ingenieursinterpretatie die helpt de formulering te doorgronden. Het is deze praktische interpretatie die heeft geleid tot het doen van extra aannamen die de formulering aanzienlijk vereenvoudigen. Numerieke simulaties die zijn uitgevoerd op een aantal standaardproblemen laten zien dat de nieuwe formulering nauwkeurig is en dat de voorgestelde extra aannamen zijn gerechtvaardigd.

Preface

Dear reader,

Over the last couple of weeks, I have finished the contents of the thesis that you are currently reading. The idea that my time as a PhD-researcher is about to come to an end makes me happy and a bit emotional as well.

Six years ago, whilst in the middle of my master project, my supervisor, who inspired me to pursue a study in dynamics, got terminally ill. Directly after I obtained my master's degree, I took over his lecture series. This period was an absolute mayhem. With only a couple of days in between each lecture, I spent the days and nights preparing them. Although my lectures were far from perfect, the students were very respectful, told me that they liked the lectures anyway and they appreciated that I did my very best. We managed to get through the lecture series together. It was in this period that I learned that as a teacher I was making a difference: by sharing my passion for the field and my dedication to teach properly, I could actually mean something to my students. In the next year, I worked hard to get better and I could not have been prouder when later that year I was awarded the university's central educational price.

Of course, in that year I did not do much about my research at all. When I talked to colleagues about what I was doing, sooner or later they warned me not to forget about my research. And here we are now. My thesis is ready and I will defend it before the end of my current contract. Of course it is difficult to judge your own work, but I honestly believe that it is a proper contribution to my field. I was able to write multiple papers about it, received very positive comments on several conferences and I foresee many opportunities for future research and applications. I am very satisfied with how my thesis turned out.

I am convinced that I could only reach this point because of all my teaching activities. Whenever I pursued a complicated strategy or whenever I finished a tedious mathematical derivation, it did not take very long before I wondered how I could explain this to my students. The wish to explain my research clearly forced me to look for the hidden elegance in my work, to find understandable interpretations of the math, to add intuition, to make it appear simple and clean. I think this really made it better.

As it is written on the title page, this thesis is "to obtain the degree of doctor," which means it serves to demonstrate that I am capable of doing solid academic research. However, I have not written it for the brilliant generations before me, to proof that I righteously belong to their family of doctors. It is dedicated to the future generations instead, although I understand that my thesis is far from a perfect textbook. It is for those who desire to understand my field in the future, that I want to be little lantern in the night. It is to lift them up to the greatest of heights.

I sincerely hope that you can sense my good intentions throughout my thesis and that even if some sections appear complicated, you can appreciate my efforts to write them to the best of my ability.

With warm regards,

Jurnan Schilder
Enschede, October 2018

List of symbols

Numerals

0	null matrix	[-]
1	identity matrix	[-]

Roman symbols

A	assembly of kinematic transformation matrices	[multiple]
A	adjoint matrix	[multiple]
a	acceleration vector	[m/s^2]
a	arbitrary vector	[-]
B	arbitrary matrix	[-]
b	arbitrary vector	[-]
C	fictitious inertia force matrix	[multiple]
C	identifier for the center of mass	[-]
E	coordinate frame	[-]
f	body force vector	[N/m^3]
F	force vector	[N]
H	homogenous transformation matrix	[multiple]
I	second moment of mass matrix	[kgm^2]
i	material point *i*	[-]
j	material point *j*	[-]
K	stiffness matrix	[multiple]
k	summation index	[-]
L	length	[m]
l	summation index	[-]
M	moment vector	[Nm]
M	mass matrix	[multiple]
M	number of deformation shapes	[-]
m	mass	[kg]
m	size of the interface points' subspace	[-]
N	number of deformation shapes	[-]
O	inertial frame	[-]
P	modal participation factors	[multiple]
P	material point	[-]

p	augmented position vector	[m]
Q	generalized force vector	[multiple]
q	generalized coordinates	[multiple]
R	rotation matrix	[-]
r	position vector	[m]
s	first moment of mass vector	[kgm]
T	transformation matrix, interface coordinates	[multiple]
t	time	[s]
U	matrix of eigenvectors	[multiple]
u	elastic displacement vector	[m]
u	axial displacement	[m]
V	inertia integrals quadratic in velocity	[multiple]
V	volume	[m^3]
v	transverse displacement	[m]
W	work	[Nm]
w	wrench vector	[Nm]
w	transverse displacement	[m]
x	position vector on undeformed body	[m]
x	axial position	[m]
Z	transformation matrix, floating frame coordinates	[multiple]

Greek symbols

α	angular acceleration vector	[rad/s^2]
ζ	generalized coordinate of a deformation shape	[multiple]
η	generalized coordinate of a deformation shape	[multiple]
θ	elastic rotation vector	[rad]
θ	vector of modal derivatives	[multiple]
Λ	matrix of eigenvalues	[multiple]
ξ	twist vector	[m/s]
π	rotation parameter vector	[-]
ρ	mass density	[kg/m^3]
Φ	matrix of deformation shapes	[-]
φ	deformation shape	[-]
Ψ	matrix of internal Craig-Bampton modes	[-]
ψ	internal Craig-Bampton modes	[-]
ω	angular velocity vector	[rad/s]

Operators

$(\bar{\ })$	particular assembly of matrices
$(\hat{\ })$	particular assembly of matrices
$(\tilde{\ })$	skew symmetric matrix
$(\dot{\ })$	time derivative
$(\ddot{\ })$	second time derivative
$(\ )^{-1}$	inverse matrix
$(\ )^{+}$	pseudo-inverse matrix
$(\ )^{T}$	transposed matrix
$\Delta(\ )$	numerical increment
$\delta(\ )$	variation / virtual change
$\mathcal{F}(\ )$	general nonlinear function
$\nabla(\ )$	gradient

Contents

1

Introduction

Flexible multibody dynamics is concerned with the study of machines and mechanisms that consist of multiple deformable bodies. These bodies are connected to each other or to the fixed world in their so-called interface points. The joints that are located at these interface points may allow for large relative rigid body rotations between the bodies, which causes the problem to be of a geometric nonlinear nature. However, the elastic strains and deformations within a single body can often be considered as small.

The kinematics of a flexible body can be described in many different ways. Different multibody formulations use different degrees of freedom. The generalized coordinates used as degrees of freedom determine the way in which kinematic constraints between bodies are enforced and also the form of the system's equations of motion. In this work, it is considered that the motion of a flexible body can be described by the motion of coordinate frames that are attached to the body's interface points: the so-called interface frames. An appropriate choice of deformation shapes defines the elastic deformation of the body uniquely.

A coordinate frame can be rigidly attached to an interface point if the material in the immediate surroundings of the interface point can be assumed to be rigid. From a practical point of view, this is often the case when a physical joint is located at such an interface point, as this typically comes with a local structural reinforcement. Also, in the specific case of for instance slender beams, cross sections are assumed undeformable. In this, a coordinate frame attached to the beam's ends can be related to its axial deformation, torsion and bending. For more complex elastic bodies, initially perpendicular axes attached to a material point need not be perpendicular in the body's deformed configuration due to shear. However, also for these cases it is still possible to uniquely define the orientation of a coordinate frame that has its origin attached to a material point. For the sake of simplicity, it is considered in this work that the interface frames can be rigidly attached to the corresponding interface points.

1.1   Existing formulations for flexible multibody dynamics

The methods suitable for the simulation of flexible multibody systems can be divided into three general classes: the inertial frame formulations, the corotational frame formulations and the floating frame formulations. These formulations have essential differences in the way the kinematics of a flexible body is described. An extensive literature overview of the different formulations was presented in [1].

The inertial frame formulation is based on the nonlinear Green-Lagrange strain definition. Each body is discretized in finite elements using global interpolation functions. The degrees of freedom are the absolute nodal coordinates: the generalized coordinates corresponding to the nodes of the finite element mesh, measured with respect to a fixed inertial reference frame. When a body's interface points coincide with finite element nodes, the absolute interface coordinates are part of the degrees of freedom. In this case, constraints between bodies can be enforced directly, by equating the degrees of freedom of the nodes shared by both bodies. Due to the use of the nonlinear strain definition, no distinction is made between a body's large rigid body motion and small elastic deformation. Figure 1.1 shows a graphical representation of the inertial frame formulation. Details of this formulation can be found in textbooks on the nonlinear finite element method, such as [2].
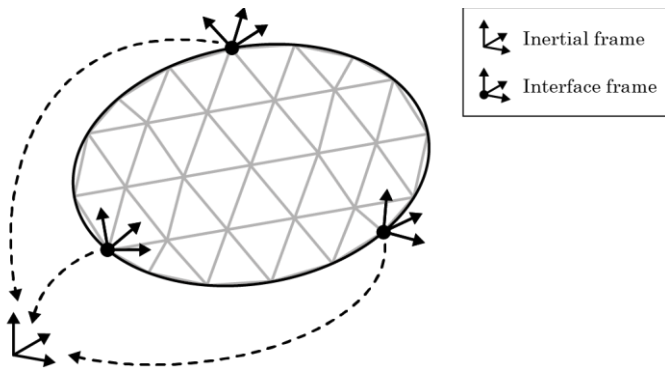

Fig. 1.1   Inertial frame formulation for a flexible body. Degrees of freedom are the absolute nodal coordinates. The absolute interface coordinates are part of the degrees of freedom.

The corotational frame formulation can be interpreted as the nonlinear extension of the standard linear finite element formulation. Alternatively, it can be interpreted as a simplification of the inertial frame formulation by using the linear strain definition instead of the nonlinear strain definition. Each element of the body's finite element mesh is given a corotational frame that describes the large rigid body motion of the element with respect to the inertial frame. Small elastic deformations within the element are superimposed using the linear finite element matrices, based on the linear Cauchy strain definition [3, 4]. The nonlinear finite element model is obtained from the linear finite element model by pre- and post-multiplying the element mass and stiffness matrices with the rotation matrices corresponding to the corotational frames. The absolute nodal coordinates are used as degrees of freedom, such that constraints are satisfied similarly as in inertial frame formulations. At every iteration, the absolute orientation of the corotational frames is determined from the absolute nodal coordinates. Figure 1.2 shows a graphical representation of the corotational frame formulation. Details of this formulation can be found in textbooks such as [2].
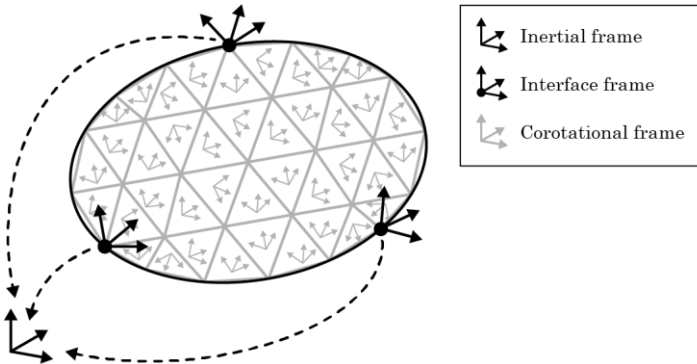

Fig. 1.2   Corotational frame formulation for a flexible body. Degrees of freedom are the absolute nodal coordinates. The absolute interface coordinates are part of the degrees of freedom.

The floating frame formulation can be interpreted as the extension of rigid multibody formulations to flexible multibody systems. In this formulation, a body's large rigid body motion is described by the absolute coordinates of a floating frame that moves along with the body. Elastic deformation is described locally, relative to the floating frame using a linear combination of deformation shapes. Within the framework of linear elasticity theory, the deformation shapes can be determined from a body's linear finite element model. To this end, powerful model order reduction techniques can be used. The degrees of freedom consist of the absolute floating frame coordinates and the generalized coordinates corresponding to the deformation shapes. Since the absolute interface coordinates are not part of the set of degrees of freedom, the kinematic constraint equations are nonlinear and in general difficult to solve analytically. Hence, Lagrange multipliers are required to satisfy the constraint equations when formulating the equations of motion. This increases the total number of unknowns in the constrained equations of motion and makes them of the differential-algebraic type instead of the ordinary differential type. Figure 1.3 shows a graphical representation of the floating frame formulation. Details of this formulation for both rigid and flexible multibody systems can be found in textbooks such as [5, 6]. An overview of its essentials will be presented in Chapter 2.
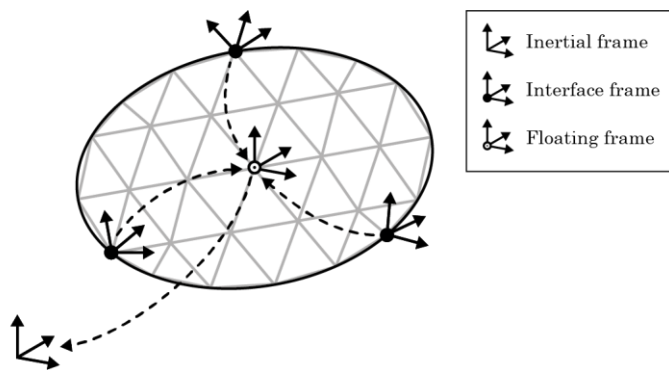

Fig. 1.3   Floating frame formulation for a flexible body. The degrees of freedom are the absolute floating frame coordinates and generalized coordinates corresponding to local deformation.

1.2 Purpose of this work

The fact that the floating frame formulation is able to exploit the advantages of linear model order reduction techniques makes it a very efficient formulation when the elastic deformation of bodies can be considered as small. In order to develop a more efficient formulation, it is desired to combine this advantage with the convenient way in which the inertial frame formulation and corotational formulation satisfy the kinematic constrains. To this end, the Lagrange multipliers need to be eliminated from the floating frame formulation. This can be done if the absolute interface coordinates uniquely describe the body's kinematics. In other words, if it is possible to express both the floating frame coordinates and the generalized coordinates corresponding to local elastic mode shapes in terms of the absolute interface coordinates, the Lagrange multipliers can be eliminated.

One could say that in this case a so-called **superelement** is created: the motion of a flexible body is described entirely by the motion of its interface points. The term superelement refers to the similar way in which the displacement field of a finite element is described uniquely by the displacements of its nodes. In the linear finite element method, the use of superelements is well-developed for the purpose of model order reduction. For geometric nonlinear problems, the development of superelements is less straightforward.

The idea to create superelements based on the floating frame formulation is not new. The fundamental problem for every superelement formulation is how to uniquely determine the motion of the floating frame from the motion of the interface points. Several different formulations can be found in literature, but in particular the contributions of Cardona and Géradin [7, 8, 9] in this field are widely acknowledged in the multibody community. The essence of these formulations is discussed in Section 1.3. The principle purpose of this thesis is the presentation of a new method for creating superelements based on the floating frame formulation. The new superelement formulation offers a unique and elegant solution to the traditional problem of expressing a body's floating frame coordinates in terms of the interface coordinates. The formulation was published firstly

in [10] and presented on multibody dynamics conferences [11, 12]. This new formulation is introduced in Section 1.4

In the proposed new method, Craig-Bampton modes [13, 14] are used to describe a body's local elastic deformation. Because the required coordinate transformation involves absolute and relative interface coordinates, it is suggested naturally to use the Craig-Bampton modes. After all, the generalized coordinates corresponding to the static Craig-Bampton modes (also known as interface modes or boundary modes) are in fact equal to the local interface coordinates. However, it is important to emphasize that the proposed method is not limited to the use of Craig-Bampton modes. In literature, many different model order reduction techniques are described and a convenient overview of the most standard ones can be found in textbooks such as [15]. For this reason, a generalization of the new method suitable for any choice of the local deformation shapes is included in Chapter 8.

Essential for the presented method is the fact that the static Craig-Bampton modes are able to describe rigid body motions. Because rigid body motion is already being described by the motion of the floating frame, the rigid body modes must be eliminated from the Craig-Bampton modes in order to describe the system's motion uniquely. At the same time, this property can be used to establish a coordinate transformation that expresses both the floating frame coordinates and the local interface coordinates corresponding to the Craig-Bampton modes in terms of the absolute interface coordinates. This is done by demanding that the elastic body has no deformation at the location of the floating frame. Although there are several ways to meet this demand, in all cases the rigid body motion is removed from the Craig-Bampton modes and the floating frame coordinates are related to the absolute interface coordinates simultaneously.

It is interesting to note that the problem of relating a flexible body's floating frame to the absolute interface coordinates is very similar to the problem of relating an element's corotational frame to its absolute nodal coordinates, as for instance addressed in [16, 17]. In this work, the parallel between a flexible body in a superelement formulation and a finite element in the corotational frame formulation will be demonstrated in more detail in Chapter 4. The standard corotational frame formulation in fact neglects higher order deformation terms in an element's mass matrix as well as fictitious forces due to quadratic velocity terms. However, in many standard textbooks on nonlinear finite element methods and the corotational formulation, such as [2], these simplifications are often not mentioned. The mathematical derivation of the new superelement formulation that is presented in this work can be used to understand the exact form of these terms that are often left out of the corotational frame formulation. Moreover, by simulating benchmark problems, these simplifications will also be justified. In this view, it is also an important contribution of this work to demonstrate relevant relations between the different flexible multibody formulations. These relations will be addressed on several occasions throughout this thesis.

1.3 Existing superelement formulations

When each individual Craig-Bampton mode equals zero at the location of the floating frame, the motion is described uniquely. A first possibility for which this is true is when the floating frame is located at an interface point, and the Craig-Bampton modes of that specific interface point are not taken into account [7]. Figure 1.4 shows a graphical representation of this situation. An important disadvantage of this method is that simulation results become dependent on which interface point is chosen. Moreover, it is known from literature that better accuracy can be expected when the floating frame is located close to the body's center of mass [9]. The effect of the floating frame location on simulation accuracy is studied, using the new formulation, by simulation of several benchmark problems. The results confirm this statement and are presented in Chapter 5.
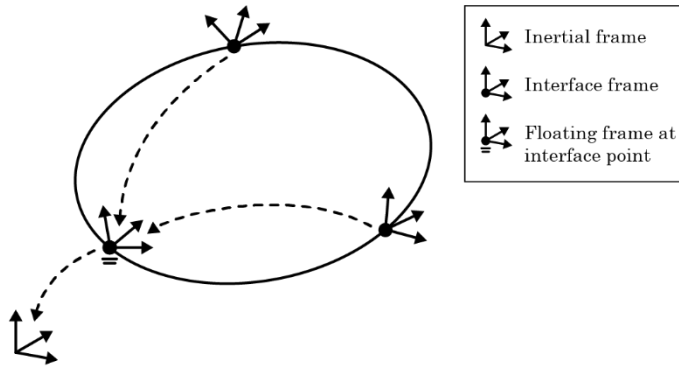
Fig. 1.4   Floating frame located in an interface point.

An alternative with which the floating frame can be positioned in the center of mass of the undeformed body is to add an auxiliary interface point at the material point that coincides with the center of mass of the undeformed body. The Craig-Bampton modes are then determined while keeping this auxiliary interface point fixed [9]. Figure 1.5 shows a graphical representation of this situation. The accuracy of the second method is method is better, in general, than that of the first, but it also requires 6 additional degrees of freedom per body. Moreover, the location of the floating frame has to be determined before computing the Craig-Bampton modes. Consequently, if one wants to relocate the floating frame, these modes need to be recomputed.
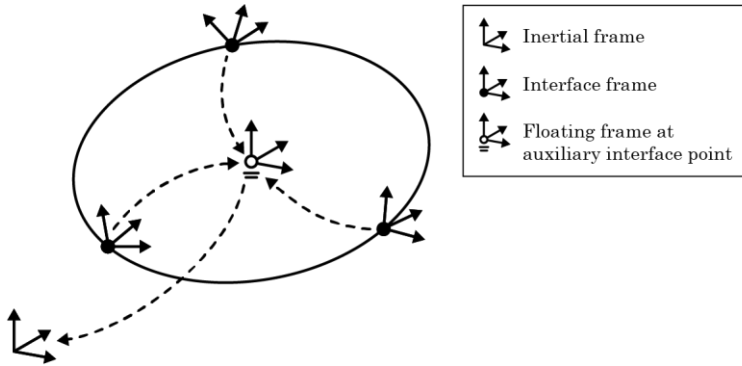
Fig. 1.5   Floating frame treated at an auxiliary interface point located at the center of mass of the undeformed body.

Finally, it is possible to compute the position and orientation of the floating frame as a (weighted) average of the interface coordinates. This strategy is used in some corotational frame formulations, but has the disadvantage that the floating frame is no longer rigidly attached to a material point on the body. As such, the motion of the floating frame has no physical meaning other than that it represents the body's rigid body motion in a certain averaged sense.

1.4 The new superelement formulation

The strength of the new superelement formulation, is that it allows the floating frame to be located at the center of mass of the undeformed body, without using an auxiliary interface point. Hence, it does not introduce 6 additional degrees of freedom. Figure 1.6 shows a graphical representation of this situation. In order to arrive at this formulation, no demands are made on the Craig-Bampton modes individually. The central thought is that as long as any linear combination of Craig-Bampton modes is zero at the location of the floating frame, the location of the floating frame can be derived uniquely from the absolute interface coordinates.
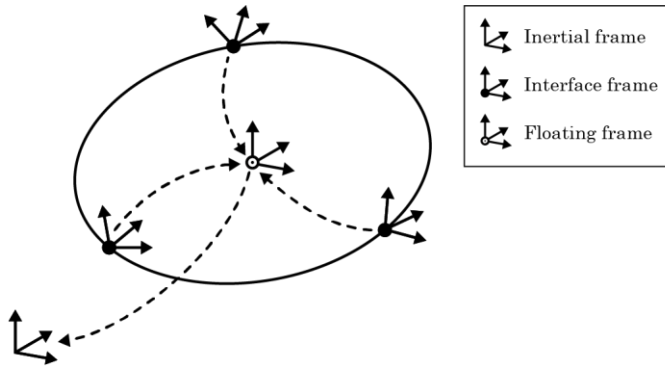
Fig. 1.6 Floating frame located at the center of mass of the undeformed body, which is not an interface point.

The development of the new superelement formulation is discussed in detail in this work. Starting from the floating frame formulation, it is shown that by using a sophisticated coordinate transformation, it is possible to express the equations of motion of a flexible body in terms of the absolute interface coordinates. This enables a new way of including flexibility in a multibody simulation, which is efficient due to the reuse of a body's linear finite element model and the application of the kinematic constraints without Lagrange multipliers.

Not only will the mathematical details of the new formulation be presented, but it is also the purpose of this work to add geometric interpretation to the various terms that will be encountered. The author wishes to demonstrate that many details can be understood using engineering intuition. To this end, interesting and relevant relations between the inertial frame, corotational frame and floating frame formulations are explained. Complex coordinate transformations are supported by graphic and geometric interpretations. In many ways, the new superelement formulation may make a significant contribution to creating a practical understanding of the various aspects of flexible multibody dynamics.

Finally, it is the intention of the author to make the new formulation easily understandable for experts in fields closely related to flexible multibody dynamics, such as mechanism design, robotics, and precision engineering. For this purpose, relevant generalizations of the superelement formulation are included at the end of this work.

1.5   Outline of this work

Chapter 2 presents an overview of the floating frame formulation. Because the new method is based on the floating frame formulation, its essentials must be introduced properly. To this end, the kinematics of a flexible body are discussed and the equations of motion of a flexible body are derived.

Chapter 3 describes the kinematics of a flexible body in terms of the absolute interface coordinates. Kinematic transformations are derived that express the absolute floating frame coordinates and local interface coordinates in terms of the absolute interface coordinates. These transformation matrices are interpreted geometrically.

Chapter 4 describes the kinetics of a flexible body in terms of the absolute interface coordinates. The equation of motion of a flexible body in the new superelement formulation is presented here. Moreover, the numerical solution procedure with which this equation of motion is solved incrementally is discussed and interpreted. It will be explained that the geometric interpretation introduced in Chapter 3 has led to the discovery of justifiable additional assumptions that improve the computational efficiency of the method.

Chapter 5 presents simulation results that were performed in order to validate the new method. A wide variety of benchmark problems have been simulated using many different formulations. The new method is compared with these simulations and found to be accurate. Also, the effect of additional simplifications and assumptions within the new method on the accuracy of simulation results is tested.

Chapter 6 presents the conclusions related to the new superelement formulation.

Chapter 7 presents an overview of the author's recommendations for future research.

Chapter 8 contains theoretical elaborations of the given recommendations. For future applications, the new superelement formulation is generalized to account for a general set of deformation modes, such that model order reduction methods other than the Craig-Bampton method can be used as well. In addition, a generalization to include large deformations within a body is described. Preliminary validation results of bodies that have more than two interface points are presented. Finally, a formulation in terms of screw theory is presented to support the implementation of the new theory in for example robotics.

2

The floating frame formulation

In order to establish a flexible multibody dynamics formulation, the equations of motion of a flexible body need to be derived. This requires the kinematics of any arbitrary material point on a flexible body to be described uniquely in a chosen set of generalized coordinates. In Section 2.1 the relevant kinematics of the floating frame formulation will be discussed. This includes the expressions for the position, velocity, acceleration and virtual displacement of an arbitrary point on a flexible body.

In Section 2.2, the equations of motion of a flexible body in the floating frame formulation are derived. To this end, first the Newton-Euler equations of motion for a rigid body are discussed. The extension from Newton's second law to the Newton-Euler equations can be seen as the extension from infinitesimal bodies to finite bodies. Subsequently, the extension from rigid bodies to flexible bodies is explained. The equations of motion of a flexible body are derived from the principle of virtual work, which serves as a fundamental physical concept.

This chapter is written after consulting many well-known standard textbooks on both rigid and flexible multibody dynamics, among which [5, 6] as well as the PhD Thesis by M.H.M. Ellenbroek [18]. The work presented in this chapter was reused by the author as a basis for the reader "Dynamics 3" that was written as study material for the course "Dynamics & Control" in the Master's programme of Mechanical Engineering at the University of Twente [19]. A digital copy of this reader is available upon request for personal use.

2.1 Kinematics of the floating frame formulation

Consider a flexible body moving in a three-dimensional space. In any arbitrary material point of the body, a Cartesian coordinate frame is rigidly attached. The kinematics of the body can be described by the motion of a set of such coordinate frames. Consider two arbitrarily chosen material points P_i and P_j, with coordinate frames E_i and E_j rigidly attached. Because a pair such as $\{P_i, E_i\}$ defines both the position and orientation of the frame attached to P_i, it will be referred to as the generalized position, or simply the position of P_i.

The position of P_i relative to P_j can be expressed by the (3×1) position vector $\mathbf{r}_i^{j,j}$ and the (3×3) rotation matrix $\mathbf{R}_i^j$. In this notation, the position vector $\mathbf{r}_i^{j,j}$ defines the position of P_i (lower index i) relative to P_j (second upper index j) and its components are expressed in the coordinate system $\{P_j, E_j\}$ (first upper index j). The rotation matrix $\mathbf{R}_i^j$ defines the orientation of E_i (lower index i) relative to E_j (upper index j) expressed in $\{P_j, E_j\}$. The graphical representation of the position of P_i relative to P_j using the position vector and rotation matrix is included in Figure 2.1.
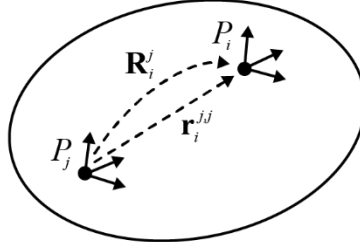
Fig. 2.1   Position of P_i relative to P_j in terms of a position vector and rotation matrix.

$\mathbf{R}_i^j$ defines a coordinate transformation that can be used to transform a vector that is expressed in frame j into a vector that is expressed in frame i. For example, the components of position vector $\mathbf{r}_i^{j,j}$ can also be expressed in the frame i, which is denoted by $\mathbf{r}_i^{i,j}$, changing the first upper index.

The two vectors $\mathbf{r}_i^{j,j}$ and $\mathbf{r}_i^{i,j}$ are related as:

$$\mathbf{r}_i^{j,j} = \mathbf{R}_i^j \mathbf{r}_i^{i,j} \qquad (2.1)$$

The rotation matrix is an orthogonal matrix of the proper kind, which means that its determinant equals +1 and its transpose equals its inverse, which also represents the inverse coordinate transformation, such that:

$$\left(\mathbf{R}_i^j\right)^{-1} = \mathbf{R}_j^i, \qquad \mathbf{R}_i^j \mathbf{R}_j^i = \mathbf{1} \qquad (2.2)$$

with $\mathbf{1}$ the (3×3) identity matrix. Expressions for the virtual displacement and virtual rotation of a material point on a flexible body are obtained by taking the variation of the current position. The virtual displacement of P_i relative to P_j expressed in frame E_j is denoted by $\delta\mathbf{r}_i^{j,j}$. The variation in the rotation matrix $\mathbf{R}_i^j$ is denoted by $\delta\mathbf{R}_i^j$, which is equal to a skew symmetric matrix times the rotation matrix itself. This can be proved by taking the variation of (2.2) using the product rule:

$$\delta\left(\mathbf{R}_i^j \mathbf{R}_j^i\right) = \delta\mathbf{R}_i^j \mathbf{R}_j^i + \mathbf{R}_i^j \delta\mathbf{R}_j^i = \mathbf{0} \qquad (2.3)$$

This can be rewritten to:

$$\delta\mathbf{R}_i^j \mathbf{R}_j^i = -\mathbf{R}_i^j \delta\mathbf{R}_j^i = -\left(\delta\mathbf{R}_i^j \mathbf{R}_j^i\right)^T \qquad (2.4)$$

From this it follows that $\delta\mathbf{R}_i^j \mathbf{R}_j^i$ is skew symmetric and has zeros on its main diagonal. Let this skew symmetric matrix be denoted by $\delta\widetilde{\boldsymbol{\pi}}_i^{j,j}$:

$$\delta\mathbf{R}_i^j \mathbf{R}_j^i = \delta\widetilde{\boldsymbol{\pi}}_i^{j,j} \qquad (2.5)$$

Post-multiplying (2.5) by $\mathbf{R}_i^j$ shows that the variation in the rotation matrix equals a skew symmetric matrix times the rotation matrix itself:

$$\boxed{\delta\mathbf{R}_i^j = \delta\widetilde{\boldsymbol{\pi}}_i^{j,j} \mathbf{R}_i^j} \qquad (2.6)$$

This is an important property of the rotation matrix which follows directly from the fact that the rotation matrix is an orthogonal matrix. In the above, the tilde operator $\widetilde{(\cdot)}$ is introduced such that when applied to a (3×1) vector $\mathbf{a}$, it yields the skew symmetric (3×3) matrix $\tilde{\mathbf{a}}$:

$$
\mathbf{a} = \begin{bmatrix} a_1 \\ a_2 \\ a_3 \end{bmatrix}, \qquad \tilde{\mathbf{a}} = \begin{bmatrix} 0 & -a_3 & a_2 \\ a_3 & 0 & -a_1 \\ -a_2 & a_1 & 0 \end{bmatrix} \tag{2.7}
$$

In (2.6), the tilde operator is applied on the vector $\delta\boldsymbol{\pi}_i^{j,j}$, which is the vector of virtual rotations of frame $\{P_i, E_i\}$ with respect to $\{P_j, E_j\}$ with its components expressed in $\{P_j, E_j\}$. The expressions for the velocity of a material point on a flexible body are similar to the expressions for the variations. The linear velocity of P_i is simply the time derivative of $\mathbf{r}_i^{j,j}$, which is denoted by $\dot{\mathbf{r}}_i^{j,j}$. The time derivative of a rotation matrix can be expressed as a skew symmetric matrix times the rotation matrix itself:

$$
\boxed{\dot{\mathbf{R}}_i^j = \tilde{\boldsymbol{\omega}}_i^{j,j} \mathbf{R}_i^j} \tag{2.8}
$$

This can be derived by taking the time derivative of (2.2) and following the same steps as for the variation. In (2.8), $\tilde{\boldsymbol{\omega}}_i^{j,j}$ is the skew symmetric matrix containing the elements of the vector $\boldsymbol{\omega}_i^{j,j}$, which is the instantaneous angular velocity vector of frame $\{P_i, E_i\}$ with respect to $\{P_j, E_j\}$ with its components expressed in $\{P_j, E_j\}$.

Expressions for the acceleration of a material point on a flexible body are obtained by differentiating the expressions for the velocity once more with respect to time. The second time derivative of the position vector $\mathbf{r}_i^{j,j}$ is the linear acceleration vector $\ddot{\mathbf{r}}_i^{j,j}$. The time derivative of the angular velocity vector $\boldsymbol{\omega}_i^{j,j}$ is the angular acceleration vector $\dot{\boldsymbol{\omega}}_i^{j,j}$. The second time derivative of the rotation matrix $\mathbf{R}_i^j$ is obtained by differentiating (2.8) with respect to time using the product rule:

$$
\ddot{\mathbf{R}}_i^j = \dot{\tilde{\boldsymbol{\omega}}}_i^{j,j} \mathbf{R}_i^j + \tilde{\boldsymbol{\omega}}_i^{j,j} \tilde{\boldsymbol{\omega}}_i^{j,j} \mathbf{R}_i^j \tag{2.9}
$$

Many derivations throughout this work involve manipulations with skew symmetric matrices. Many properties that are used for these derivations originate from the fact that the cross product between two arbitrary (3×1) vectors **a** and **b** can be expressed in terms of a skew symmetric matrix:

$$\mathbf{a} \times \mathbf{b} = \tilde{\mathbf{a}}\mathbf{b} \tag{2.10}$$

The components of a skew symmetric matrix can be transformed from one frame to another by pre- and post-multiplication with the appropriate rotation matrices. For example, let $\tilde{\mathbf{a}}^j$ be a skew symmetric matrix of which its components are expressed in frame E_j. Then, expressing its components in frame E_i is denoted by $\tilde{\mathbf{a}}^i$ and realized as follows:

$$\tilde{\mathbf{a}}^j = \mathbf{R}_i^j \tilde{\mathbf{a}}^i \mathbf{R}_j^i \quad \leftrightarrow \quad \tilde{\mathbf{a}}^j \mathbf{R}_i^j = \mathbf{R}_i^j \tilde{\mathbf{a}}^i \tag{2.11}$$

This expression can be obtained by expressing the components of the $\mathbf{a}^j$ in frame E_i and constructing the skew symmetric matrix $\tilde{\mathbf{a}}^i$ from the result:

$$\mathbf{a}^j = \mathbf{R}_i^j \mathbf{a}^i \quad \leftrightarrow \quad \tilde{\mathbf{a}}^j = \left(\widetilde{\mathbf{R}_i^j \mathbf{a}^i}\right) = \mathbf{R}_i^j \tilde{\mathbf{a}}^i \mathbf{R}_j^i \tag{2.12}$$

In the floating frame formulation, the absolute position of an arbitrary point on a flexible body is expressed in terms of the absolute position of the body's floating frame and the relative position of the point to the floating frame. Figure 2.2 shows a graphical representation of how the position of an arbitrary point P_i on a flexible body with respect to inertial frame P_O is described using the body's floating frame located in P_j. In the floating frame formulation, the position vector $\mathbf{r}_i^{O,O}$ is expressed as:

$$\mathbf{r}_i^{O,O} = \mathbf{r}_j^{O,O} + \mathbf{R}_j^O \mathbf{r}_i^{j,j} \tag{2.13}$$
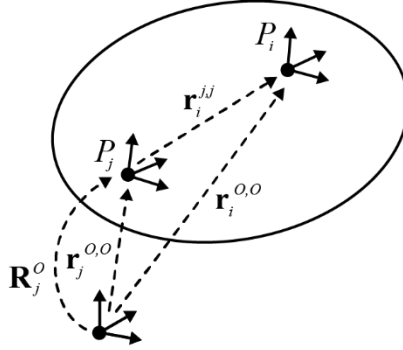
Fig. 2.2 Position of P_i relative to P_O using floating frame P_j.

In the case of a flexible body, the local position vector $\mathbf{r}_i^{j,j}$ is not constant. Instead, it is expressed as the sum of the position vector of P_i relative to P_j on the undeformed body $\mathbf{x}_i^{j,j}$ and the elastic displacement $\mathbf{u}_i^{j,j}$ of this point:

$$\mathbf{r}_i^{j,j} = \mathbf{x}_i^{j,j} + \mathbf{u}_i^{j,j} \tag{2.14}$$

Assuming that elastic strains and deformations within a single body remain small, the linear theory of elasticity can be used to describe local elastic deformations based on the linear Cauchy strain definition. This allows for the local elastic displacement field to be generally described by a linear combination of a set of N deformation shapes $\boldsymbol{\phi}$:

$$\mathbf{u}_i^{j,j} = \sum_{k=1}^{N} \boldsymbol{\phi}_k\big(\mathbf{x}_i^{j,j}\big)\eta_k = \boldsymbol{\Phi}_i \boldsymbol{\eta}, \qquad \boldsymbol{\Phi}_i \equiv \big[\boldsymbol{\phi}_1\big(\mathbf{x}_i^{j,j}\big) \quad \dots \quad \boldsymbol{\phi}_N\big(\mathbf{x}_i^{j,j}\big)\big] \tag{2.15}$$

In this, η_k is the time dependent generalized coordinate corresponding to position dependent deformation shape $\boldsymbol{\phi}_k$. Since $\mathbf{x}_i^{j,j}$ is constant, the following holds for the variation and time derivatives of the local position vector $\mathbf{r}_i^{j,j}$:

$$\delta\mathbf{r}_i^{j,j} = \boldsymbol{\Phi}_i \delta\boldsymbol{\eta}, \qquad \dot{\mathbf{r}}_i^{j,j} = \boldsymbol{\Phi}_i \dot{\boldsymbol{\eta}}, \qquad \ddot{\mathbf{r}}_i^{j,j} = \boldsymbol{\Phi}_i \ddot{\boldsymbol{\eta}} \tag{2.16}$$

Recall Figure 2.2 and (2.13) which show how the absolute position of P_i is expressed using the floating frame. The expression for the virtual displacement of P_i is obtained by taking the variation, using (2.6):

$$\delta \mathbf{r}_i^{0,O} = \delta \mathbf{r}_j^{0,O} + \delta \tilde{\boldsymbol{\pi}}_j^{0,O} \mathbf{R}_j^O \mathbf{r}_i^{j,j} + \mathbf{R}_j^O \delta \mathbf{r}_i^{j,j} \tag{2.17}$$

Using the transformation rule (2.11) and the cross product property that for any two (3×1) vectors $\mathbf{a}$ and $\mathbf{b}$ holds that $\tilde{\mathbf{a}}\mathbf{b} = -\tilde{\mathbf{b}}\mathbf{a}$, the second term on the right hand side of (2.17) can be rewritten. Together with substitution of (2.16), this allows (2.17) to be rewritten in the following matrix-vector notation:

$$\delta \mathbf{r}_i^{0,O} = \begin{bmatrix} \mathbf{1} & \mathbf{R}_j^O \left(\tilde{\mathbf{r}}_i^{j,j}\right)^T \mathbf{R}_O^j & \mathbf{R}_j^O \boldsymbol{\Phi}_i \end{bmatrix} \begin{bmatrix} \delta \mathbf{r}_j^{0,O} \\ \delta \boldsymbol{\pi}_j^{0,O} \\ \delta \boldsymbol{\eta} \end{bmatrix} \tag{2.18}$$

The expression for the absolute linear velocity of P_i in the inertial frame is obtained by differentiating (2.13) with respect to time. The result is similar to (2.17):

$$\dot{\mathbf{r}}_i^{0,O} = \dot{\mathbf{r}}_j^{0,O} + \tilde{\boldsymbol{\omega}}_j^{0,O} \mathbf{R}_j^O \mathbf{r}_i^{j,j} + \mathbf{R}_j^O \dot{\mathbf{r}}_i^{j,j} \tag{2.19}$$

The expression for the absolute linear acceleration of P_i is obtained by differentiating once more:

$$\ddot{\mathbf{r}}_i^{0,O} = \ddot{\mathbf{r}}_j^{0,O} + \dot{\tilde{\boldsymbol{\omega}}}_j^{0,O} \mathbf{R}_j^O \mathbf{r}_i^{j,j} + \mathbf{R}_j^O \ddot{\mathbf{r}}_i^{j,j} + \tilde{\boldsymbol{\omega}}_j^{0,O} \tilde{\boldsymbol{\omega}}_j^{0,O} \mathbf{R}_j^O \mathbf{r}_i^{j,j} + 2\tilde{\boldsymbol{\omega}}_j^{0,O} \mathbf{R}_j^O \dot{\mathbf{r}}_i^{j,j} \tag{2.20}$$

Substitution of (2.16) and rewriting in matrix-vector form yields:

$$\ddot{\mathbf{r}}_i^{0,O} = \begin{bmatrix} \mathbf{1} & \mathbf{R}_j^O \left(\tilde{\mathbf{r}}_i^{j,j}\right)^T \mathbf{R}_O^j & \mathbf{R}_j^O \boldsymbol{\Phi}_i \end{bmatrix} \begin{bmatrix} \ddot{\mathbf{r}}_j^{0,O} \\ \tilde{\boldsymbol{\omega}}_j^{0,O} \\ \ddot{\boldsymbol{\eta}} \end{bmatrix}$$
$$+ \begin{bmatrix} \mathbf{0} & \mathbf{R}_j^O \tilde{\boldsymbol{\omega}}_j^{j,O} \left(\tilde{\mathbf{r}}_i^{j,j}\right)^T \mathbf{R}_O^j & 2\mathbf{R}_j^O \tilde{\boldsymbol{\omega}}_j^{j,O} \boldsymbol{\Phi}_i \end{bmatrix} \begin{bmatrix} \dot{\mathbf{r}}_j^{0,O} \\ \boldsymbol{\omega}_j^{0,O} \\ \dot{\boldsymbol{\eta}} \end{bmatrix} \tag{2.21}$$

2.2   Kinetics of the floating frame formulation

Kinetics of a point mass

Newton's second law of motion represents the equation of motion of a freely moving point mass. It must be understood that this physical law is defined for a point mass of mass m and that both the resultant force $\mathbf{F}$ and acceleration $\mathbf{a}$ are defined with respect to an inertial frame. In its best known form, it is expressed as:

$$\mathbf{F} = m\mathbf{a} \tag{2.22}$$

Kinetics of a rigid body

For a freely moving rigid body, the equations of motion are known as the Newton-Euler equations. They can be considered as an extension of the above in the sense that Newton's second law is applied on every infinitesimally small mass particle within the rigid body. In the Newton-Euler equations, integration of all infinitesimal contributions yields independent equations for the translational and rotational degrees of freedom in the form of a force balance and a moment balance. In fact, the extension from Newton's second law to the Newton-Euler equations is the extension from infinitesimal bodies to finite bodies. In their popular form, they are expressed as:

$$\mathbf{F} = m\mathbf{a}$$
$$\mathbf{M} = \mathbf{I}\boldsymbol{\alpha} + \tilde{\boldsymbol{\omega}}\mathbf{I}\boldsymbol{\omega} \tag{2.23}$$

In the force balance, $\mathbf{F}$ represents the resultant applied force on the body, m is the body's total mass and $\mathbf{a}$ is the absolute acceleration of the body's center of mass. The force balance is expressed globally, with respect to an inertial frame, which in this work will be the global reference frame $\{P_O, E_O\}$. In the moment balance, $\mathbf{M}$ is the resultant moment about the body's principal axes, $\mathbf{I}$ is the second moment of mass matrix about the body's principal axes and $\boldsymbol{\omega}$ and $\boldsymbol{\alpha}$ are the angular velocity and acceleration vectors respectively. The moment balance is expressed locally, with respect to a coordinate system located at the body's center of mass $\{P_C, E_C\}$, which is the origin of the body's principal axes.

Kinetics of a flexible body

When extending from a point mass to a rigid body, it is relatively intuitive to understand that the moment balance equations are the required additional equations of motion. However, when considering the motion of a flexible body, additional generalized coordinates are required to describe a body's local elastic deformation. Because the physical interpretation of these coordinates is not straightforward, it is hard to imagine the precise form of the required additional equations of motion. For that reason, the principle of virtual work is used as a fundamental physical principle from which the equations of motion can be derived. It is commonly attributed to D'Alembert to reformulate Newton's second law using the concept of virtual displacements. In its well-known form, it is expressed as:

$$\delta \mathbf{r}^T (m\ddot{\mathbf{r}} - \mathbf{F}) = 0, \qquad \forall \, \delta \mathbf{r} \tag{2.24}$$

which is equivalent to Newton's second law as the equation must hold for all arbitrary virtual displacements $\delta \mathbf{r}$. Upon integration of (2.24), the principle of virtual work is obtained, which equates the virtual work by internal forces to the virtual work by external forces. For a flexible body, the virtual work by internal forces consists of the virtual work by inertia forces δW_{in} and the virtual work by elastic forces δW_{el}. These are equated to the virtual work by external forces δW_{ex}:

$$\boxed{\delta W_{in} + \delta W_{el} = \delta W_{ex}} \tag{2.25}$$

The virtual work by elastic forces equals the variation in the internal strain energy. In the case of a rigid body, the virtual internal work equals the virtual work by inertia forces only, because a rigid body cannot deform. For the virtual external work, concentrated forces are summed and body forces are integrated over the volume of the body. Each of the three terms in (2.25) will now be elaborated on. The development of the virtual work by inertia forces is the most cumbersome and will be presented first.

Virtual work by inertia forces δW_{in}

Let $\rho_i dV$ denote the infinitesimally small mass located at P_i on a body. Then, in terms of the notation used in this work, the virtual internal work by inertia forces δW_{in} is expressed as:

$$\delta W_{in} = \int_V \left(\delta \mathbf{r}_i^{0,0}\right)^T \ddot{\mathbf{r}}_i^{0,0}\, \rho_i dV \tag{2.26}$$

In the expression for virtual work by inertia forces (2.26), the integrand consists of the multiplication $\left(\delta\mathbf{r}_i^{0,0}\right)^T \ddot{\mathbf{r}}_i^{0,0}$. Since (2.21) consists of two terms, the required integrand in (2.26) consists of two matrices: a matrix that is multiplied by the acceleration of the floating frame and a matrix that is multiplied by the velocity of the floating frame. By using the appropriate matrix-vector product identities, the result can be written in the following form:

$$
\begin{aligned}
\left(\delta\mathbf{r}_i^{0,0}\right)^T \ddot{\mathbf{r}}_i^{0,0} =
&\begin{bmatrix} \delta\mathbf{r}_j^{0,0} \\ \delta\boldsymbol{\pi}_j^{0,0} \\ \delta\boldsymbol{\eta} \end{bmatrix}^T
\left[\begin{array}{cc|c}
\mathbf{1} & \mathbf{R}_j^O \left(\tilde{\mathbf{r}}_i^{j,j}\right)^T \mathbf{R}_O^j & \mathbf{R}_j^O \boldsymbol{\Phi}_i \\
\mathbf{R}_j^O \tilde{\mathbf{r}}_i^{j,j} \mathbf{R}_O^j & \mathbf{R}_j^O \tilde{\mathbf{r}}_i^{j,j} \left(\tilde{\mathbf{r}}_i^{j,j}\right)^T \mathbf{R}_O^j & \mathbf{R}_j^O \tilde{\mathbf{r}}_i^{j,j} \boldsymbol{\Phi}_i \\
\hline
(\boldsymbol{\Phi}_i)^T \mathbf{R}_O^j & (\boldsymbol{\Phi}_i)^T \left(\tilde{\mathbf{r}}_i^{j,j}\right)^T \mathbf{R}_O^j & (\boldsymbol{\Phi}_i)^T \boldsymbol{\Phi}_i
\end{array}\right]
\begin{bmatrix} \ddot{\mathbf{r}}_j^{0,0} \\ \dot{\tilde{\boldsymbol{\omega}}}_j^{0,0} \\ \ddot{\boldsymbol{\eta}} \end{bmatrix} \\[2em]
+ &\begin{bmatrix} \delta\mathbf{r}_j^{0,0} \\ \delta\boldsymbol{\pi}_j^{0,0} \\ \delta\boldsymbol{\eta} \end{bmatrix}^T
\left[\begin{array}{cc|c}
\mathbf{0} & \mathbf{R}_j^O\, \tilde{\boldsymbol{\omega}}_j^{j,O} \left(\tilde{\mathbf{r}}_i^{j,j}\right)^T \mathbf{R}_O^j & 2\mathbf{R}_j^O\, \tilde{\boldsymbol{\omega}}_j^{j,O} \boldsymbol{\Phi}_i \\
\mathbf{0} & \mathbf{R}_j^O\, \tilde{\boldsymbol{\omega}}_j^{j,O} \tilde{\mathbf{r}}_i^{j,j} \left(\tilde{\mathbf{r}}_i^{j,j}\right)^T \mathbf{R}_O^j & 2\mathbf{R}_j^O \tilde{\mathbf{r}}_i^{j,j} \tilde{\boldsymbol{\omega}}_j^{j,O} \boldsymbol{\Phi}_i \\
\hline
\mathbf{0} & (\boldsymbol{\Phi}_i)^T \tilde{\boldsymbol{\omega}}_j^{j,O} \left(\tilde{\mathbf{r}}_i^{j,j}\right)^T \mathbf{R}_O^j & 2(\boldsymbol{\Phi}_i)^T \tilde{\boldsymbol{\omega}}_j^{j,O} \boldsymbol{\Phi}_i
\end{array}\right]
\begin{bmatrix} \dot{\mathbf{r}}_j^{0,0} \\ \boldsymbol{\omega}_j^{0,0} \\ \dot{\boldsymbol{\eta}} \end{bmatrix}
\end{aligned}
\tag{2.27}
$$

In this, the partitioning lines are used to conveniently distinguish between the terms that are related to the rigid body motion and the terms that are related to the body's flexible behavior.

Integration of (2.27) yields the expression for the virtual work by inertia forces:

$$\delta W_{in} = \begin{bmatrix} \delta\mathbf{r}_j^{0,0} \\ \delta\boldsymbol{\pi}_j^{0,0} \\ \delta\boldsymbol{\eta} \end{bmatrix}^T \int_V \begin{bmatrix} \mathbf{1} & \mathbf{R}_j^O\left(\tilde{\mathbf{r}}_i^{j,j}\right)^T\mathbf{R}_O^j & \mathbf{R}_j^O\boldsymbol{\Phi}_i \\ \mathbf{R}_j^O\tilde{\mathbf{r}}_i^{j,j}\mathbf{R}_O^j & \mathbf{R}_j^O\tilde{\mathbf{r}}_i^{j,j}\left(\tilde{\mathbf{r}}_i^{j,j}\right)^T\mathbf{R}_O^j & \mathbf{R}_j^O\tilde{\mathbf{r}}_i^{j,j}\boldsymbol{\Phi}_i \\ (\boldsymbol{\Phi}_i)^T\mathbf{R}_O^j & (\boldsymbol{\Phi}_i)^T\left(\tilde{\mathbf{r}}_i^{j,j}\right)^T\mathbf{R}_O^j & (\boldsymbol{\Phi}_i)^T\boldsymbol{\Phi}_i \end{bmatrix}\rho_i dV \begin{bmatrix} \ddot{\mathbf{r}}_j^{0,0} \\ \dot{\tilde{\boldsymbol{\omega}}}_j^{0,0} \\ \ddot{\boldsymbol{\eta}} \end{bmatrix}$$

$$+ \begin{bmatrix} \delta\mathbf{r}_j^{0,0} \\ \delta\boldsymbol{\pi}_j^{0,0} \\ \delta\boldsymbol{\eta} \end{bmatrix}^T \int_V \begin{bmatrix} \mathbf{0} & \mathbf{R}_j^O\,\tilde{\boldsymbol{\omega}}_j^{j,0}\left(\tilde{\mathbf{r}}_i^{j,j}\right)^T\mathbf{R}_O^j & 2\mathbf{R}_j^O\tilde{\boldsymbol{\omega}}_j^{j,0}\boldsymbol{\Phi}_i \\ \mathbf{0} & \mathbf{R}_j^O\,\tilde{\boldsymbol{\omega}}_j^{j,0}\tilde{\mathbf{r}}_i^{j,j}\left(\tilde{\mathbf{r}}_i^{j,j}\right)^T\mathbf{R}_O^j & 2\mathbf{R}_j^O\tilde{\mathbf{r}}_i^{j,j}\tilde{\boldsymbol{\omega}}_j^{j,0}\boldsymbol{\Phi}_i \\ \mathbf{0} & (\boldsymbol{\Phi}_i)^T\tilde{\boldsymbol{\omega}}_j^{j,0}\left(\tilde{\mathbf{r}}_i^{j,j}\right)^T\mathbf{R}_O^j & 2(\boldsymbol{\Phi}_i)^T\tilde{\boldsymbol{\omega}}_j^{j,0}\boldsymbol{\Phi}_i \end{bmatrix}\rho_i dV \begin{bmatrix} \dot{\mathbf{r}}_j^{0,0} \\ \boldsymbol{\omega}_j^{0,0} \\ \dot{\boldsymbol{\eta}} \end{bmatrix} \tag{2.28}$$

The first matrix in (2.28) is identified as the global mass matrix $\mathbf{M}^O$ of the flexible body:

$$\mathbf{M}^O \equiv \int_V \begin{bmatrix} \mathbf{1} & \mathbf{R}_j^O\left(\tilde{\mathbf{r}}_i^{j,j}\right)^T\mathbf{R}_O^j & \mathbf{R}_j^O\boldsymbol{\Phi}_i \\ \mathbf{R}_j^O\tilde{\mathbf{r}}_i^{j,j}\mathbf{R}_O^j & \mathbf{R}_j^O\tilde{\mathbf{r}}_i^{j,j}\left(\tilde{\mathbf{r}}_i^{j,j}\right)^T\mathbf{R}_O^j & \mathbf{R}_j^O\tilde{\mathbf{r}}_i^{j,j}\boldsymbol{\Phi}_i \\ (\boldsymbol{\Phi}_i)^T\mathbf{R}_O^j & (\boldsymbol{\Phi}_i)^T\left(\tilde{\mathbf{r}}_i^{j,j}\right)^T\mathbf{R}_O^j & (\boldsymbol{\Phi}_i)^T\boldsymbol{\Phi}_i \end{bmatrix}\rho_i dV \tag{2.29}$$

The second matrix in (2.28) is identified as the velocity dependent matrix of fictitious forces $\mathbf{C}^O$ of the flexible body:

$$\mathbf{C}^O \equiv \int_V \begin{bmatrix} \mathbf{0} & \mathbf{R}_j^O\,\tilde{\boldsymbol{\omega}}_j^{j,0}\left(\tilde{\mathbf{r}}_i^{j,j}\right)^T\mathbf{R}_O^j & 2\mathbf{R}_j^O\tilde{\boldsymbol{\omega}}_j^{j,0}\boldsymbol{\Phi}_i \\ \mathbf{0} & \mathbf{R}_j^O\,\tilde{\boldsymbol{\omega}}_j^{j,0}\tilde{\mathbf{r}}_i^{j,j}\left(\tilde{\mathbf{r}}_i^{j,j}\right)^T\mathbf{R}_O^j & 2\mathbf{R}_j^O\tilde{\mathbf{r}}_i^{j,j}\tilde{\boldsymbol{\omega}}_j^{j,0}\boldsymbol{\Phi}_i \\ \mathbf{0} & (\boldsymbol{\Phi}_i)^T\tilde{\boldsymbol{\omega}}_j^{j,0}\left(\tilde{\mathbf{r}}_i^{j,j}\right)^T\mathbf{R}_O^j & 2(\boldsymbol{\Phi}_i)^T\tilde{\boldsymbol{\omega}}_j^{j,0}\boldsymbol{\Phi}_i \end{bmatrix}\rho_i dV \tag{2.30}$$

It can be observed that the integrands in both $\mathbf{M}^O$ and $\mathbf{C}^O$ contain terms that are being pre- and post-multiplied with rotation matrices. These rotation matrices can be taken outside of the integral. In this way, both global matrices $\mathbf{M}^O$ and $\mathbf{C}^O$ can be expressed in terms of local matrices $\mathbf{M}^j$ and $\mathbf{C}^j$ that are being transformed to the global frame as follows:

$$\mathbf{M}^O = \left[\mathbf{R}_j^O\right]\mathbf{M}^j\left[\mathbf{R}_O^j\right], \qquad \mathbf{C}^O = \left[\mathbf{R}_j^O\right]\mathbf{C}^j\left[\mathbf{R}_O^j\right] \tag{2.31}$$

In this the local mass matrix $\mathbf{M}^j$ is defined as:

$$\mathbf{M}^j \equiv \int_V \begin{bmatrix} \mathbf{1} & \left(\tilde{\mathbf{r}}_i^{j,j}\right)^T & \boldsymbol{\Phi}_i \\ \tilde{\mathbf{r}}_i^{j,j} & \tilde{\mathbf{r}}_i^{j,j}\left(\tilde{\mathbf{r}}_i^{j,j}\right)^T & \tilde{\mathbf{r}}_i^{j,j}\boldsymbol{\Phi}_i \\ \left(\boldsymbol{\Phi}_i\right)^T & \left(\boldsymbol{\Phi}_i\right)^T\left(\tilde{\mathbf{r}}_i^{j,j}\right)^T & \left(\boldsymbol{\Phi}_i\right)^T\boldsymbol{\Phi}_i \end{bmatrix} \rho_i dV \qquad (2.32)$$

The local matrix of fictitious forces $\mathbf{C}^j$ is defined as:

$$\mathbf{C}^j \equiv \int_V \begin{bmatrix} \mathbf{0} & \tilde{\boldsymbol{\omega}}_j^{j,O}\left(\tilde{\mathbf{r}}_i^{j,j}\right)^T & 2\tilde{\boldsymbol{\omega}}_j^{j,O}\boldsymbol{\Phi}_i \\ \mathbf{0} & \tilde{\boldsymbol{\omega}}_j^{j,O}\tilde{\mathbf{r}}_i^{j,j}\left(\tilde{\mathbf{r}}_i^{j,j}\right)^T & 2\tilde{\mathbf{r}}_i^{j,j}\tilde{\boldsymbol{\omega}}_j^{j,O}\boldsymbol{\Phi}_i \\ \mathbf{0} & \left(\boldsymbol{\Phi}_i\right)^T\tilde{\boldsymbol{\omega}}_j^{j,O}\left(\tilde{\mathbf{r}}_i^{j,j}\right)^T & 2\left(\boldsymbol{\Phi}_i\right)^T\tilde{\boldsymbol{\omega}}_j^{j,O}\boldsymbol{\Phi}_i \end{bmatrix} \rho_i dV \qquad (2.33)$$

Note that the integrals in both $\mathbf{M}^j$ and $\mathbf{C}^j$ are expressed in terms of the deformed configuration, i.e. they are expressed in terms of $\mathbf{r}_i^{j,j}$ instead of $\mathbf{x}_i^{j,j}$. Hence, they are not constant. Yet, these integrals can be expressed as a constant matrix, based on the undeformed configuration $\mathbf{x}_i^{j,j}$, and higher order terms that are either linear or quadratic in terms of the deformation $\mathbf{u}_i^{j,j}$. In this way, $\mathbf{M}^j$ and $\mathbf{C}^j$ can be expressed as follows:

$$\mathbf{M}^j = \mathbf{M}_0^j + \mathbf{M}_1^j + \mathbf{M}_2^j, \qquad \mathbf{C}^j = \mathbf{C}_0^j + \mathbf{C}_1^j + \mathbf{C}_2^j \qquad (2.34)$$

In this, the subscripts 0, 1 and 2 are used to identify the terms with zeroth, first and second order dependency on the deformation respectively. By recalling from (2.15) that $\mathbf{u}_i^{j,j} = \boldsymbol{\Phi}_i\boldsymbol{\eta}$, the time dependency of the higher order terms can be taken outside the integral. In this way, the higher order terms are in fact integrals of the deformation shapes $\boldsymbol{\Phi}_i$, which are constant. Consequently, even for the higher order terms it is not necessary to recompute integrals at every iteration step.

In order to be able to express the elastic displacement field as a linear combination of deformation shapes, it is assumed that local elastic deformations are small. This suggests the effect of elastic deformation on the matrices $\mathbf{M}^j$ and $\mathbf{C}^j$ will indeed be of a higher order. In Chapter 5,

simulations of various benchmark problems are performed in which the effect of these higher order terms is investigated. The validation simulations have demonstrated that ignoring higher order terms, i.e. taking into account $\mathbf{M}_0^j$ and $\mathbf{C}_0^j$ only, still produces accurate results. For this reason, no further elaboration on the exact form of the higher order terms is given here.

In the partition of the mass matrix (2.32) that is related to the rigid body motion, the mass, first moment of mass and second moment of mass integrals can be recognized:

$$m^j \equiv \int_V \rho_i dV$$

$$\tilde{\mathbf{s}}^j \equiv \int_V \left(\tilde{\mathbf{r}}_i^{j,j}\right)^T \rho_i dV \qquad (2.35)$$

$$\mathbf{I}^j \equiv \int_V \tilde{\mathbf{r}}_i^{j,j}\left(\tilde{\mathbf{r}}_i^{j,j}\right)^T \rho_i dV$$

Recall that the first moment of mass $\mathbf{s}^j$ defines the body's center of mass P_C: the center of mass is located such that $\mathbf{s}^C \equiv \mathbf{0}$ by construction. Consequently, if the floating frame is located at the center of mass of the undeformed body, and the higher order terms are neglected, the coupling between the force and moment balances conveniently vanishes.

Due to the flexibility, other inertia integrals appear in (2.32) as well. In the mass matrix, the submatrix $\mathbf{M}_\Phi$, can be recognized. The coupling between the rigid body motion and elastic deformations is governed by the modal participation factors for the translation $\mathbf{P}_1$ and rotation $\mathbf{P}_2$:

$$\mathbf{M}_\Phi \equiv \int_V (\mathbf{\Phi}_i)^T \mathbf{\Phi}_i \, \rho_i \, dV$$

$$\mathbf{P}_1 \equiv \int_V \mathbf{\Phi}_i \, \rho_i \, dV \qquad\qquad (2.36)$$

$$\mathbf{P}_2 \equiv \int_V \tilde{\mathbf{r}}_i^{j,j} \mathbf{\Phi}_i \, \rho_i \, dV$$

For the purpose of this work, it is considered that these integrals are determined based on the body's linear finite element model. In that case $\mathbf{M}_\Phi$ really represents the finite element mass matrix, reduced to the basis spanned by the chosen deformation shapes $\mathbf{\Phi}$. As $\mathbf{P}_1$ and $\mathbf{P}_2$ represent the coupling between rigid and flexible behavior, they will be equal to zero when the deformation shapes are chosen such that they are orthogonal to the rigid body modes. This is the case when the deformation shapes are the body's mode shapes determined with all-free boundaries. As the rigid body modes are eigenvectors of the all-free boundary eigenvalue problem, their orthogonality with the flexible mode shapes follows directly from the orthogonality conditions posed on the eigenmodes. The fact that these mode shapes are able to diagonalise the local mass matrix explains their common use. However, many alternatives exist for choosing a set of deformation shapes, which may have other advantages. Among them are the Craig-Bampton modes, which will be used in this work and discussed in Chapter 3.

In the fictitious force matrix (2.33), two additional inertia integrals can be identified:

$$\mathbf{V}_1 \equiv \int_V \tilde{\mathbf{r}}_i^{j,j} \tilde{\boldsymbol{\omega}}_j^{j,O} \mathbf{\Phi}_i \, \rho_i \, dV$$

$$\mathbf{V}_2 \equiv \int_V (\mathbf{\Phi}_i)^T \tilde{\boldsymbol{\omega}}_j^{j,O} \mathbf{\Phi}_i \, \rho_i \, dV \qquad\qquad (2.37)$$

The presence of $\tilde{\boldsymbol{\omega}}_j^{j,O}$ in these integrals would require to recompute these integrals at every iteration step. Fortunately, the integrals can be rewritten such that $\tilde{\boldsymbol{\omega}}_j^{j,O}$ is taken outside the integral. To this end, the product $\tilde{\boldsymbol{\omega}}_j^{j,O}\boldsymbol{\Phi}_i$ is rewritten as follows:

$$\tilde{\boldsymbol{\omega}}_j^{j,O}\boldsymbol{\Phi}_i = -[\tilde{\boldsymbol{\Phi}}_i][\boldsymbol{\omega}_j^{j,O}] \tag{2.38}$$

In (2.38), $[\tilde{\boldsymbol{\Phi}}_i]$ is the $3 \times 3N$ matrix of skew symmetric mode shape matrices and $[\boldsymbol{\omega}_j^{j,O}]$ is the $3N \times N$ block diagonal matrix of $\boldsymbol{\omega}_j^{j,O}$:

$$[\tilde{\boldsymbol{\Phi}}_i] \equiv [\tilde{\boldsymbol{\phi}}_1(\mathbf{x}_i^{j,j}) \quad \dots \quad \tilde{\boldsymbol{\phi}}_N(\mathbf{x}_i^{j,j})], \qquad [\boldsymbol{\omega}_j^{j,O}] \equiv \begin{bmatrix} \boldsymbol{\omega}_j^{j,O} & & \\ & \ddots & \\ & & \boldsymbol{\omega}_j^{j,O} \end{bmatrix} \tag{2.39}$$

Using (2.38), the inertia integrals V_1 and V_2 in (2.37) can be rewritten as:

$$\mathbf{V}_1 = -\int_V \tilde{\mathbf{r}}_i^{j,j}[\tilde{\boldsymbol{\Phi}}_i]\,\rho_i dV \,[\boldsymbol{\omega}_j^{j,O}]$$

$$\mathbf{V}_2 = -\int_V (\boldsymbol{\Phi}_i)^T[\tilde{\boldsymbol{\Phi}}_i]\,\rho_i dV \,[\boldsymbol{\omega}_j^{j,O}] \tag{2.40}$$

Hence, the inertia integrals that actually need to be computed only consist of multiplications of entries $\mathbf{r}_i^{j,j}$ and $\boldsymbol{\Phi}_i$. These products are, however, different from the integrals encountered in the mass matrix. Moreover, it is not straightforward to relate the integrals to finite element modes. Only with additional approximations, such as using a lumped mass approximation, can the relation with finite element mass matrix be established [18].

Virtual work by elastic forces δW_{el}
The virtual work by elastic forces δW_{el} equals the variation in the strain energy. Because the strain energy is independent of rigid body motion, the result will only be in terms of the generalized coordinates corresponding

to the elastic modes $\boldsymbol{\eta}$ by means of a stiffness matrix $\mathbf{K}_\phi$. This stiffness matrix can be obtained directly from a linear finite element model by reducing it to the basis spanned by the chosen set of deformation shapes. The virtual work by elastic forces can be written as:

$$\delta W_{el} = (\delta\boldsymbol{\eta})^T \mathbf{K}_\phi \boldsymbol{\eta} \tag{2.41}$$

In terms of all generalized coordinates that are used in the floating frame equation, this can be written as:

$$\delta W_{el} = \begin{bmatrix} \delta\mathbf{r}_j^{0,0} \\ \delta\boldsymbol{\pi}_j^{0,0} \\ \delta\boldsymbol{\eta} \end{bmatrix}^T \mathbf{K}^j \begin{bmatrix} \mathbf{r}_j^{0,0} \\ \boldsymbol{\pi}_j^{0,0} \\ \boldsymbol{\eta} \end{bmatrix}, \qquad \mathbf{K}^j \equiv \begin{bmatrix} \mathbf{0} & \mathbf{0} & \vdots & \mathbf{0} \\ \mathbf{0} & \mathbf{0} & \vdots & \mathbf{0} \\ \mathbf{0} & \mathbf{0} & \vdots & \mathbf{K}_\phi \end{bmatrix} \tag{2.42}$$

Note that $\boldsymbol{\pi}_j^{0,0}$ is used here to denote the parameters that parameterize the rotation matrix. They can be interpreted as the summed or integrated contributions of all small increments $\Delta\boldsymbol{\pi}_j^{0,0}$. Its presence in (2.42) is merely a matter of notation, as computation of the elastic forces only requires multiplication of $\mathbf{K}_\phi$ with $\boldsymbol{\eta}$.

Virtual work by external forces δW_{ex}
The virtual work due to external forces can be expressed as:

$$\delta W_{ext} = \begin{bmatrix} \delta\mathbf{r}_j^{0,0} \\ \delta\boldsymbol{\pi}_j^{0,0} \\ \delta\boldsymbol{\eta} \end{bmatrix}^T \begin{bmatrix} \mathbf{F}_j^O \\ \mathbf{M}_j^O \\ \mathbf{Q}_\Phi \end{bmatrix} \tag{2.43}$$

where $\mathbf{F}_j^O$ is the vector of external forces expressed in the inertial frame E_O and $\mathbf{M}_j^O$ is the vector of external moments about the axes of the inertial frame E_O. $\mathbf{Q}_\Phi$ represents the generalized forces acting on the elastic deformation shapes. They are the projection of the externally applied forces on the shapes $\boldsymbol{\Phi}$.

For body forces, this requires the computation of the following integral:

$$\mathbf{Q}_{\Phi} = \int_V (\mathbf{\Phi}_i)^T \mathbf{f}_i^j \; \rho_i dV \tag{2.44}$$

Point forces can be included directly by multiplying them by the value of the deformation shapes at the point where they apply. Alternatively, point forces can be written in terms of a body force $\mathbf{f}_i^j$ with the appropriate use of the Dirac-delta function.

Equations of motion of a flexible body

Substitution of the expressions for the virtual work by inertia forces, elastic forces and external forces in the principle of virtual work (2.25), realizing that this principle must hold for arbitrary $\delta \mathbf{r}_j^{0,0}$, $\delta \mathbf{\pi}_j^{0,0}$, and $\delta \mathbf{\eta}$, yields the equations of motion of a single flexible body in the floating frame formulation. These can be written in the following form:

$$\boxed{\left[\mathbf{R}_j^O\right]\mathbf{M}^j\left[\mathbf{R}_O^j\right]\ddot{\mathbf{q}}^O + \left[\mathbf{R}_j^O\right]\mathbf{C}^j\left[\mathbf{R}_O^j\right]\dot{\mathbf{q}}^O + \mathbf{K}^j\mathbf{q}^O = \mathbf{Q}^O} \tag{2.45}$$

where it should be understood that the stiffness matrix does not need to be pre- and post-multiplied with rotation matrices, because it contains only nonzero terms related to the elastic coordinates $\mathbf{\eta}$, which are local. Also, it should be noted that constraint forces are still included in $\mathbf{Q}^O$. When formulating the equations of motion of the entire multibody system, these constraint forces will be expressed in terms of the Lagrange multipliers.

The notations $\mathbf{q}^O$, $\dot{\mathbf{q}}^O$, and $\ddot{\mathbf{q}}^O$ are introduced for the global generalized coordinates, velocities and accelerations respectively and $\mathbf{Q}^O$ for the global generalized forces:

$$\mathbf{q}^O = \begin{bmatrix} \mathbf{r}_j^{0,0} \\ \mathbf{\pi}_j^{0,0} \\ \mathbf{\eta} \end{bmatrix}, \qquad \dot{\mathbf{q}}^O = \begin{bmatrix} \dot{\mathbf{r}}_j^{0,0} \\ \mathbf{\omega}_j^{0,0} \\ \dot{\mathbf{\eta}} \end{bmatrix}, \qquad \ddot{\mathbf{q}}^O = \begin{bmatrix} \ddot{\mathbf{r}}_j^{0,0} \\ \dot{\mathbf{\omega}}_j^{0,0} \\ \ddot{\mathbf{\eta}} \end{bmatrix}, \qquad \mathbf{Q}^O = \begin{bmatrix} \mathbf{F}_j^O \\ \mathbf{M}_j^O \\ \mathbf{Q}_{\Phi} \end{bmatrix} \tag{2.46}$$

It is interesting to mention that in case of a rigid body, when the floating frame is located in the body's center of mass P_C and its orientation E_C is aligned with the body's principle axes, the force balance has a diagonal mass matrix and a zero velocity matrix. When the moment balance is expressed in the floating frame, the equations of motion indeed reduce to the Newton-Euler equations:

$$m\ddot{\mathbf{r}}_C^{O,O} = \mathbf{F}_C^O$$

$$\mathbf{I}^C \dot{\tilde{\boldsymbol{\omega}}}_C^{C,O} + \tilde{\boldsymbol{\omega}}_C^{C,O} \mathbf{I}^C \boldsymbol{\omega}_C^{C,O} = \mathbf{M}_C^O$$

(2.47)

For the dynamic analysis of a flexible multibody system, the equations of motion of each flexible body are of the form (2.45). Because the absolute interface coordinates are not part of the generalized coordinates $\mathbf{q}^O$, the kinematic constraints between bodies cannot be enforced directly. Instead, Lagrange multipliers are required to satisfy the constraints when formulating the multibody system's equations of motion. In the next Chapter, a coordinate transformation will be established with which the equations of motion (2.45) can be expressed in terms of the absolute interface coordinates. In this way, a body's linear finite element model can be used to create a superelement for each flexible body and the use of Lagrange multipliers is prevented.

3

Kinematics of a flexible body in absolute interface coordinates

In this chapter, a coordinate transformation is derived with which the floating frame coordinates and local interface coordinates are expressed in terms of the absolute interface coordinates. This is required so as to express a flexible body's equation of motion in terms of the absolute interface coordinates. For this purpose, Craig-Bampton modes are used for a local description of a flexible body's kinematics. After the relevant transformation matrices have been derived, additional geometric interpretation will be given to them, for more engineering understanding of the method.

This new method was published online in the journal paper "On the use of absolute interface coordinates in the floating frame of reference formulation for flexible multibody dynamics" in Multibody System Dynamics on 14-12-2017. The additional geometric interpretation of the various matrices involved in this method is based on the journal paper "Geometric interpretation of superelements in the floating frame of reference formulation" that was submitted for review on 31-07-2018.

3.1 Local kinematics of a flexible body using Craig-Bampton modes

In the floating frame formulation, many different choices can be made for the set of deformation shapes $\mathbf{\Phi}$ that describe the local elastic deformation of a body, as mentioned in the previous chapter. For the reduction of a body's linear finite element model, the Craig-Bampton method is one of the most commonly used techniques. This method makes a distinction between two types of deformation shapes: static interface modes and internal vibration modes. The static Craig-Bampton modes are a body's deformed shape when one of its interface coordinates is given a unit displacement, while keeping all other interface coordinates fixed. Using these modes only is in fact a static condensation, also known as the Irons-Guyan reduction. The internal Craig-Bampton modes are the natural vibration modes of the body when all interface coordinates are fixed. The use of Craig-Bampton modes for the model order reduction of linear finite element models can be found in standard textbooks such as [15].

The development of superelements requires a coordinate transformation towards absolute interface coordinates. Because the local interface coordinates are in fact the generalized coordinates corresponding to the static Craig-Bampton modes, it is natural to choose these as the deformation shapes. For this reason it is assumed in the remainder of this chapter that the static Craig-Bampton modes are indeed used for describing local elastic deformations. However, it is important to mention that taking into account the internal Craig-Bampton modes as well does not introduce any problems for the method whatsoever. This generalization is explained in more detail in Chapter 8, which also includes thoughts on how any arbitrary reduction basis might be used.

Consider a three-dimensional flexible body of which the position and orientation of the floating frame are denoted by the pair $\{P_j, E_j\}$. Let N be the number of interface points on the flexible body. Then the number of interface coordinates and thus the number of Craig-Bampton modes is $6N$. Let P_k identify the interface point with index k. The local interface coordinates corresponding to this point, which are also the generalized

coordinates of the Craig-Bampton modes related to this interface point, are denoted by the (6×1) vector $\mathbf{q}_k^{j,j}$. The generalized coordinates $\mathbf{q}_k^{j,j}$ are the small elastic local displacements $\mathbf{u}_k^{j,j}$ and rotations $\boldsymbol{\theta}_k^{j,j}$ of the interface points P_k on the body expressed in the body's floating frame E_j:

$$\mathbf{q}_k^{j,j} = \begin{bmatrix} \mathbf{u}_k^{j,j} \\ \boldsymbol{\theta}_k^{j,j} \end{bmatrix} \tag{3.1}$$

The local elastic deformation of an arbitrary point P_i on the body can be expressed in terms of the local interface coordinates as:

$$\mathbf{q}_i^{j,j} = \sum_{k=1}^{N} \boldsymbol{\Phi}_k\big(\mathbf{x}_i^{j,j}\big)\, \mathbf{q}_k^{j,j} \tag{3.2}$$

Here $\boldsymbol{\Phi}_k$ is the (6×6) matrix of Craig-Bampton modes of P_k. It describes the local elastic displacements and rotations of the material point P_i, which has position $\mathbf{x}_i^{j,j}$ on the undeformed body. Equation (3.2) can be written in compact matrix-vector form as:

$$\mathbf{q}_i^{j,j} = [\boldsymbol{\Phi}_i]\mathbf{q}^{j,j} \tag{3.3}$$

Note that whereas in (2.15) $\boldsymbol{\Phi}_i$ could still be any set of deformation shapes evaluated at P_i, in (3.3) $[\boldsymbol{\Phi}_i]$ denotes specifically the $(6 \times 6N)$ matrix of Craig-Bampton modes evaluated at P_i. The $(1 \times 6N)$ vector $\mathbf{q}^{j,j}$ is the set of all local interface coordinates:

$$[\boldsymbol{\Phi}_i] \equiv \begin{bmatrix} \boldsymbol{\Phi}_1\big(\mathbf{x}_i^{j,j}\big) & \dots & \boldsymbol{\Phi}_N\big(\mathbf{x}_i^{j,j}\big) \end{bmatrix}, \quad \mathbf{q}^{j,j} \equiv \begin{bmatrix} \mathbf{q}_1^{j,j} \\ \vdots \\ \mathbf{q}_N^{j,j} \end{bmatrix} \tag{3.4}$$

When using the Craig-Bampton modes in the floating frame formulation, the total number of degrees of freedom will be $6 + 6N$: there are 6 absolute floating frame coordinates and $6N$ local interface coordinates. Now, recall the fact that a formulation is desired in terms of the $6N$ absolute interface coordinates and that the rigid body motions should be eliminated from the

Craig-Bampton modes to avoid problems of non-uniqueness. Consequently, 6 constraints should be imposed on the local interface coordinates $\mathbf{q}^{j,j}$, corresponding to the Craig-Bampton modes. In general these constraints can be expressed as:

$$\mathcal{F}(\mathbf{q}^{j,j}) = \mathbf{0} \tag{3.5}$$

Due to the possible nonlinearities in the general form of (3.5), these constraints might not be solved analytically. However, by taking its variation, 6 linear equations are obtained in terms of the virtual displacements of the interface points $\delta\mathbf{q}^{j,j}$:

$$\delta\mathcal{F} = \nabla\mathcal{F} \cdot \delta\mathbf{q}^{j,j} = \mathbf{0} \tag{3.6}$$

If (3.6) is satisfied, the virtual displacements of the interface points do not allow for a rigid body motion. In most superelement formulations, among which the one presented in this work, this is realized by defining the floating frame such that there is zero elastic deformation at its location. By taking the variation of (3.3) and evaluating the Craig-Bampton modes at the location of the floating frame P_j, i.e. letting the arbitrary point P_i be floating frame P_j, a constraint is obtained of the form of (3.6):

$$\boxed{\delta\mathbf{q}_j^{j,j} = [\mathbf{\Phi}_{CB}]\delta\mathbf{q}^{j,j} = \mathbf{0}} \tag{3.7}$$

where $[\mathbf{\Phi}_{CB}]$ is used to denote the $(6 \times 6N)$ matrix of Craig-Bampton (CB) modes evaluated at the location of floating frame P_j. Each column of $[\mathbf{\Phi}_{CB}]$ contains the deformation of the floating frame when the body is deformed according to a certain Craig-Bampton mode. Figure 3.1 shows a graphical interpretation of $[\mathbf{\Phi}_{CB}]$ for a translational (a) and rotational (b) Craig-Bampton mode of an arbitrarily shaped flexible body.
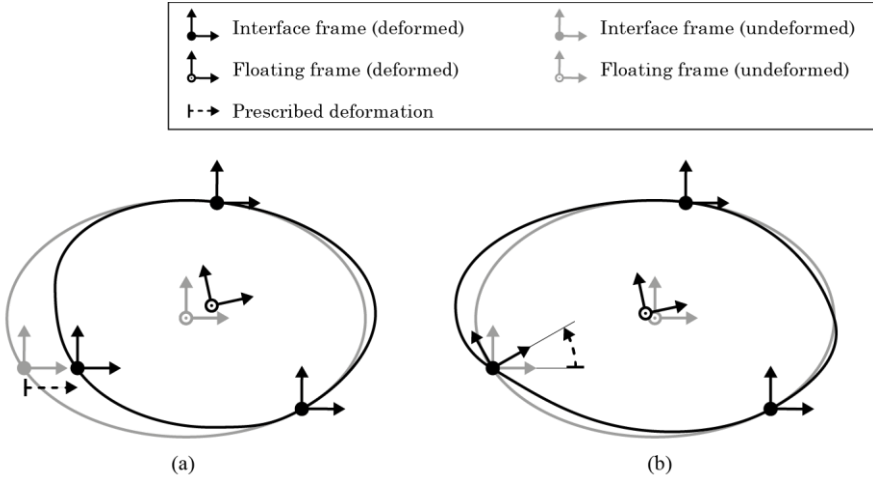
Fig. 3.1 Graphical interpretation of $[\mathbf{\Phi}_{CB}]$. This shows the displacement of the floating frame when the body is deformed according to a prescribed translational (a) or rotational (b) Craig-Bampton mode.

As mentioned in Chapter 1 and illustrated by Figures 1.4 to 1.6, there are multiple ways in which (3.7) can be satisfied. Most methods encountered in literature treat the floating frame as an interface point: either the floating frame is located at an actual interface point or an auxiliary interface point is created at the location of the floating frame. The method presented here does not require this. In the next section, it will be shown how the location of the floating frame follows from satisfying the constraint equation (3.7), without the need that P_j is an interface point.

3.2 Kinematics of a flexible body in terms of absolute interface coordinates

In Chapter 2, kinematic relations were derived for the virtual displacement of an arbitrary point on a flexible body with respect to the inertial frame. In (2.17), let the arbitrary point P_i be interface point P_k, such that for its virtual position holds:

$$\delta \mathbf{r}_k^{0,0} = \delta \mathbf{r}_j^{0,0} + \delta \widetilde{\boldsymbol{\pi}}_j^{0,0} \mathbf{R}_j^O \mathbf{r}_k^{j,j} + \mathbf{R}_j^O \delta \mathbf{r}_k^{j,j} \tag{3.8}$$

Because the Craig-Bampton modes involve both translational and rotational degrees of freedom, an expression is also required for the virtual rotation at P_k:

$$\delta \boldsymbol{\pi}_k^{0,0} = \delta \boldsymbol{\pi}_j^{0,0} + \mathbf{R}_j^O \delta \boldsymbol{\pi}_k^{j,j} \tag{3.9}$$

Using the identities $\widetilde{\mathbf{a}}^j \mathbf{R}_i^j = \mathbf{R}_i^j \widetilde{\mathbf{a}}^i$ and $\widetilde{\mathbf{a}} \mathbf{b} = -\widetilde{\mathbf{b}} \mathbf{a}$, as introduced in Chapter 2, the second term on the right hand side of (3.8) can be rewritten such that it can be combined with (3.9) to:

$$\begin{bmatrix} \delta \mathbf{r}_k^{0,0} \\ \delta \boldsymbol{\pi}_k^{0,0} \end{bmatrix} = \begin{bmatrix} \mathbf{R}_j^O & \mathbf{0} \\ \mathbf{0} & \mathbf{R}_j^O \end{bmatrix} \begin{bmatrix} \delta \mathbf{r}_k^{j,j} \\ \delta \boldsymbol{\pi}_k^{j,j} \end{bmatrix} + \begin{bmatrix} \mathbf{R}_j^O & \mathbf{0} \\ \mathbf{0} & \mathbf{R}_j^O \end{bmatrix} \begin{bmatrix} \mathbf{1} & -\widetilde{\mathbf{r}}_k^{j,j} \\ \mathbf{0} & \mathbf{1} \end{bmatrix} \begin{bmatrix} \mathbf{R}_O^j & \mathbf{0} \\ \mathbf{0} & \mathbf{R}_O^j \end{bmatrix} \begin{bmatrix} \delta \mathbf{r}_j^{0,0} \\ \delta \boldsymbol{\pi}_j^{0,0} \end{bmatrix} \tag{3.10}$$

In compact form this can be written as:

$$\delta \mathbf{q}_k^{0,0} = [\mathbf{R}_j^O] \delta \mathbf{q}_k^{j,j} + [\mathbf{R}_j^O][-\widetilde{\mathbf{r}}_k^{j,j}][\mathbf{R}_O^j] \delta \mathbf{q}_j^{0,0} \tag{3.11}$$

in which

$$[\mathbf{R}_j^O] \equiv \begin{bmatrix} \mathbf{R}_j^O & \mathbf{0} \\ \mathbf{0} & \mathbf{R}_j^O \end{bmatrix}, \qquad [-\widetilde{\mathbf{r}}_k^{j,j}] \equiv \begin{bmatrix} \mathbf{1} & -\widetilde{\mathbf{r}}_k^{j,j} \\ \mathbf{0} & \mathbf{1} \end{bmatrix} \tag{3.12}$$

From (3.11), it can be understood that the columns of the (6×6) matrix $\left[-\tilde{\mathbf{r}}_k^{j,j}\right]$ contain the displacements and rotations of interface point P_k when the deformed body is subjected to infinitesimal rigid body motions: the first three columns represent the displacements and rotations due to rigid body translations and the last three columns represent the displacements and rotations due to rigid body rotations about the origin of the floating frame P_j. These are both expressed with respect to the floating frame. Equation (3.11) can be established for all interface points:

$$\delta\mathbf{q}^{O,O} = \left[\overline{\mathbf{R}}_j^O\right]\delta\mathbf{q}^{j,j} + \left[\overline{\mathbf{R}}_j^O\right]\left[\mathbf{\Phi}_{rig}\right]\left[\mathbf{R}_O^j\right]\delta\mathbf{q}_j^{O,O} \qquad (3.13)$$

in which $\delta\mathbf{q}^{O,O}$ and $\delta\mathbf{q}^{j,j}$ are the $(6N \times 1)$ vectors containing all variations of the absolute and local interface coordinates respectively, $\left[\overline{\mathbf{R}}_j^O\right]$ is the $(6N \times 6N)$ block diagonal rotation matrix and $\left[\mathbf{\Phi}_{rig}\right]$ is the column-wise assembly of all matrices $\left[-\tilde{\mathbf{r}}_k^{j,j}\right]$:

$$\left[\overline{\mathbf{R}}_O^j\right] \equiv \begin{bmatrix} \left[\mathbf{R}_O^j\right] & & \\ & \ddots & \\ & & \left[\mathbf{R}_O^j\right] \end{bmatrix}, \qquad \left[\mathbf{\Phi}_{rig}\right] \equiv \begin{bmatrix} \left[-\tilde{\mathbf{r}}_1^{j,j}\right] \\ \vdots \\ \left[-\tilde{\mathbf{r}}_N^{j,j}\right] \end{bmatrix} \qquad (3.14)$$

Each column of $\left[\mathbf{\Phi}_{rig}\right]$ contains the displacement and rotation of all interface coordinates when the body is subjected to a rigid body motion in a certain direction with respect to the floating frame. Figure 3.2 shows a graphical interpretation of $\left[\mathbf{\Phi}_{rig}\right]$ for a translational (a) and rotational (b) rigid body motion of an arbitrarily shaped flexible body.
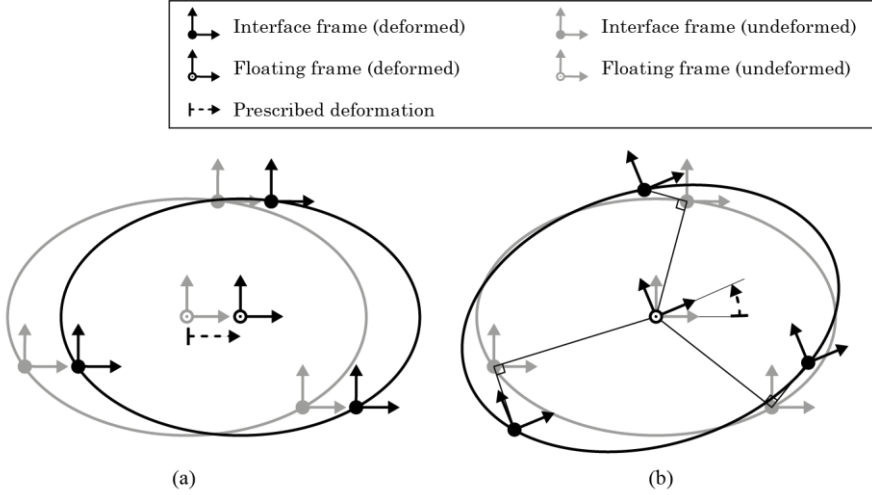
Fig. 3.2 Graphical interpretation of $[\mathbf{\Phi}_{rig}]$. This shows is the displacement of all interface points when the floating frame is subjected to a prescribed translational (a) or rotational (b) rigid body mode.

Using the property (2.2) that $\mathbf{R}_O^j \mathbf{R}_j^O = \mathbf{1}$, equation (3.13) can be rewritten such that the virtual change in the local interface coordinates is expressed as the difference between the absolute interface coordinates and the absolute floating frame coordinates:

$$\delta\mathbf{q}^{j,j} = \left[\overline{\mathbf{R}}_O^j\right]\delta\mathbf{q}^{O,O} - \left[\mathbf{\Phi}_{rig}\right]\left[\mathbf{R}_O^j\right]\delta\mathbf{q}_j^{O,O} \tag{3.15}$$

At this point, (3.15) can be substituted in the constraint equation (3.7), eliminating the rigid body motions. This results in 6 equations from which the variation of the absolute floating frame coordinates can be expressed in terms of the variation of the absolute interface coordinates:

$$\delta\mathbf{q}_j^{O,O} = \left[\mathbf{R}_j^O\right]\left(\left[\mathbf{\Phi}_{CB}\right]\left[\mathbf{\Phi}_{rig}\right]\right)^{-1}\left[\mathbf{\Phi}_{CB}\right]\left[\overline{\mathbf{R}}_O^j\right]\delta\mathbf{q}^{O,O} \tag{3.16}$$

In compact form, this can be written as:

$$\boxed{\delta\mathbf{q}_j^{O,O} = \left[\mathbf{R}_j^O\right][\mathbf{Z}]\left[\overline{\mathbf{R}}_O^j\right]\delta\mathbf{q}^{O,O}, \qquad [\mathbf{Z}] \equiv \left(\left[\mathbf{\Phi}_{CB}\right]\left[\mathbf{\Phi}_{rig}\right]\right)^{-1}\left[\mathbf{\Phi}_{CB}\right]} \tag{3.17}$$

In Section 3.3, it will be explained that the (6×6) matrix product $[\mathbf{\Phi}_{CB}][\mathbf{\Phi}_{rig}]$ equals the identity matrix $\mathbf{1}$ on leading order. If the elastic deformations remain small, the inverse of this matrix, as it appears in definition of $[\mathbf{Z}]$, can always be computed. By back substitution of (3.17) in (3.15) it is also possible to express the variations in the local interface coordinates in terms of the variations in the global interface coordinates. In short form, this can be written as:

$$\delta\mathbf{q}^{j,j} = [\mathbf{T}][\bar{\mathbf{R}}_O^j]\delta\mathbf{q}^{O,O}, \qquad [\mathbf{T}] \equiv \mathbf{1} - [\mathbf{\Phi}_{rig}][\mathbf{Z}] \qquad (3.18)$$

The combination of (3.17) and (3.18) can be used to express the degrees of freedom used in the standard floating frame formulation in terms of the absolute interface coordinates. This can be applied on the equations of motion of each flexible body within the multibody system. The equations of motion of the entire flexible multibody system can then be formulated without Lagrange multipliers. In compact form, these coordinate transformations can be written as:

$$\begin{bmatrix} \delta\mathbf{q}_j^{O,O} \\ \delta\mathbf{q}^{j,j} \end{bmatrix} = \mathbf{A}\delta\mathbf{q}^{O,O}, \qquad \mathbf{A} \equiv \begin{bmatrix} [\mathbf{R}_j^O][\mathbf{Z}][\bar{\mathbf{R}}_O^j] \\ [\mathbf{T}][\bar{\mathbf{R}}_O^j] \end{bmatrix} \qquad (3.19)$$

3.3 Geometric interpretation of the matrices $[\mathbf{\Phi}_{rig}]$, $[\mathbf{Z}]$ and $[\mathbf{T}]$

Geometric interpretation of $[\mathbf{\Phi}_{rig}]$

Because $[\mathbf{\Phi}_{rig}]$ is based on matrices $[-\tilde{\mathbf{r}}_k^{j,j}]$, it contains the rigid body modes of a deformed body. This means that a flexible body is considered in a deformed configuration and in this configuration the floating frame is subjected to rigid body motions. Because the local deformations are considered small, it could be argued that the effect of the body's deformation on $[\mathbf{\Phi}_{rig}]$ might be neglected. After all, the contribution of the displacement field is of higher order than that of the constant terms in $[\mathbf{\Phi}_{rig}]$.

To study the effect of this simplification, $[\mathbf{\Phi}_{rig,0}]$ is introduced as the matrix of rigid body modes, based on the undeformed body, which is defined as:

$$[\mathbf{\Phi}_{rig,0}] \equiv \begin{bmatrix} [-\tilde{\mathbf{x}}_1^{j,j}] \\ \vdots \\ [-\tilde{\mathbf{x}}_N^{j,j}] \end{bmatrix} \tag{3.20}$$

$[\mathbf{\Phi}_{rig,0}]$ plays an interesting role in the reuse of a body's linear finite element model during the development of the equations of motion in the floating frame formulation. To explain this, consider that a body's linear finite element matrices are reduced using the Craig-Bampton modes. The reduced local mass matrix is denoted by $\mathbf{M}_{CB}^j$ and is constant, where the superscript j denotes that this mass matrix is expressed locally, relative to the floating frame. Because the Craig-Bampton modes are able to describe rigid body motions, the rigid body mass matrix $\mathbf{M}_{rig}^j$ can be obtained from $\mathbf{M}_{CB}^j$ by projecting it onto the rigid body modes $[\mathbf{\Phi}_{rig,0}]$:

$$\mathbf{M}_{rig}^j = [\mathbf{\Phi}_{rig,0}]^T \mathbf{M}_{CB}^j [\mathbf{\Phi}_{rig,0}] \tag{3.21}$$

When the floating frame is located in the center of mass of the undeformed body and its axes are aligned with the body's principal axes, $\mathbf{M}_{rig}^{j}$ is a diagonal matrix with the mass and second moments of mass on its main diagonal. This can be understood since $\mathbf{M}_{CB}^{j}\left[\mathbf{\Phi}_{rig,0}\right]$ are the generalized inertia forces acting on the interface points due to rigid body motions. Pre-multiplication by $\left[\mathbf{\Phi}_{rig,0}\right]^{T}$ in fact sums all inertia forces due to rigid body motions, which yields the resulting inertia forces in the local frame. Hence, for translations this must result in the total mass of the body and for rotations in the second moment of mass about the principal axes of rotation. At this point, recall the partitioned form of the local mass matrix (2.32). When the higher order terms in the mass matrix are neglected, it is found that the partition corresponding to the rigid body motion exactly equals $\mathbf{M}_{rig}^{j}$.

When one wants to take into account the higher order terms in the mass matrix $\mathbf{M}^{j}$ of a body in its deformed configuration, the partition corresponding to the rigid body motion can be approximated by projecting $\mathbf{M}_{CB}^{j}$ onto $\left[\mathbf{\Phi}_{rig}\right]$ instead of $\left[\mathbf{\Phi}_{rig,0}\right]$. Hence, when all Craig-Bampton modes are retained to describe the body's flexible behavior, the local mass matrix $\mathbf{M}^{j}$ as defined in (2.32) can be expressed as:

$$\mathbf{M}^{j} \approx \begin{bmatrix} \mathbf{\Phi}_{rig}^{T} \\ \mathbf{1} \end{bmatrix} \mathbf{M}_{CB}^{j} [\mathbf{\Phi}_{rig} \quad \mathbf{1}] \tag{3.22}$$

Hence, using $\left[\mathbf{\Phi}_{rig}\right]$ it is possible to construct the mass matrix in the floating frame formulation directly from a body's finite element model. For the local stiffness matrix in $\mathbf{K}_{\phi}$ in (2.42) holds that it can be replaced by the finite element stiffness matrix that is reduced using Craig-Bampton modes $\mathbf{K}_{CB}^{j}$. Unfortunately, for the velocity dependent matrix of fictitious forces $\mathbf{C}^{j}$ this cannot be done without additional assumptions [18].

Geometric interpretation of [Z]

The $(6 \times 6N)$ transformation matrix $[\mathbf{Z}]$ defines the relation between the absolute motion of the interface coordinates and the absolute motion of the floating frame. In this definition, the matrix product $[\mathbf{\Phi}_{CB}][\mathbf{\Phi}_{rig}]$ appears. This product can be given a very interesting geometrical interpretation for which first the product $[\mathbf{\Phi}_{CB}][\mathbf{\Phi}_{rig,0}]$ is considered [20]. To this end, recall that $[\mathbf{\Phi}_{rig,0}]$ describes the displacement of the interface points when the undeformed body is subjected to a rigid body mode and that $[\mathbf{\Phi}_{CB}]$ describes the displacement of the floating frame when the interface points are displaced. Hence, the matrix $[\mathbf{\Phi}_{CB}][\mathbf{\Phi}_{rig,0}]$ describes the displacement of the floating frame, when the interface points are given a displacement according to a rigid body motion of the floating frame. This is simply a (6×6) identity matrix. Figure 3.3 shows a graphical interpretation of this identity for a translational (a) and rotational (b) rigid body motion of an arbitrarily shaped flexible body.
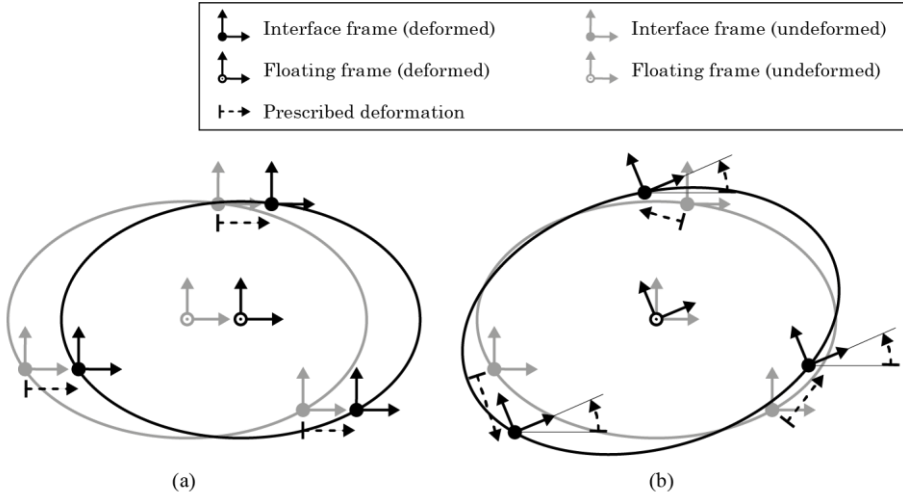

Fig. 3.3 Graphical interpretation of $[\mathbf{\Phi}_{CB}][\mathbf{\Phi}_{rig,0}]$. Shown is the displacement of the floating frame when the interface points are subjected to a prescribed translational (a) or rotational (b) rigid body mode.

The product $[\mathbf{\Phi}_{CB}][\mathbf{\Phi}_{rig}]$ can be interpreted similarly, but for the fact the rigid body modes are determined based on the body's deformed configuration. This means that one imagines the body in a deformed

configuration, determines the actual rigid body modes and then uses the Craig-Bampton modes to determine the displacement of the floating frame when the interface points of the undeformed body are subjected to the deformed body's rigid body modes. Because it might be reasonable to assume only little difference between the rigid body modes of the deformed and undeformed body, as explained in the previous chapter, $[\mathbf{\Phi}_{CB}][\mathbf{\Phi}_{rig}]$ will be close to the identity matrix.

By approximating $[\mathbf{\Phi}_{rig}]$ by $[\mathbf{\Phi}_{rig,0}]$ in (3.17), $[\mathbf{Z}]$ can be approximated by $[\mathbf{\Phi}_{CB}]$ itself:

$$\boxed{[\mathbf{Z}] \approx [\mathbf{\Phi}_{CB}]} \qquad (3.23)$$

Consequently, the relation between the absolute motion of the interface coordinates and the absolute motion of the floating frame could be simplified by:

$$\delta\mathbf{q}_j^{O,O} \approx [\mathbf{R}_j^O][\mathbf{\Phi}_{CB}][\bar{\mathbf{R}}_O^j]\delta\mathbf{q}^{O,O} \qquad (3.24)$$

In this way, it can be understood that $[\mathbf{Z}]$ as defined as in (3.17) can be interpreted in as the Craig-Bampton modes of a flexible body in its deformed configuration. Since $[\mathbf{\Phi}_{CB}]$ is constant, the relation between $\delta\mathbf{q}_j^{O,O}$ and $\delta\mathbf{q}^{O,O}$ depends only on the orientation of the floating frame. Because determination of $\delta\mathbf{q}_j^{O,O}$ using (3.24) instead of (3.17) is more computationally efficient, it is interesting to investigate the validity of this approximation. In Chapter 5, simulation results of benchmark problems show that when the approximation (3.23) is applied, accurate results are still obtained.

Geometric interpretation of $[\mathbf{T}]$

The $(6N \times 6N)$ transformation matrix $[\mathbf{T}]$ defines the relation between the absolute and local motion of the interface coordinates. In its definition, the matrix product $[\mathbf{\Phi}_{rig}][\mathbf{Z}]$ appears. Also this product can be given a geometrical interpretation for which it is useful to consider that the approximation (3.24) is allowed. Under the same assumptions, $[\mathbf{\Phi}_{rig}][\mathbf{Z}]$

could be approximated as $[\mathbf{\Phi}_{rig,0}][\mathbf{\Phi}_{CB}]$. For the interpretation of this matrix, imagine that the floating frame is displaced according to a Craig-Bampton mode in $[\mathbf{\Phi}_{CB}]$. Pre-multiplication of this base motion by $[\mathbf{\Phi}_{rig,0}]$ yields the displacement of the interface points required to cause this floating frame configuration, assuming the body is rigid. Figure 3.4 shows a graphical interpretation of this for a translational Craig-Bampton mode of an arbitrarily shaped flexible body.
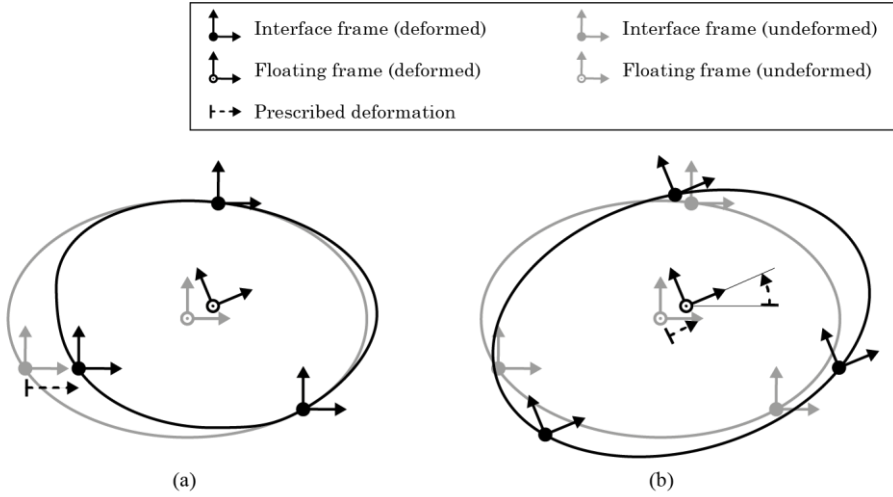

Fig. 3.4   Graphical interpretation of $[\mathbf{\Phi}_{rig,0}][\mathbf{\Phi}_{CB}]$. Shown is the displacement of the floating frame when the body is deformed according to a prescribed Craig-Bampton mode (a). $[\mathbf{\Phi}_{rig,0}][\mathbf{\Phi}_{CB}]$ represents the displacements that the interface points need to make in a rigid body motion, such that the deformation of floating frame is the same (b).

With this approximation, the matrix $[\mathbf{T}]$ can be written as:

$$[\mathbf{T}] \approx \mathbf{1} - [\mathbf{\Phi}_{rig,0}][\mathbf{\Phi}_{CB}]$$

(3.25)

Consequently, the relation between the absolute and local motion of the interface coordinates could be simplified by:

$$\delta\mathbf{q}^{j,j} \approx \left(\mathbf{1} - [\mathbf{\Phi}_{rig,0}][\mathbf{\Phi}_{CB}]\right)[\bar{\mathbf{R}}_O^j]\delta\mathbf{q}^{O,O}$$

(3.26)

Now, consider any variation in the absolute interface coordinates. Using the matrix $[\mathbf{Z}]$ and (3.17), it is possible to determine the corresponding variation in the absolute floating frame coordinates. Because $\left[\mathbf{\Phi}_{rig,0}\right][\mathbf{\Phi}_{CB}]$ determines the local displacement of the interface coordinates when the body would have been rigid, $\mathbf{1} - \left[\mathbf{\Phi}_{rig,0}\right][\mathbf{\Phi}_{CB}]$ must describe the difference from this due to the body's elastic deformation. Hence, the matrix $[\mathbf{T}]$ can be interpreted as the transformation from absolute to local variations of the interface coordinates, while it simultaneously removes the contribution of rigid body motion. When the above approximations of neglecting small deformations are not applied, $[\mathbf{T}]$ can still be interpreted in the same way, except for the fact that the matrix is based on the body's deformed configuration.

The fact that $[\mathbf{T}]$ can be interpreted as a coordinate transformation which removes the rigid body motions led to the idea that another multiplication by $[\mathbf{T}]$ has no influence. After all, the rigid body motions are already removed. Based on this, it can be understood that $[\mathbf{T}]$ is idempotent. It can be shown mathematically that this is the case. By direct computation, it can be shown that $\left[\mathbf{\Phi}_{rig}\right][\mathbf{Z}]$ is idempotent:

$$
\begin{aligned}
&\left[\mathbf{\Phi}_{rig}\right][\mathbf{Z}]\left[\mathbf{\Phi}_{rig}\right][\mathbf{Z}] \\
&= \left[\mathbf{\Phi}_{rig}\right]\left([\mathbf{\Phi}_{CB}]\left[\mathbf{\Phi}_{rig}\right]\right)^{-1}[\mathbf{\Phi}_{CB}]\left[\mathbf{\Phi}_{rig}\right]\left([\mathbf{\Phi}_{CB}]\left[\mathbf{\Phi}_{rig}\right]\right)^{-1}[\mathbf{\Phi}_{CB}] \quad (3.27) \\
&= \left[\mathbf{\Phi}_{rig}\right][\mathbf{Z}]
\end{aligned}
$$

Now consider the property that when an idempotent matrix is subtracted from the identity matrix, the result is another idempotent matrix. Because $[\mathbf{T}] = \mathbf{1} - \left[\mathbf{\Phi}_{rig}\right][\mathbf{Z}]$ and $\left[\mathbf{\Phi}_{rig}\right][\mathbf{Z}]$ is idempotent, it follows that $[\mathbf{T}]$ is indeed idempotent.

Except for the identity matrix, any idempotent matrix is singular, is diagonalizable and has eigenvalues that are either 0 or 1. In the case of $[\mathbf{T}]$, there will be six eigenvalues 0, corresponding to the rigid body modes and $6N - 6$ eigenvalues 1, corresponding to the elastic deformations.

Consider the eigendecomposition of $[\mathbf{T}]$:

$$[\mathbf{T}] = \mathbf{U}^{-1}\mathbf{\Lambda}\mathbf{U} \qquad (3.28)$$

where $\mathbf{U}$ is the columnwise assembly of eigenvectors of $[\mathbf{T}]$ and $\mathbf{\Lambda}$ is the diagonal matrix of eigenvalues (0s and 1s).

The fact that $[\mathbf{T}]$ removes the rigid body motion from a set of coordinates can now be understood mathematically: due to the multiplication by $\mathbf{U}$, the coordinates are projected in the subspace of the rigid body modes. The zeros in $\mathbf{\Lambda}$ eliminate this contribution and $\mathbf{U}^{-1}$ applies the inverse map. Hence, only contributions that are not part of any rigid body motion are retained by the transformation.

In the next chapter, the coordinate transformations (3.17) and (3.18) are applied on the equations of motion in the floating frame formulation (2.45). In this way a flexible body's equation of motion is expressed in terms of the absolute interface coordinates.

4

Kinetics of a flexible body in absolute interface coordinates

In this chapter, the coordinate transformations from the absolute floating frame coordinates and local interface coordinates towards absolute interface coordinates are used to establish the equations of motion of a superelement in absolute interface coordinates. For the purpose of static analysis, the tangent stiffness matrix is derived by taking the variation of the equilibrium equations.

This chapter presents the equations of motion of the new superelement method that was published online in the journal paper "On the use of absolute interface coordinates in the floating frame of reference formulation flexible multibody dynamics" in Multibody System Dynamics on 14-12-2017. The derivation of the tangent stiffness matrix is based on the journal paper "The tangent stiffness matrix for an absolute interface coordinates floating frame of reference formulation" that was submitted to Multibody System Dynamics on 05-03-2018.

4.1 Equations of motion in absolute interface coordinates

In order to derive the equations of motion of a flexible body in terms of its absolute interface coordinates, the principle of virtual work can be used as a starting point. When expressions for the virtual position, velocity and acceleration of an arbitrary point on a flexible body in terms of the absolute interface coordinates are known, a similar approach as discussed in Chapter 2 will result in the relevant equations of motion. However, since the equations of motion in the floating frame formulation (2.45) are well-established, these can be used as a starting point too:

$$\left[\mathbf{R}_j^O\right]\mathbf{M}^j\left[\mathbf{R}_O^j\right]\ddot{\mathbf{q}}^O + \left[\mathbf{R}_j^O\right]\mathbf{C}^j\left[\mathbf{R}_O^j\right]\dot{\mathbf{q}}^O + \mathbf{K}^j\mathbf{q}^O = \mathbf{Q}^O \tag{4.1}$$

Or expressed in terms of global matrices:

$$\mathbf{M}^O\ddot{\mathbf{q}}^O + \mathbf{C}^O\dot{\mathbf{q}}^O + \mathbf{K}^j\mathbf{q}^O = \mathbf{Q}^O \tag{4.2}$$

Recall that in this floating frame formulation, the generalized coordinates $\mathbf{q}^O$ consist of the absolute floating frame coordinates, which describe the rigid body motion and the local interface coordinates corresponding to the Craig-Bampton modes, which describe local elastic deformations. In Chapter 3, the kinematic transformation matrices (3.17) and (3.18) were derived that express a virtual change in these coordinates in terms of a virtual change in the absolute interface coordinates. In combined form these coordinate transformations were written as (3.19):

$$\begin{bmatrix}\delta\mathbf{q}_j^{O,O}\\\delta\mathbf{q}^{j,j}\end{bmatrix} = \begin{bmatrix}[\mathbf{R}_j^O][\mathbf{Z}][\bar{\mathbf{R}}_O^j]\\[\mathbf{T}][\bar{\mathbf{R}}_O^j]\end{bmatrix}\delta\mathbf{q}^{O,O} = \mathbf{A}\delta\mathbf{q}^{O,O} \tag{4.3}$$

Following the same procedure, it can be shown that the transformation matrix $\mathbf{A}$ can be used on the level of velocities, and upon differentiation with respect to time a transformation is obtained for the accelerations:

$$\begin{bmatrix}\dot{\mathbf{q}}_j^{O,O}\\\dot{\mathbf{q}}^{j,j}\end{bmatrix} = \mathbf{A}\dot{\mathbf{q}}^{O,O}, \qquad \begin{bmatrix}\ddot{\mathbf{q}}_j^{O,O}\\\ddot{\mathbf{q}}^{j,j}\end{bmatrix} = \mathbf{A}\ddot{\mathbf{q}}^{O,O} + \dot{\mathbf{A}}\dot{\mathbf{q}}^{O,O} \tag{4.4}$$

This coordinate transformation is now substituted in the equations of motion (4.1), which yields:

$$\mathbf{A}^T \mathbf{M}^O \mathbf{A} \ddot{\mathbf{q}}^O + \mathbf{A}^T \left(\mathbf{M}^O \dot{\mathbf{A}} + \mathbf{C}^O \mathbf{A} \right) \dot{\mathbf{q}}^O + \mathbf{A}^T \mathbf{K}^j \mathbf{q}^O = \mathbf{A}^T \mathbf{Q}^O \qquad (4.5)$$

This can be rewritten to the following form:

$$\left[\bar{\mathbf{R}}_j^O \right] \hat{\mathbf{M}}^j \left[\bar{\mathbf{R}}_O^j \right] \mathbf{A} \ddot{\mathbf{q}}^{O,O} + \left[\bar{\mathbf{R}}_j^O \right] \hat{\mathbf{C}}^j \left[\bar{\mathbf{R}}_O^j \right] \dot{\mathbf{q}}^{O,O} + \left[\bar{\mathbf{R}}_j^O \right] \hat{\mathbf{K}}^j \mathbf{q}^O = \mathbf{Q}^{O,O} \qquad (4.6)$$

In this, $\hat{\mathbf{M}}^j$, $\hat{\mathbf{C}}^j$ and $\hat{\mathbf{K}}^j$ are the transformed local system matrices and $\mathbf{Q}^{O,O}$ contains the generalized external forces acting on the interface points, expressed in the global frame. Let the exact expression of the local mass matrix $\mathbf{M}^j$ (2.32) be approximated up to second order by (3.22), which conveniently reuses the reduced finite element mass matrix $\mathbf{M}_{CB}^j$. With this, the transformed global mass matrix can be expressed as:

$$\mathbf{A}^T \mathbf{M}^O \mathbf{A} = \left[\bar{\mathbf{R}}_j^O \right] \left[[\mathbf{Z}]^T \quad [\mathbf{T}]^T \right] \begin{bmatrix} \mathbf{\Phi}_{rig}^T \\ \mathbf{1} \end{bmatrix} \mathbf{M}_{CB}^j \left[\mathbf{\Phi}_{rig} \quad \mathbf{1} \right] \begin{bmatrix} [\mathbf{Z}] \\ [\mathbf{T}] \end{bmatrix} \left[\bar{\mathbf{R}}_O^j \right] \qquad (4.7)$$

By direct substitution of the definitions for $[\mathbf{Z}]$ (3.17) and $[\mathbf{T}]$ (3.18), it follows that:

$$\left[\mathbf{\Phi}_{rig} \quad \mathbf{1} \right] \begin{bmatrix} [\mathbf{Z}] \\ [\mathbf{T}] \end{bmatrix} = \mathbf{1} \qquad (4.8)$$

With this, the transformed mass matrix becomes simply:

$$\mathbf{A}^T \mathbf{M}^O \mathbf{A} = \left[\bar{\mathbf{R}}_j^O \right] \mathbf{M}_{CB}^j \left[\bar{\mathbf{R}}_O^j \right] \qquad (4.9)$$

Note that (4.9) is exact when the approximation (3.22) is used. In other words, it is not only exact for the zeroth order terms, but also for the approximation of the higher order terms in the deformation. The local stiffness matrix $\mathbf{K}^j$ in the floating frame formulation only contains nonzero terms in the partition related to the elastic coordinates. This partition simply equals $\mathbf{K}_{CB}^j$.

For this reason, the transformed stiffness matrix can be expressed as:

$$\mathbf{A}^T \mathbf{K}^j = \left[\bar{\mathbf{R}}_j^O\right][\mathbf{T}]^T \mathbf{K}_{CB}^j \tag{4.10}$$

With (4.9) and (4.10), the transformed equation of motion reduce to:

$$\boxed{\left[\bar{\mathbf{R}}_j^O\right]\mathbf{M}_{CB}^j\left[\bar{\mathbf{R}}_O^j\right]\mathbf{A}\ddot{\mathbf{q}}^{O,O} + \left[\bar{\mathbf{R}}_j^O\right]\hat{\mathbf{C}}^j\left[\bar{\mathbf{R}}_O^j\right]\dot{\mathbf{q}}^{O,O} + \left[\bar{\mathbf{R}}_j^O\right][\mathbf{T}]^T\mathbf{K}_{CB}^j\mathbf{q} = \mathbf{Q}^{O,O}} \tag{4.11}$$

It is worth mentioning that the transformed mass matrix in (4.11) that holds for a flexible body is of a similar form as one obtains in the corotational formulation for a finite element. In the corotational frame formulation, the global mass matrix of an individual element is obtained by pre- and post-multiplying each local finite element mass matrix by the rotation matrices corresponding to the element's corotational frame.

Moreover, the fictitious forces that are quadratic in the velocities are typically not included in standard corotational frame formulations. Because in (4.11) the absolute interface coordinates are the degrees of freedom, the interface forces due to fictitious forces are in fact only the forces that arise due to the relative acceleration of the internal elastic deformation relative to the interface points. As elastic deformations are assumed small, these forces can in general be expected to be small as well. The benchmark problems simulated for validation in Chapter 5 did not include these fictitious forces and still show accurate results. Therefore, the exact form of the transformed matrix $\hat{\mathbf{C}}^j$ will not be elaborated on further.

In the elastic term in the transformed equation of motion (4.11), the Craig-Bampton stiffness matrix is multiplied by the local interface coordinates, resulting in the local elastic force vector. The pre-multiplication by $[\mathbf{T}]^T$ can be interpreted as an operation that eliminates the rigid body component, as discussed in Chapter 3. For an undeformed body, this does not influence the elastic forces, such that when $[\mathbf{T}]$ is approximated using (3.25), the result of the elastic term is just $\left[\bar{\mathbf{R}}_j^O\right]\mathbf{K}_{CB}^j\mathbf{q}$. In this, the local

elastic forces are simply rotated to the global frame. This is also how the elastic forces are described in the corotational frame formulation.

Hence, the standard corotational frame formulation uses a number of simplifications to establish the equation of motion of a corotational finite element. These simplifications are rarely emphasized in literature dedicated specifically to the corotational frame formulation. However, from precise formulation presented in this work it can be understood that the standard corotational frame formulation:
- ignores higher order terms in the mass matrix of an element;
- ignores fictitious forces caused by the elastic deformation within an element;
- ignores elastic deformations when computing the elastic forces within an element.

4.2   Solving the equation of motion

Equation of motion (4.11) can be interpreted as the equation of motion of a superelement, suitable for flexible multibody dynamics simulations. The mass and stiffness matrix of the superelement can be conveniently obtained from a body's linear finite element model, by applying Craig-Bampton reduction. In most practical situations, simulation accuracy is sufficient when the fictitious forces are either approximated using terms from $\mathbf{M}_{CB}^j$, or even neglected, as discussed above.

The fact that it is not possible to establish a coordinate transformation on the position level is the reason that the elastic forces in (4.11) are still expressed in terms of the local instead of the absolute interface coordinates. For this reason, some remarks about the procedure with which the equation of motion (4.11) is solved numerically are appropriate. To this end, it is important to realize that the equation of motion will indeed be solved numerically. This means that the equation of motion is not solved directly for the large absolute position of the interface points. Instead, it is solved for the small increment in the absolute interface coordinates that occurs during the time increment. The time-discretized equations are linear in this position increment and tangent to the current configuration space. Consequently, the transformation matrix in (4.3) can be used to ensure that at every time increment, the increment in the absolute interface coordinates is solved.

At the start of the next time increment, the floating frame coordinates and local interface coordinates are calculated to find expressions for rotation matrix $\mathbf{R}_J^O$ and the elastic forces. As the increment in the absolute interface coordinates is known, the increment for the floating frame coordinates can be determined from (4.3). However, the error introduced by numerical integration may cause the floating frame to drift. For that reason additional Newton-Raphson iterations can be applied in which the current floating frame coordinates are used as an initial estimate. In simulations that were performed for validation purposes in [10, 20, 21], it was found that only few Newton-Raphson iterations are actually required. Once both the absolute interface coordinates and the absolute floating frame

coordinates are determined with sufficient accuracy, the local interface coordinates and thus the local elastic deformation can be determined consistently. At this point, the equation of motion can be solved.

Depending on the time integration method chosen, computational costs may be reduced when aside from the system matrices also the Jacobian of these matrices is obtained. In particular, it is found that for both static and dynamic simulation the inclusion of the tangent stiffness matrix is often essential for both stability and accuracy. This tangent stiffness matrix consists of the standard material stiffness matrix and the geometric stiffness matrix. The geometric stiffness matrix is required to properly include stress-stiffening effects. These are important in the case of for instance the equilibrium analysis of structures that undergo large deformations or for the dynamic analysis of pre-tensioned structures. For this reason, it is useful to derive the expression for the tangent stiffness matrix. To this end, the equations of motion (4.11) are reduced to the equilibrium equations, which can be rewritten as:

$$\boxed{\left[\overline{\mathbf{R}}_j^O\right][\mathbf{T}]^T\mathbf{Q}_{int}^j = \mathbf{Q}_{ext}^O, \qquad \mathbf{Q}_{int}^j \equiv \mathbf{K}_{CB}^j\mathbf{q}} \qquad (4.12)$$

The equilibrium equations can be solved incrementally using load stepping, which requires a set of linear equations to be solved repeatedly in terms of small increments in the generalized coordinates. To this end, the variation of (4.12) is taken. In order to emphasize that these equations are intended to solve incrementally, $\Delta(\cdot)$ is used for a small numerical increment.

$$\left[\overline{\mathbf{R}}_j^O\right][\mathbf{T}]^T\Delta\mathbf{Q}_{int}^j + \left[\overline{\mathbf{R}}_j^O\right]\Delta[\mathbf{T}]^T\mathbf{Q}_{int}^j + \Delta\left[\overline{\mathbf{R}}_j^O\right][\mathbf{T}]^T\mathbf{Q}_{int}^j = \Delta\mathbf{Q}_{ext}^O \qquad (4.13)$$

On the left hand side of (4.13), the terms $\Delta\mathbf{Q}_{int}^j$, $\Delta[\mathbf{T}]$ and $\Delta\left[\overline{\mathbf{R}}_j^O\right]$ all contain variations in the generalized coordinates. Using the coordinate transformations presented in Chapter 3, these terms can all be expressed as a matrix times a vector of variations in the absolute interface coordinates.

Hence, the equilibrium equation can be rewritten to the following form:

$$\mathbf{K}_t^O \Delta \mathbf{q}^{O,O} = \Delta \mathbf{Q}_{ext}^O \qquad (4.14)$$

where $\mathbf{K}_t^O$ is the global tangential stiffness matrix that depends on the orientation of the floating frame and the elastic deformation of the body. Equation (4.14) can be solved incrementally for the global position of the interface coordinates. Given a certain load increment $\Delta \mathbf{Q}_{ext}^O$, (4.14) can be solved for the corresponding displacement increment $\Delta \mathbf{q}^{O,O}$ by applying Newton-Raphson iterations. Then, the global position of the interface coordinates can be updated by adding the obtained $\Delta \mathbf{q}^{O,O}$ to the current position of the interface points. After this, the external load can be increased with the next load increment and a possible residual from the current step. This procedure can be repeated until the external load is applied entirely. Clearly, the full expression for the tangential stiffness matrix $\mathbf{K}_t^O$ is needed for this procedure, which requires the rewriting of all three terms on the left hand side of (4.13). To this end, the variation of the transformation matrix [**T**] must be derived, for which the variation of the transformation matrix [**Z**] is required.

4.3   The tangent stiffness matrix

The variation in $[\mathbf{Z}]$ is obtained by taking the virtual change of its definition (3.17):

$$\delta[\mathbf{Z}] \equiv \delta\big([\mathbf{\Phi}_{CB}][\mathbf{\Phi}_{rig}]\big)^{-1}[\mathbf{\Phi}_{CB}] \qquad (4.15)$$

For an arbitrary invertible matrix $\mathbf{B}$ the following holds for the variation of its inverse:

$$\delta\mathbf{B}^{-1} = -\mathbf{B}^{-1}\delta\mathbf{B}\,\mathbf{B}^{-1} \qquad (4.16)$$

Using (4.16) and the fact that $[\mathbf{\Phi}_{CB}]$ is constant, the variation in $[\mathbf{Z}]$ is expressed as:

$$\delta[\mathbf{Z}] = -\big([\mathbf{\Phi}_{CB}][\mathbf{\Phi}_{rig}]\big)^{-1}[\mathbf{\Phi}_{CB}]\delta\big[\mathbf{\Phi}_{rig}\big]\big([\mathbf{\Phi}_{CB}][\mathbf{\Phi}_{rig}]\big)^{-1}[\mathbf{\Phi}_{CB}] \qquad (4.17)$$

which can be written in compact form as:

$$\boxed{\delta[\mathbf{Z}] = -[\mathbf{Z}]\delta\big[\mathbf{\Phi}_{rig}\big][\mathbf{Z}]} \qquad (4.18)$$

Here, the virtual change in $\big[\mathbf{\Phi}_{rig}\big]$ is:

$$\delta\big[\mathbf{\Phi}_{rig}\big] = \begin{bmatrix} \delta\big[-\tilde{\mathbf{r}}_1^{j,j}\big] \\ \vdots \\ \delta\big[-\tilde{\mathbf{r}}_N^{j,j}\big] \end{bmatrix}, \qquad \delta\big[-\tilde{\mathbf{r}}_k^{j,j}\big] = \begin{bmatrix} \mathbf{0} & -\delta\tilde{\mathbf{r}}_k^{j,j} \\ \mathbf{0} & \mathbf{0} \end{bmatrix} \qquad (4.19)$$

To find the variation in $[\mathbf{T}]$, take the virtual change of its definition (3.18):

$$\delta[\mathbf{T}] = -\delta\big[\mathbf{\Phi}_{rig}\big][\mathbf{Z}] - \big[\mathbf{\Phi}_{rig}\big]\delta[\mathbf{Z}] \qquad (4.20)$$

Substitution of (4.18) in (4.20) yields:

$$\delta[\mathbf{T}] = -\delta\big[\mathbf{\Phi}_{rig}\big][\mathbf{Z}] + \big[\mathbf{\Phi}_{rig}\big][\mathbf{Z}]\delta\big[\mathbf{\Phi}_{rig}\big][\mathbf{Z}] \qquad (4.21)$$

In compact form, this can be rewritten to:

$$\delta[\mathbf{T}] = -[\mathbf{T}]\delta[\boldsymbol{\Phi}_{rig}][\mathbf{Z}] \qquad (4.22)$$

The expressions for $\delta[\mathbf{Z}]$ and $\delta[\mathbf{T}]$ as established in (4.18) and (4.22) will now be used to obtain the tangent stiffness matrix. For the first term in (4.13), the virtual change in internal forces $\delta\mathbf{Q}_{int}^{j}$ is required. Since the local material stiffness matrix $\mathbf{K}_{CB}$ is constant, this can simply be written as:

$$\delta\mathbf{Q}_{int}^{j} = \mathbf{K}_{CB}^{j}\delta\mathbf{q}^{j,j} \qquad (4.23)$$

In this expression, with the help of (3.18), the virtual change in local interface coordinates is expressed in terms of the virtual change in global interface coordinates:

$$\delta\mathbf{Q}_{int}^{j} = \mathbf{K}_{CB}^{j}[\mathbf{T}][\bar{\mathbf{R}}_{O}^{j}]\delta\mathbf{q}^{O,O} \qquad (4.24)$$

With (4.24), the increment in the first term in (4.13) can be expressed as:

$$[\bar{\mathbf{R}}_{j}^{O}][\mathbf{T}]^{T}\Delta\mathbf{Q}_{int}^{j} = [\bar{\mathbf{R}}_{j}^{O}][\mathbf{K}_{1}^{j}][\bar{\mathbf{R}}_{O}^{j}]\Delta\mathbf{q}^{O,O}, \quad [\mathbf{K}_{1}^{j}] \equiv [\mathbf{T}]^{T}\mathbf{K}_{CB}^{j}[\mathbf{T}] \qquad (4.25)$$

$[\mathbf{K}_{1}^{j}]$ can be recognized as the transformed local material stiffness matrix. The transformation matrices $[\mathbf{T}]$ remove the rigid body component from the local material stiffness matrix $\mathbf{K}_{CB}^{j}$ and the rotation matrices $[\bar{\mathbf{R}}_{O}^{j}]$ transform the local material stiffness matrix to the global frame. Note again that when the elastic forces are not influenced by rigid body motion, such that when $[\mathbf{T}]$ is based on the body's undeformed configuration, approximation (3.25) applies and it follows simply that $[\mathbf{K}_{1}^{j}] = \mathbf{K}_{CB}^{j}$.

In order to rewrite the second term in (4.13), the following notation is introduced first:

$$\hat{\mathbf{Q}}_{int}^{j} = [\mathbf{T}]^{T}\mathbf{Q}_{int}^{j} \qquad (4.26)$$

The virtual change in $[\mathbf{T}]$ is required in (4.13). Upon substitution of (4.22) and (4.26), this can be written as:

$$\left[\overline{\mathbf{R}}_j^O\right]\delta[\mathbf{T}]^T\mathbf{Q}_{int}^j = -\left[\overline{\mathbf{R}}_j^O\right][\mathbf{Z}]^T\,\delta\left[\boldsymbol{\Phi}_{rig}\right]^T\widehat{\mathbf{Q}}_{int}^j \tag{4.27}$$

The multiplication of $\delta\left[\boldsymbol{\Phi}_{rig}\right]^T\widehat{\mathbf{Q}}_{int}^j$ can be expanded as:

$$\delta\left[\boldsymbol{\Phi}_{rig}\right]^T\widehat{\mathbf{Q}}_{int}^j = \left[\begin{bmatrix} \mathbf{0} & \mathbf{0} \\ \delta\tilde{\mathbf{r}}_1^{j,j} & \mathbf{0} \end{bmatrix} \quad \cdots \quad \begin{bmatrix} \mathbf{0} & \mathbf{0} \\ \delta\tilde{\mathbf{r}}_N^{j,j} & \mathbf{0} \end{bmatrix}\right]\begin{bmatrix} \begin{bmatrix} \widehat{\mathbf{F}}_{int,1}^j \\ \widehat{\mathbf{M}}_{int,1}^j \end{bmatrix} \\ \vdots \\ \begin{bmatrix} \widehat{\mathbf{F}}_{int,N}^j \\ \widehat{\mathbf{M}}_{int,N}^j \end{bmatrix} \end{bmatrix} \tag{4.28}$$

The generalized forces $\widehat{\mathbf{Q}}_{int,k}^j$ of interface point k are decomposed in the forces $\widehat{\mathbf{F}}_{int,k}^j$ and moments $\widehat{\mathbf{M}}_{int,k}^j$. Equation (4.28) can be rewritten to:

$$\delta\left[\boldsymbol{\Phi}_{rig}^j\right]^T\widehat{\mathbf{Q}}_{int}^j = \left[\widehat{\mathbf{F}}_{int}^j\right]^T\delta\mathbf{q}^{j,j}, \qquad \left[\widehat{\mathbf{F}}_{int}^j\right] \equiv \begin{bmatrix} \begin{bmatrix} \mathbf{0} & \tilde{\widehat{\mathbf{F}}}_{int,1}^j \\ \mathbf{0} & \mathbf{0} \end{bmatrix} \\ \vdots \\ \begin{bmatrix} \mathbf{0} & \tilde{\widehat{\mathbf{F}}}_{int,N}^j \\ \mathbf{0} & \mathbf{0} \end{bmatrix} \end{bmatrix} \tag{4.29}$$

With this, the second term in (4.13) becomes:

$$\left[\overline{\mathbf{R}}_j^O\right]\delta[\mathbf{T}]^T\mathbf{Q}_{int}^j = -\left[\overline{\mathbf{R}}_j^O\right][\mathbf{Z}]^T\left[\widehat{\mathbf{F}}_{int}^j\right]^T\delta\mathbf{q}^{j,j} \tag{4.30}$$

At this point, the transformation from the local interface coordinates to the global interface coordinates can again be made using (3.18):

$$\left[\overline{\mathbf{R}}_j^O\right]\delta[\mathbf{T}]^T\mathbf{Q}_{int}^j = -\left[\overline{\mathbf{R}}_j^O\right][\mathbf{Z}]^T\left[\widehat{\mathbf{F}}_{int}^j\right]^T[\mathbf{T}]\left[\overline{\mathbf{R}}_O^j\right]\delta\mathbf{q}^{O,O} \tag{4.31}$$

With (4.31), the increment in the second term in (4.13) can be expressed as:

$$\boxed{\left[\overline{\mathbf{R}}_j^O\right]\Delta[\mathbf{T}]^T\mathbf{Q}_{int}^j = \left[\overline{\mathbf{R}}_j^O\right]\left[\mathbf{K}_2^j\right]\left[\overline{\mathbf{R}}_O^j\right]\Delta\mathbf{q}^{O,O}, \quad \left[\mathbf{K}_2^j\right] \equiv -[\mathbf{Z}]^T\left[\hat{\mathbf{f}}_{int}^j\right]^T[\mathbf{T}]} \quad (4.32)$$

For the third term in (4.13), the variation of the rotation matrix is rewritten with (2.8):

$$\delta\left[\overline{\mathbf{R}}_j^O\right][\mathbf{T}]^T\mathbf{Q}_{int}^j = \left[\overline{\mathbf{R}}_j^O\right]\delta\tilde{\boldsymbol{\pi}}_j^{j,O}\hat{\mathbf{Q}}_{int}^j \quad (4.33)$$

Now $\delta\boldsymbol{\pi}_j^{j,O}$ and $\hat{\mathbf{Q}}_i^j$ can be interchanged by considering the following:

$$\delta\tilde{\boldsymbol{\pi}}_j^{j,O}\hat{\mathbf{Q}}_i^j = \begin{bmatrix}\delta\tilde{\boldsymbol{\pi}}_j^{j,O} & & \\ & \ddots & \\ & & \delta\tilde{\boldsymbol{\pi}}_j^{j,O}\end{bmatrix}\begin{bmatrix}\hat{\mathbf{Q}}_{i,1}^j \\ \vdots \\ \hat{\mathbf{Q}}_{i,N}^j\end{bmatrix} = -\begin{bmatrix}\begin{bmatrix}\mathbf{0} & \tilde{\tilde{\mathbf{F}}}_{i,1}^j \\ \mathbf{0} & \tilde{\mathbf{M}}_{i,1}^j\end{bmatrix} \\ \vdots \\ \begin{bmatrix}\mathbf{0} & \tilde{\tilde{\mathbf{F}}}_{i,N}^j \\ \mathbf{0} & \tilde{\mathbf{M}}_{i,N}^j\end{bmatrix}\end{bmatrix}[\mathbf{R}_j^O]\begin{bmatrix}\delta\mathbf{r}_j^{O,O} \\ \delta\boldsymbol{\pi}_j^{O,O}\end{bmatrix} \quad (4.34)$$

This can be written in compact form as:

$$\delta\tilde{\boldsymbol{\pi}}_j^{j,O}\hat{\mathbf{Q}}_i^j = -\left(\left[\hat{\mathbf{f}}_{int}^j\right] + \left[\hat{\mathbf{M}}_{int}^j\right]\right)[\mathbf{R}_j^O]\begin{bmatrix}\delta\mathbf{r}_j^{O,O} \\ \delta\boldsymbol{\pi}_j^{O,O}\end{bmatrix}, \quad \left[\hat{\mathbf{M}}_{int}^j\right] \equiv \begin{bmatrix}\begin{bmatrix}\mathbf{0} & \mathbf{0} \\ \mathbf{0} & \tilde{\mathbf{M}}_{i,1}^j\end{bmatrix} \\ \vdots \\ \begin{bmatrix}\mathbf{0} & \mathbf{0} \\ \mathbf{0} & \tilde{\mathbf{M}}_{i,N}^j\end{bmatrix}\end{bmatrix} \quad (4.35)$$

Substitution of (4.35) and using the transformation (3.17) to express the virtual position of the floating frame in terms of the virtual position of the interface coordinates yields for the third term in (4.13):

$$\delta\left[\overline{\mathbf{R}}_j^O\right][\mathbf{T}]^T\mathbf{Q}_{int}^j = -\left[\overline{\mathbf{R}}_j^O\right]\left(\left[\hat{\mathbf{f}}_{int}^j\right] + \left[\hat{\mathbf{M}}_{int}^j\right]\right)[\mathbf{Z}]\left[\overline{\mathbf{R}}_O^j\right]\delta\mathbf{q}^{O,O} \quad (4.36)$$

And so the increment in the third term in (4.13) can be expressed as:

$$\Delta[\overline{\mathbf{R}}_j^O][\mathbf{T}]^T \mathbf{Q}_{int}^j = [\overline{\mathbf{R}}_j^O][\mathbf{K}_3^j][\overline{\mathbf{R}}_O^j]\Delta\mathbf{q}^{O,O}, \quad [\mathbf{K}_3^j] \equiv -([\hat{\mathbf{f}}_{int}^j] + [\hat{\mathbf{M}}_{int}^j])\,[\mathbf{Z}] \qquad (4.37)$$

Combining (4.25), (4.32) and (4.37) yields an expression for the incremental change in the equilibrium equation in terms of the incremental change in global interface coordinates:

$$[\overline{\mathbf{R}}_j^O]([\mathbf{K}_1^j] + [\mathbf{K}_2^j] + [\mathbf{K}_3^j])[\overline{\mathbf{R}}_O^j]\Delta\mathbf{q}^{O,O} = \Delta\mathbf{Q}_{ext}^O \qquad (4.38)$$

And thus the expression for the tangential stiffness matrix is obtained:

$$\mathbf{K}_t^O = [\overline{\mathbf{R}}_j^O]([\mathbf{K}_1^j] + [\mathbf{K}_2^j] + [\mathbf{K}_3^j])[\overline{\mathbf{R}}_O^j] \qquad (4.39)$$

It can be seen that $\mathbf{K}_t^O$ consists of a local stiffness matrix, rotated to the global frame. The local tangential stiffness matrix contains the local material stiffness matrix in $[\mathbf{K}_1^j]$. The matrices $[\mathbf{K}_2^j]$ and $[\mathbf{K}_3^j]$ together form the local geometric stiffness matrix $\mathbf{K}_g^j$, which depends explicitly on the internal forces by means of $[\hat{\mathbf{f}}_{int}^j]$ and $[\hat{\mathbf{M}}_{int}^j]$. Moreover, the geometric stiffness matrix depends on the deformation of the body by means of the transformation matrices $[\mathbf{Z}]$ and $[\mathbf{T}]$.

The equations of motion presented in this chapter, including the tangent stiffness matrix, are implemented in a numerical program that can be used to perform flexible multibody dynamics simulations. In this, the finite element mass and stiffness matrices of a body are reused in the superelement formulation. Validation of this formulation with benchmark problems has shown that it produces reliable results. These validation simulations are discussed in the next chapter.

5

Validation

In this chapter, simulations are presented in which the new superelement formulation is compared with other software packages (Spacar, Ansys and Adams) that use different formulations. Therefore, it is important to make a clear distinction between the several methods before presenting the simulation results. Because of different customs in the terminology of different methods, the term *component* is introduced here to identify a part of a system with clear physical boundaries. A component is discretized in *bodies*. Each body has a floating frame attached to it, such that is able to describe large translations and rotations. *Elements* that are also able to describe this, such as corotational elements or fully nonlinear elements are, in this sense bodies. To emphasize the difference, linear finite elements cannot do this and are therefore not regarded as bodies. In the floating frame formulation, bodies are discretized in linear elements, which describe elastic deformations with respect to the body's floating frame.

In the new superelement formulation, all Craig-Bampton modes of all interface points are taken into account for all bodies in the system. This means six Craig-Bampton modes per interface point for three-dimensional analysis and three Craig-Bampton modes per interface point for two-dimensional analysis. In all cases, the floating frame is located at the center of mass of the undeformed body, unless stated otherwise.

Spacar is a finite element based multibody software package that uses the corotational formulation [22]. For each beam element, a fixed number of physically meaningful deformation modes is defined which are expressed as analytical functions of the absolute nodal coordinates. Flexible elements are modelled by allowing non-zero deformations. If the deformations remain sufficiently small, they can be described in a single co-rotational frame and related to dual stress resultants using linear beam models. In the present validation examples, the standard beam element is used [23], but it is interesting to note that a superelement formulation has been developed for general two-node beam-like elements in Spacar [24, 25].

The formulation used in Spacar is different than the standard corotational formulation, because it uses a consistent mass formulation and fictitious forces are not ignored [26]. Due to these similarities with the new superelement formulation presented in this work, it is expected that when the number of bodies in the new superelement formulation equals the number of elements in Spacar, simulation results are very close.

Ansys is used for nonlinear finite element analysis. Standard two-node beam elements are used in the analysis. Ansys uses an inertial frame formulation and a nonlinear strain definition. This is a fundamentally different formulation from the new superelement formulation. For that reason, small differences might occur when a small number of elements / bodies are used. This is not expected, because the nonlinear strain definition is able to properly describe large rigid body motions.

Adams uses the floating frame formulation in combination with Lagrange multipliers in all simulations. For each body, flexibility is included by means of local deformation shapes. These deformation shapes are included in Adams by means of a modal neutral file. This file contains the body's free-free natural modes that are determined from a linear finite element model in Ansys. In the simulations presented here, the number of free-free modes taken into account equals the number of degrees of freedom of the finite element model minus the rigid body modes. For example, a three-dimensional beam that consists of 2 elements has 18 nodal degrees of freedom. Hence, $18 - 6 = 12$ free-free modes are taken into account. As explained in Chapter 4, the reuse of a body's linear finite element model, causes that some inertia terms cannot be determined exactly. Terms related to the rigid-flexible coupling and fictitious forces are approximated using a lumped mass matrix. It can be expected that these approximations may cause differences in simulations when a small number of elements is used.

In Section 5.1, the general validation of the new superelement formulation is presented. These simulations show excellent accuracy of the new method. In Section 5.2, the effect of the floating frame location on simulation accuracy is investigated. It is found that better accuracy is obtained when the floating frame is located in a body's center of mass than when the floating frame is located in an interface point. In Section 5.3, the effect of simplifications in the coordinate transformation matrices involved in the new superelement formulation is studied. It is found that neglecting the effect of elastic deformation on the transformation matrices is acceptable when the elastic deformations within a body remain small.

5.1   Validation of the superelement formulation

For validation purposes, the simulation of several benchmark problems has been performed. The validation problems consist of a static cantilever beam subjected to a large vertical tip force, a 2D and 3D slider-crank mechanism with a flexible connector and a 3D spinning beam on a spherical joint.

Equilibrium analysis of a cantilever beam

A cantilever beam with circular cross section was modelled with 10 bodies. The total length of the beam is 1 m. The outer radius of the cross section is 0.01 m with a wall thickness of 1 mm. The Young's modulus is 70 GPa. The beam was incrementally loaded at its tip starting at 100 N and increasing to 10 kN. The load acts in vertical direction at all times. Results have been obtained with the new method, Spacar and Ansys. The computed deformed beam shapes are shown in Figure 5.1 for applied loads of 100 N, 500 N, 2000 N and 10000 N. The figure shows good agreement between the new code and both Spacar and Ansys for this number of bodies. Differences occur when fewer bodies are used. This will be discussed in Section 5.2.
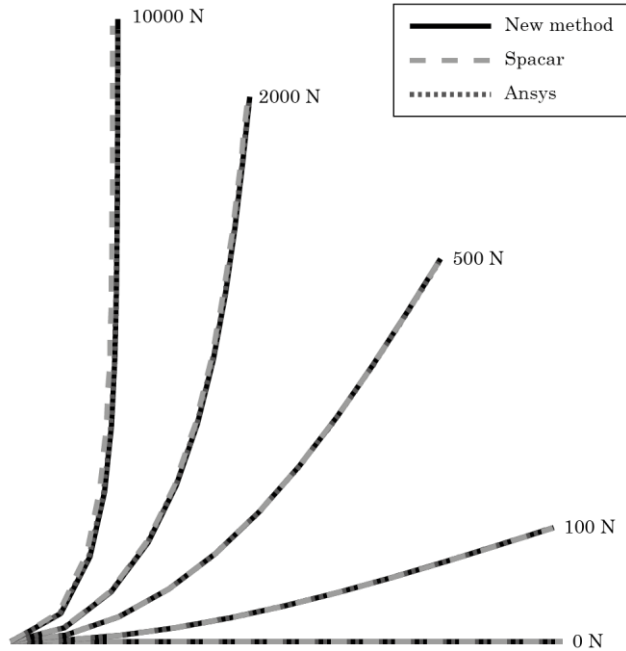
Fig. 5.1   Deflection of a cantilever beam subjected to a vertical tip force.

Transient analysis of a 2D slider-crank mechanism

The dynamic 2D slider-crank problem is adopted from [23] and shown in Figure 5.2. The rigid crank 0.15 m in length is rotating with a constant angular velocity of 150 rad/s. The flexible connector 0.3 m in length has a uniform circular cross section with a diameter of 6 mm. In the simulation a Young's modulus of 200 GPa and a mass density of 7870 kg/m^3 are used. The end of the connector is attached to a slider with a mass that equals half the mass of the connector. The slider is able to translate without friction on its base.

The angular velocity of the crank introduces an initial linear velocity and an angular velocity of the connector, assuming no deformation. In the new superelement formulation, the connector is modeled with two bodies. In Spacar, two elements are used. In Adams, a modal neutral file is created based on the 6 free-free modes of the connector's linear finite element model that consists of 2 elements.
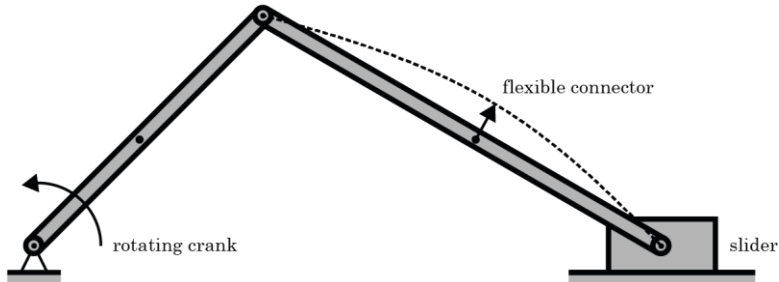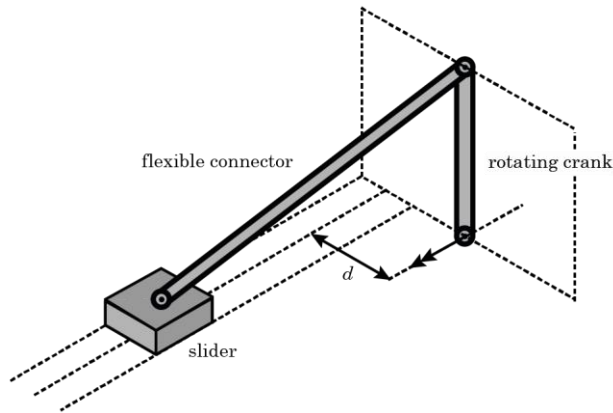
Fig. 5.2   2D Slider-crank mechanism with flexible connector.

As output, the displacement of the midpoint of the connector perpendicular to the undeformed beam was determined and plotted against the crank angle. The results are shown in Figure 5.3. This figure also shows the results obtained with Spacar and Adams. It can be seen that the new method agrees very well with the results obtained with Spacar. The results obtained with Adams show small differences. Apart from the possible approximations mentioned before, it should also be noted that the Adams model only has 1 floating frame for the connector. In the new superelement formulation, both bodies have a floating frame, which may describe the deformed configuration of the connector better than the Adams model.
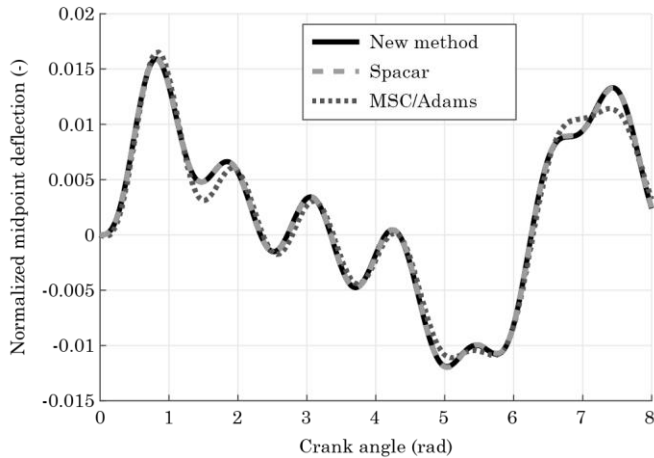
Fig. 5.3   Midpoint deformation of the flexible connector as a function of the crank angle.

Transient analysis of a 3D slider-crank mechanism
The dynamic 3D slider-crank mechanism is adopted from [27] and shown in Figure 5.4. The physical properties of the mechanism are the same as in the 2D case described before. The horizontal position d of the rotation axis is 0.1 m. In the initial configuration, the crank is oriented vertically upward. The models in the new superelement formulation, Spacar and Adams are similar as described before, but now expanded to the three-dimensional case.

Fig. 5.4   3D Slider-crank mechanism with flexible connector.

As output, the displacement of the midpoint of the connector in its local y-direction was determined and plotted against the crank angle. The results are shown in Figure 5.5. It can be seen that also in this case, the results obtained with the new method are very close to the results obtained with Spacar. The results obtained with Adams again show a small differences in comparison with the other two methods. In this example in particular, it can be seen that the results produced by Adams show a slightly higher frequency of vibration than the results obtained by the new method and Spacar. This might very well be due to the fact that Adams uses a lumped mass matrix, which is known to result in higher vibration frequencies.
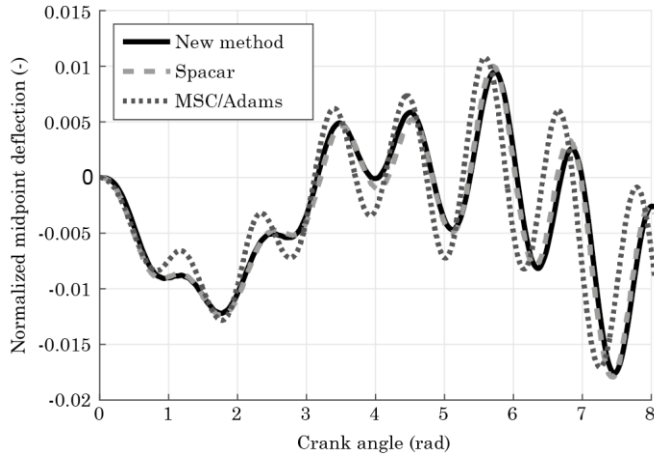
Fig. 5.5   Mid-point deformation of the flexible connector as a function of the crank angle.

Transient analysis of a 3D beam on a spherical joint

The 3D spinning beam on a spherical joint is adopted from [9] and shown in Figure 5.6. The physical properties, prescribed loads and simulation settings are the same as described in this reference: the beam has length 141.42 mm, cross section 9.0 mm^2 and area moment of inertia 6.75 mm^4. The material has a mass density 7800 kg/m^3 and Young's Modulus 210 GPa. A torque of 0.2 Nm is applied about the vertical axis during the first 10.2 seconds. 15 seconds later, at $t = 25.2$ sconds, an impulsive vertical tip force of 100 N is applied.
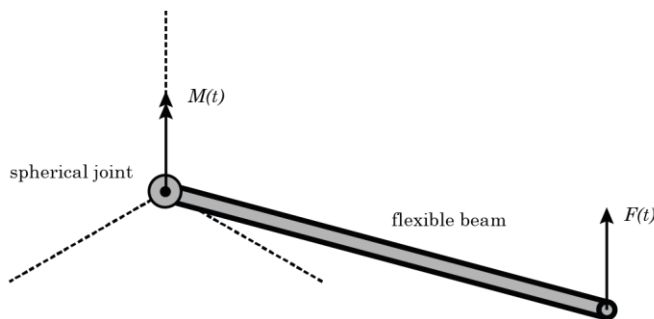
Fig. 5.6   Flexible beam on a spherical joint.

In the new superelement formulation, the connector is modelled with two bodies. In Spacar, two elements are used. In Adams, a modal neutral file is created based on the 12 free-free modes of the connector's linear finite element model that consists of 2 elements.

As output, the absolute angular velocity about the vertical axis at the base of the beam was determined and plotted as a function of time. The results are shown in Figure 5.7. It was observed in [9] that different methods show different results only after the impulsive vertical force is applied. In Figure 5.7 it can be seen that all methods used here produce very similar results even after this moment. However, it should be noted that although the new superelement formulation and Spacar predict similar vibration amplitudes after the force is applied, Adams predicts a slightly smaller vibration amplitude.
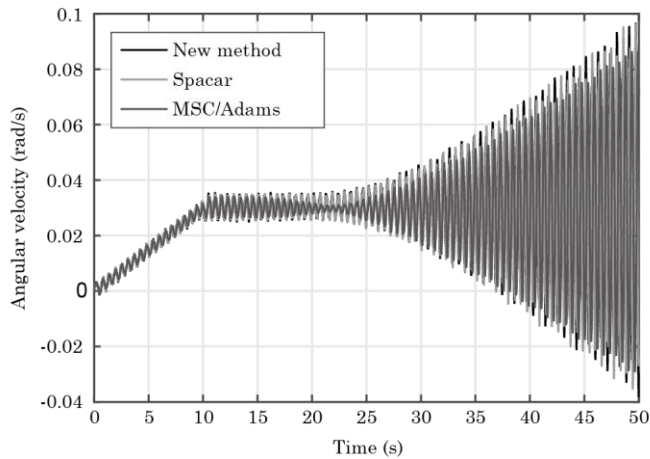

Fig. 5.7   Angular velocity about the vertical axis of the beam as a function of time.

It is also worthwhile comparing all results with the ones published in [9]. In figures 9, 10 and 11 of this work by Cardona, several floating frame formulations are compared with the results of a nonlinear finite element formulation. It can be seen that all results shown in Figure 5.7 are similar to the nonlinear finite element formulation in [9]. In fact, the difference between the new method, Spacar and Adams is very small in comparison with the difference between the nonlinear finite element formulation and

any of the floating frame formulations in [9]. For the sake of illustration, Figures 10 and 11 from [9] are reproduced here in Figure 5.8 to emphasize how good the agreement of the new method is in comparison with other formulations. When comparing these figures, take careful note of the different scales of the y-axis. It can be observed that after 50 seconds, the result of the nonlinear finite element formulation in Figure 5.8 is slightly below 0.1 rad/s, which agrees very well with Figure 5.7.
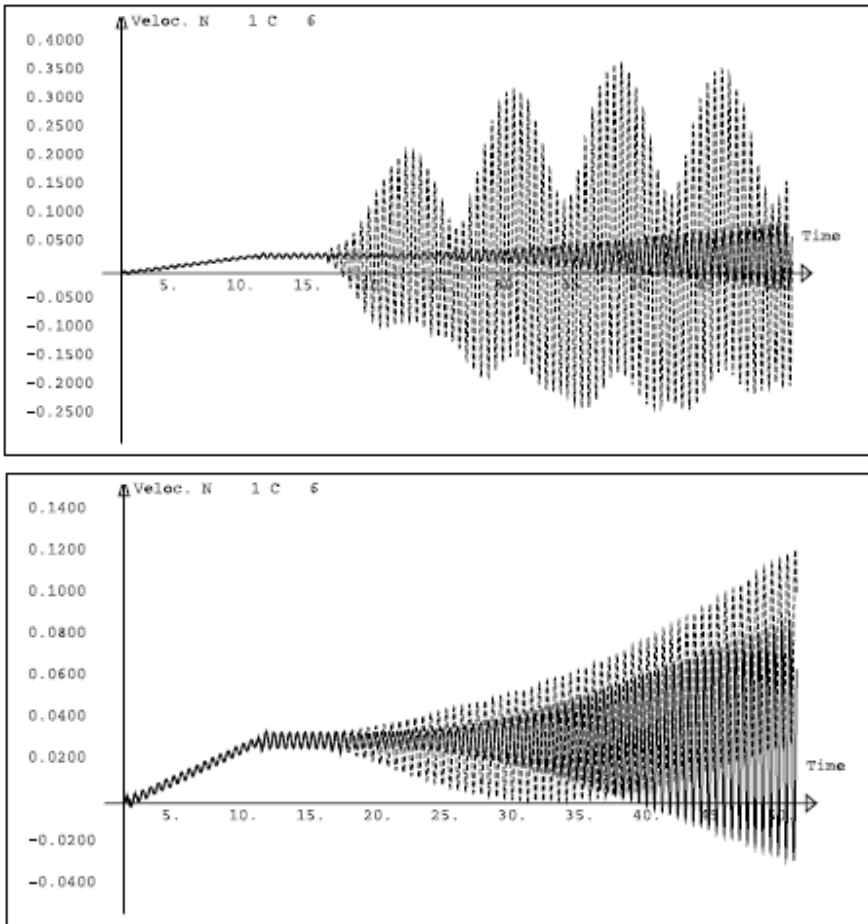

Fig. 5.8　　Figure is reproduced from Figures 10 and 11 in [9]. Solid line is the result obtained with the nonlinear finite element formulation, which is close to all the lines in Figure 5.7. Dashed lines are obtained with the floating frame formulation using different inertia options considered in [9].

Conclusion

Based on the above simulations of benchmark problems, it is concluded that the new superelement formulation yields reliable results when it is compared with other formulations.

5.2   Effect of the floating frame location

In general, better simulation accuracy is obtained when the floating frame is located in the body's center of mass than when the floating frame is located in an interface point. This can be explained by the fact that when the floating frame is located in an interface point relatively large elastic deformations are required to describe the motion of material points on the body's far end. When the floating frame is located near the center of the body, smaller elastic deformations are required to describe the same body shape. Because the assumption of small displacements is fundamental to the floating frame formulation, accuracy is best when the floating frame is located such that elastic deformations are minimized. This concept is visualized for a beam in Figure 5.9, where the dotted lines represent the undeformed shape of the beam.
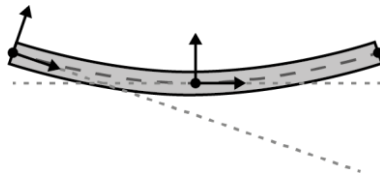

Fig. 5.9   A flexible body in its deformed configuration and its undeformed configurations (dashed lines) for floating frame locations at an interface point and at the undeformed body's center of mass.

Several simulations have been performed to validate that indeed better accuracy is obtained when the floating frame is located in the body's center of mass than when the floating frame is located in an interface point. These validation problems consist of a cantilever beam subjected to a transient tip force and a fast rotating beam subjected to a transient tip force.

Simulations in which the beams consist of 10 bodies are performed as a reference. With this number of bodies, all formulations have converged to the same solution. Then, simulations with fewer bodies are performed to illustrate the fundamental differences between the formulations. These differences are explained best when only using a small number of bodies, although the overall simulation accuracy might be unacceptable for practical purposes. However, from the simulations it is concluded that the

new superelement formulation in which the floating frame is located in the center of mass also gives reasonable results when using a smaller number of bodies.

Transient analysis of a cantilever beam

The same cantilever beam is used as in the static problem described in Section 5.1. However, in this case, a transient vertical tip force is applied. In 0.05 s, the force is increased linearly from 0 to 2500 N and maintained constant at this value after 0.05 s. First, the simulation is performed using 10 bodies and validated with Spacar, from which it is concluded that the new method yields reliable results. Then, simulations are performed with 1 body according to the new method in which the floating frame is located at the center of mass or at the left or right interface point. Figure 5.10 shows the vertical tip position as a function of time. It can be seen that when a floating frame is located in an interface point, the simulation becomes unstable. In the new formulation, the simulation is stable, yet it shows a lower frequency and also an amplitude offset with respect to the correct solution.
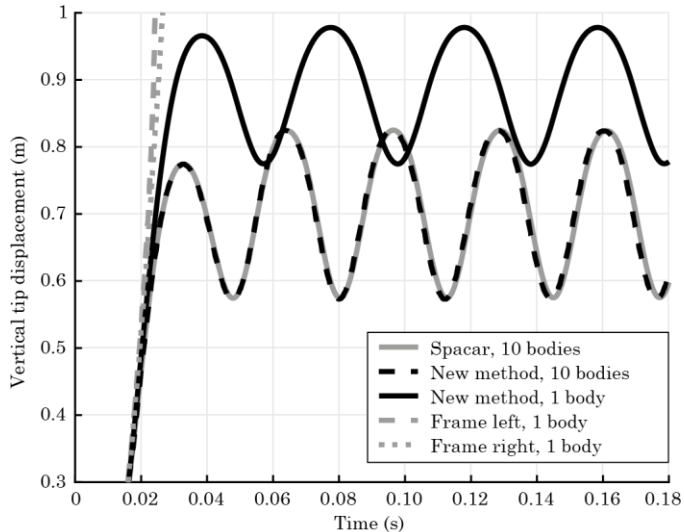

Fig. 5.10 Vertical tip position of the beam. Validation of the new method with Spacar for 10 bodies and the effect of the floating frame position for 1 body.

Figure 5.11 shows the results for the simulations that are performed with 3 bodies. In this case, all three methods produce stable results. However, the new method is found most accurate, although locating the floating frame in the left interface point is of similar accuracy. It is concluded that when increasing the number of bodies, all methods converge to the correct solution, but the new method is found most accurate.
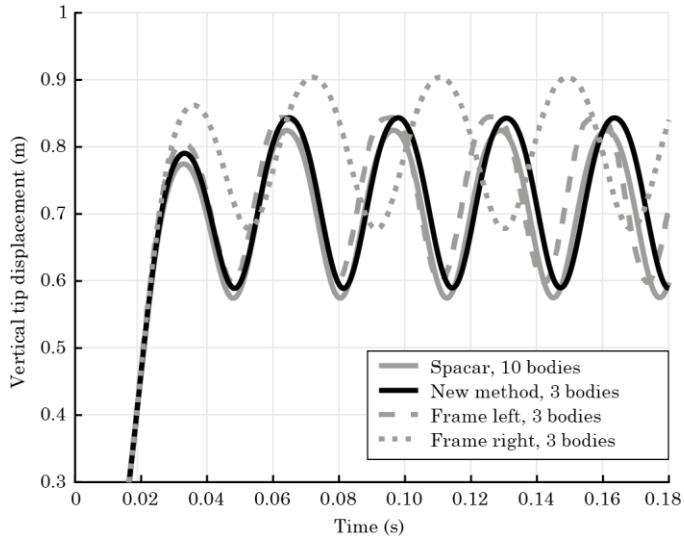

Fig. 5.11 Vertical tip position of the beam. The effect of the floating frame position for 3 bodies.

Transient analysis of a rotating beam

In the rotating beam problem, the same beam properties are used as in the previous cantilever beam problem. The beam is hinged at its left interface point and given a constant angular velocity of 100 rad/s. During the first 0.01 s of the simulation, a constant tip force of 50 N is applied perpendicular to the beam, in the plane of rotation. Figure 5.12 shows a graphical representation of the problem.
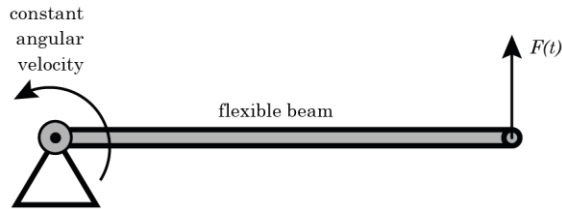
Fig. 5.12   Graphical representation of the rotating beam problem, subjected to a transient perpendicular tip force.

First, the simulation is performed using 10 bodies and validated with Spacar, from which it is concluded that the new method yields reliable results. Then, simulations are performed with 1 body using the new method and compared with the traditional floating frame formulation in which the floating frame is located in the left or right interface point. Figure 5.13 shows the tip deflection as a function of time. It can be seen that when using 1 body only, the new method is reasonably close to the 10-body simulation, although a difference is observed. Placing the floating frame in the left interface point yields simulation results that are far from the correct solution. In this case the constraints at the hinge can be satisfied exactly, but because only 1 body is used, the remaining model is simply a rotating linear beam element. Because this model is unable to include stress stiffening, larger amplitudes and longer vibration periods are observed. Placing the floating frame in the right interface point shows instable behavior after a rotation of 2 rad.
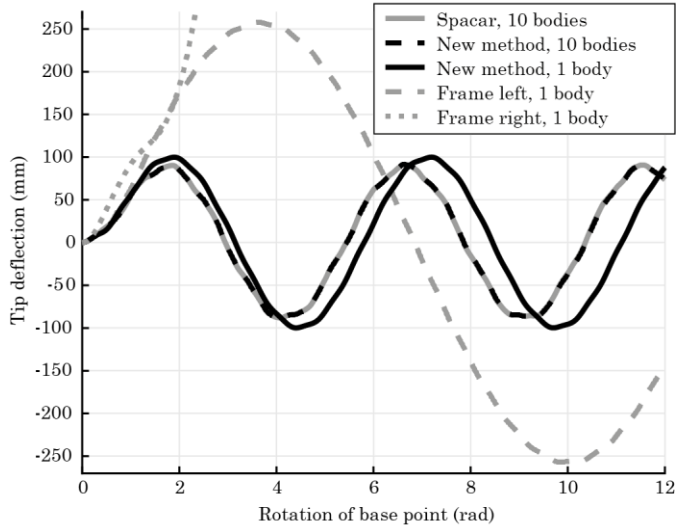
Fig. 5.13 Deflection of the tip of the beam, measured relative to its dynamic equilibrium position. Validation of the new method with Spacar for 10 bodies and the effect of the floating frame position for 1 body.

Figure 5.14 shows the results for the simulations that are performed with 2 bodies. It can be seen that all simulations are stable and that the new method produces the most accurate results. Also from this example it is concluded that when increasing the number of bodies, all methods converge to the correct solution, but the new method is found most accurate when using fewer bodies.
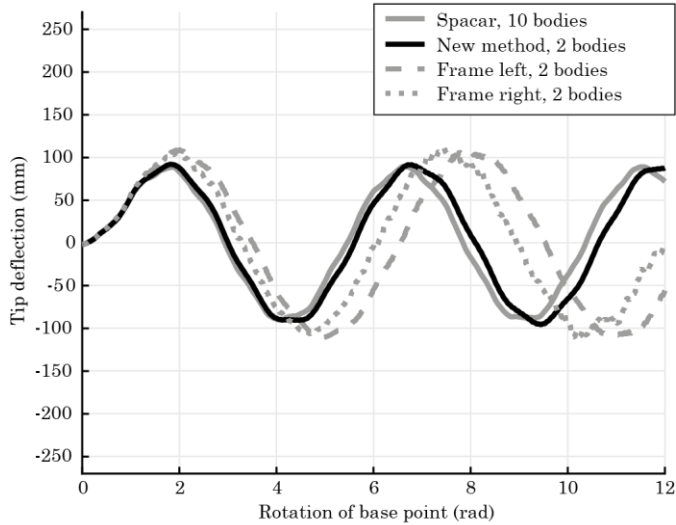
Fig. 5.14 Deflection of the tip of the beam, measured relative to its dynamic equilibrium position. The effect of the floating frame position for 2 body.

Conclusion

Based on the above simulations of benchmark problems, it is concluded that better accuracy is obtained when the floating frame is located at the center of mass of an undeformed body than when the floating frame is located at an interface point. This difference in accuracy becomes most pronounced when the number of bodies is low. This means that when the floating frame is located at a body's center of mass, fewer bodies are required to obtain the same accuracy as when the floating frame would have been located at an interface point.

5.3 Effect of the simplification of the matrices $[\boldsymbol{\Phi}_{rig}]$, $[\mathbf{Z}]$ and $[\mathbf{T}]$

It was explained in Chapter 3 that the matrices $[\boldsymbol{\Phi}_{rig}]$, $[\mathbf{Z}]$ and $[\mathbf{T}]$ can be given a very elegant geometric interpretation. For this interpretation, it was found a convenient thought experiment to consider these matrices to be based on an undeformed body instead of a deformed body. In this way it was discovered that $[\boldsymbol{\Phi}_{rig}]$ describes the motion of the interface points when the floating frame is subjected to rigid body modes, $[\mathbf{Z}]$ describes the motion of the floating frame when the interface points are subjected to rigid body modes and $[\mathbf{T}]$ describes the elastic deformation of the coordinate transformation from global to local interface coordinates. Because the local elastic deformations are small, the hypothesis is that their effect on $[\boldsymbol{\Phi}_{rig}]$, $[\mathbf{Z}]$ and $[\mathbf{T}]$ might be small as well.

As it would increase the computational efficiency to consider these matrices as constant, the effect of neglecting the higher order terms is investigated. To this end, simulations are performed on three benchmark problems that were already introduced above: the equilibrium analysis of a cantilever beam, the 2D slider-crank mechanism shown in Figure 5.2 and the rotating beam problem shown in Figure 5.12.

Equilibrium analysis of a cantilever beam
Figure 5.15 shows the equilibrium configuration of the beam when subjected to 250 N, 1000 N and 10000 N, using 10 and 3 bodies, using both the exact and approximated transformation matrices. It was already validated in Section 5.1 that the simulation results with 10 bodies are accurate. When using 10 bodies, no significant difference was observed between the exact and approximated transformation matrices.

It can be seen that when using fewer bodies, a larger deflection is obtained. Hence, a single body clearly underestimates the stiffness. One could say that when increasing the number of bodies, the exact solution is being converged to "from the soft side". It is difficult to prove that this is the case from the equations directly, yet this behavior is observed in multiple simulations. It can be seen that when the transformation matrices are based on the undeformed body, the solution is better than when using the

exact definition. When the transformation matrices are approximated, the body is assumed stiffer than in reality throughout the transformation. Based on the simulation results, it is found that this partially counteracts the fact that when using fewer bodies, a softer system is created.
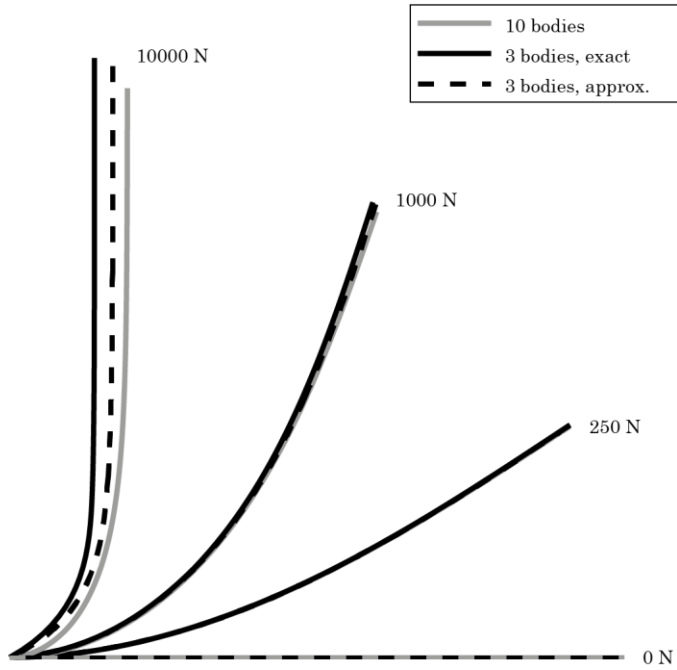

Fig. 5.15 Deflected beam configuration. Comparison with 3 and 10 bodies, using exact and approximated transformation matrices.

It should be noted that significant differences occur only for large deformations. From Figure 5.15 it can be seen that in particular near the clamping, the curvature in the beam is very large. As a result, the body that is connected to the clamping, is subjected to deformations that go beyond the linear range. In this case, the fundamental assumption that local deformations remain small is violated, such that one should anticipate inaccurate results. As a comparison, another simulation has been performed in which the three bodies are given different lengths of $L/7$, $2L/7$ and $4L/7$. Figure 5.16 shows the simulation results, from which it can be seen that high accuracy is now also obtained, even at these large deformations.
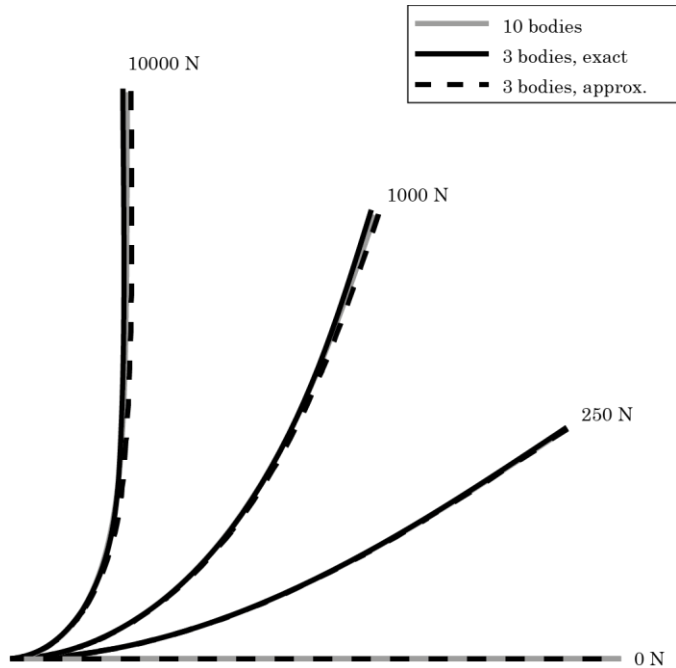
Fig. 5.16 Deflected beam configuration. Comparison with 3 and 10 bodies, using exact and approximated transformation matrices. The 3 bodies have partial lengths 1/7, 2/7, 4/7.

Transient analysis of a 2D slider-crank mechanism

Figure 5.17 shows the midpoint deformation of the flexible connector of the slider-crank mechanism for simulations using 10 and 2 bodies, using both the exact and approximated transformation matrices. It can be seen that in general all simulation results are comparable, with some minor differences between 5 and 6 rad. A zoomed-in detail of the simulation results shows that when the transformation matrices are approximated as constant, the results are closer to the exact solution.
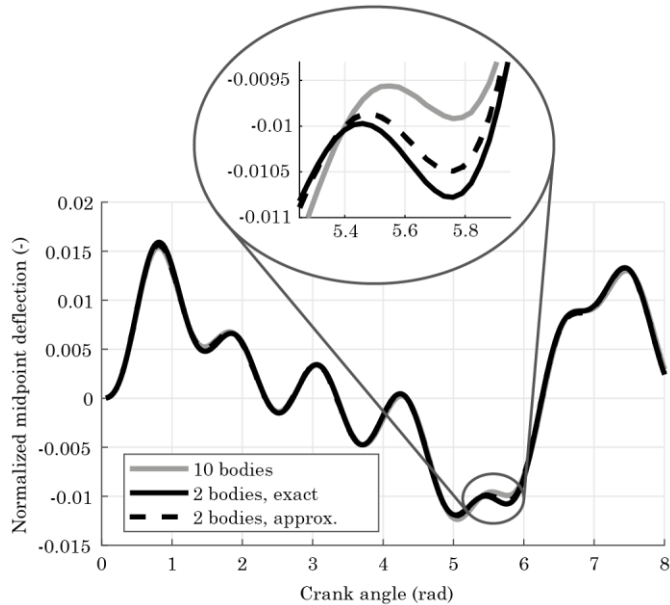
Fig. 5.17   Midpoint deformation of the connector. Comparison with 2 and 10 bodies, using exact and approximated transformation matrices.

Transient analysis of a rotating beam

For the rotating beam problem, Figure 5.18 shows the tip deflection as a function of time when using 10 and 1 bodies, using both the exact and approximated transformation matrices. It can be seen that when using only 1 body, the period of vibration becomes longer. This is consistent with the previous observation that using fewer bodies makes the system softer. Also in this example, it is found that when using the approximated transformation matrices, the simulation results get closer to the exact solution.
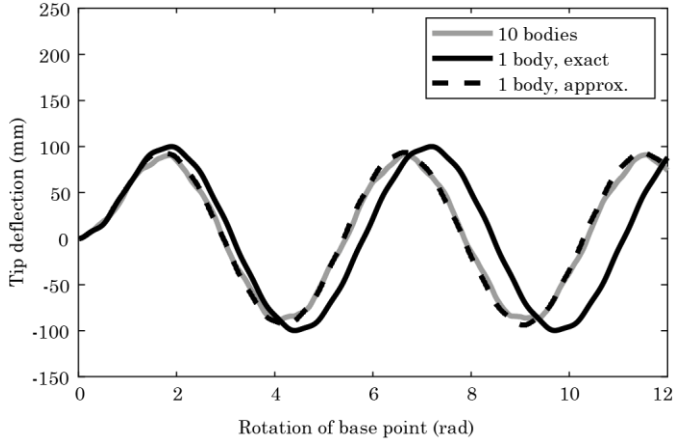
Fig. 5.18 Deflection of the tip of the beam, measured relative from its dynamic equilibrium position. Comparison with 1 and 10 bodies, using exact and approximated transformation matrices.

Conclusion

Based on the above simulations of benchmark problems, it is concluded that the influence of higher order terms in the transformation matrices is small whenever the local elastic deformations of a body remain small. In that case, the higher order terms in $[\mathbf{\Phi}_{rig}]$, $[\mathbf{Z}]$ and $[\mathbf{T}]$ can be neglected without influencing the simulation accuracy. When the number of bodies is low, the effect of this approximation is most pronounced. Yet in these cases, the error due to using too few bodies is partially compensated by the error due to large deformations within a single body. This means that when constant transformation matrices are used, fewer bodies are required to obtain the same accuracy as when this approximation is not made. It would be interesting to see if it is possible to show mathematically that the new superelement formulation underestimates the stiffness.

6

Conclusion

New superelement formulation

Describing the kinematics of a flexible multibody system comes down to the kinematic formulation of the motion of the interface points. In the inertial frame and corotational frame formulations, the absolute interface coordinates are part of the degrees of freedom, allowing for a direct application of the constraints. This is in contrast to the floating frame formulation, which requires the use of Lagrange multipliers. In this work, it has been demonstrated that the absolute floating frame coordinates, and the local elastic coordinates that appear in the equation of motion of a floating frame formulation, can be replaced by the absolute interface coordinates. Consequently, no Lagrange multipliers are required to enforce the kinematic constraints. In this way a new superelement formulation is obtained that can be used for the simulation of a system's flexible multibody dynamics. Validation of the method with static and dynamic benchmark problems described in literature has shown to yield reliable results in all cases. It was shown that the new formulation produces better results than a floating frame formulation in which the floating frame is located at an interface point. Even when a very small number of flexible bodies are used, the new method yields reasonable results.

The use of Craig-Bampton modes

In the development of the presented superelement formulation, the use of Craig-Bampton modes as a body's local deformations shapes has been crucial. The rigid body motions that can be described by these Craig-Bampton modes are employed to eliminate the floating frame coordinates from the system. This is done by imposing the constraint that any linear combination of the Craig-Bampton modes should be such that there is no elastic deformation at the location of the floating frame. Due to the nonlinear nature of the kinematic relations, this constraint is imposed on the variations in the relevant coordinates. From the kinematics it follows that variations of local interface coordinates can be expressed as the difference between variations of the absolute interface coordinates and variations of the absolute floating frame coordinates. The constraint provides the possibility of eliminating the variation of the absolute floating frame coordinates by the variation in the absolute interface coordinates. Subsequently also the variation in the local interface coordinates can be

eliminated by the variation in the absolute interface coordinates. By using Newton-Raphson iterations and the constraints, it is possible to prevent drift at the position level.

Advantages of the new superelement formulation

The new superelement formulation can be applied to systems that consist of arbitrarily shaped three-dimensional bodies that have an arbitrary number of interface points. It offers the possibility of reducing geometric nonlinear systems by applying important model order reduction techniques in a body's local frame. In this way a body's linear finite element model can be reused in the multibody analysis. Existing superelement formulations require the floating frame to be located at an interface point. It was shown that better accuracy is obtained when the floating frame is located in the body's center of mass. The strength of the new formulation is that the floating frame can be located in the center of mass, without the need for an interface point in the center of mass. In this way, the new formulation offers a unique and elegant solution to the traditional problem of how to create efficient superelements.

Similarities with corotational frame formulation

In this work, it was explained that relating a flexible body's floating frame to the absolute interface coordinates is very similar to the problem of relating an element's corotational frame to its absolute nodal coordinates. The mathematically correct formulation of the kinematics of the new superelement formulation also provides a good understanding of the approximations made in corotational methods. These approximations consist of neglecting:

- higher order terms in the mass matrix of an element
- fictitious forces caused by the elastic deformation within an element
- elastic deformations when computing the elastic forces within an element.

Geometric interpretation of the transformation matrices

Elaborate work was done to give the transformation matrices involved in the new superelement formulation a geometric interpretation. A substantial effort was made to add more engineering intuition to the mathematical formulation. For this purpose, it is crucial to understand

that $[\mathbf{\Phi}_{rig}]$ represents the motion of the interface points when a body's floating frame is given a prescribed rigid body motion. The fact that this matrix is based on the deformed configuration of the body means that neither $[\mathbf{Z}]$ nor $[\mathbf{T}]$ are constant but depend on the elastic deformation. However, when one considers the undeformed configuration of a body, $[\mathbf{Z}]$ simply describes the deformation of the floating frame when interface coordinates are moving according to Craig-Bampton modes. In this case $[\mathbf{T}]$ eliminates the contribution of rigid body motion from the absolute interface coordinates and provides the local interface coordinates. The geometric interpretations of transformation matrices $[\mathbf{Z}]$ and $[\mathbf{T}]$ as presented in this work resulted in the idea that they could be well approximated using the rigid body modes of the undeformed body $[\mathbf{\Phi}_{rig,0}]$ instead of $[\mathbf{\Phi}_{rig}]$. Simulation of benchmark problems has shown that this approximation is justified and results in good accuracy even when a small number of bodies are used.

7

Recommendations

This work has shown that the new superelement formulation is a very elegant and attractive method of creating reduced order models of flexible multibody systems. In order to employ its benefits over existing methods, it is recommended to focus future research on several generalizations and further validations to make the formulation applicable in more situations and in more fields of research.

In particular, it is worthwhile investigating the possibility of using other deformation shapes to describe a body's local displacement field. So far, only the use of static Craig-Bampton modes has been implemented. It is natural to extend this to the internal Craig-Bampton modes as well, such that more complicated deformations can be described. For further generalization it is worthwhile examining whether a coordinate transformation to absolute interface coordinates can be applied when an arbitrary set of deformation shapes is used.

In this work, the assumption that the local elastic deformations remain small was of crucial importance. However, there are many applications for which deformations of a single body will become large, for instance in the case of large stroke flexure mechanisms. For these applications, it is worthwhile investigating the possibility of combining geometric nonlinear model order reduction techniques on a body's nonlinear finite element model.

The validations performed in this work were limited to bodies with two interface points. However, the formulation allows for an arbitrary number of interface points. For this reason, it is recommended to include more complicated bodies in the benchmark portfolio. A natural expansion would be to construct superelements for - for example - plates, but ideally the possibility to include any finite element model in the multibody formulation should be implemented.

For most fields of engineering dynamics, the multibody formulation used in this work is standard. However, there are many related fields of research in which it is very common to formulate a system's dynamics in terms of screw theory and lie algebras. This is in particular the case for the likes of robotics, control engineering and mechanism design. In order to make the new superelement formulation suitable for application in these fields, it is useful to reformulate the kinematics and kinetics in terms of screw theory.

The author is aware that in order to cover all above recommendations, much additional research is required. In a certain way it is easy to list everything that can be done and has not been done yet as a recommendation. However, the research of the above topics might have very interesting practical applications. For that reason, the author expresses his dedication to execute this research in the future. To demonstrate his current thoughts on the matter, the author has presented some initial theoretical steps in the direction of the recommendations mentioned in Chapter 8. This substantiates the recommendations a little more.

8

**Generalizations
for future research**

In this chapter, the author wishes to give his current thoughts on the possibilities of the new superelement formulation for future research. This chapter presents generalizations of the current method in several directions. However, it should be understood that this contains only the mathematical formulations without the supporting numerical examples. The purpose is to substantiate the recommendations from Chapter 7 a little bit further. The author wants the reader to focus on the general direction of these thoughts. For this reason, it should be anticipated that the presented derivations will not be as elaborate as in other parts of this work. For the purpose of keeping this chapter compact, intermediate steps will be left out, briefly described by text or replaced by relevant references.

In order to create superelements based on the floating frame formulation, the absolute floating frame coordinates and local coordinates corresponding to the elastic deformation shapes need to be expressed in terms of the absolute interface coordinates. In Chapter 3, it was explained that because the local interface coordinates are in fact the generalized coordinates corresponding to the static Craig-Bampton modes, it is natural to choose these modes to describe the local elastic displacement field. However, in the Craig-Bampton method, the set of static interface modes is in general augmented with internal vibration modes. These internal Craig-Bampton modes are obtained by computing the vibration modes of the body while all interface points are fixed.

In Section 8.1, it is explained how the internal Craig-Bampton modes can be taken into account when constructing the superelements according to the method described in the previous chapters. In Section 8.2, it is explained how the method can be generalized further, by using any set of deformation modes - not necessarily Craig-Bampton modes - to describe local deformations. Section 8.3 presents the method with which it is expected to include geometrical nonlinearities within a body using a modified local reduction basis that is based on Craig-Bampton modes. This method would allow for large deformations within a flexible body. Section 8.4 presents some preliminary validation results for bodies with more than 2 interface points. In particular this contains the simulation of benchmark problems using plates. In Section 8.5, it is explained how the new superelement formulation can be obtained in terms of screw theory.

In this chapter, the author reused earlier work of conference papers "Model order reduction of large stroke flexure hinges using modal derivatives" [28] and "An absolute interface coordinates floating frame of reference formulation for plates" [29] that were accepted at the ISMA Noise and Vibration Engineering Conference 2018 in Leuven and the journal paper "A new superelement formulation for flexible multibody systems using screw theory" [30] that is being prepared for submission.

8.1 Including internal Craig-Bampton modes

Consider a flexible body with N interface points. The local elastic deformation of an arbitrary point P_i on the body is expressed in terms of the $6N$ static Craig-Bampton modes and M internal Craig-Bampton modes as follows:

$$\mathbf{q}_i^{j,j} = \sum_{k=1}^{N} \boldsymbol{\Phi}_k(\mathbf{x}_i^{j,j})\, \mathbf{q}_k^{j,j} + \sum_{l=1}^{M} \boldsymbol{\psi}_l(\mathbf{x}_i^{j,j})\, \eta_l^{j,j} \tag{8.1}$$

In this, $\boldsymbol{\Phi}_k$ is the (6×6) matrix of static Craig-Bampton modes corresponding to interface point P_k and $\boldsymbol{\psi}_l$ is the (6×1) vector of the internal Craig-Bampton mode which corresponds to the natural coordinate $\eta_l^{j,j}$. Equation (8.1) can be written in compact matrix-vector form as:

$$\mathbf{q}_i^{j,j} = [\boldsymbol{\Phi}_i]\mathbf{q}^{j,j} + [\boldsymbol{\Psi}_i]\boldsymbol{\eta}^{j,j} \tag{8.2}$$

with:

$$[\boldsymbol{\Phi}_i] \equiv \begin{bmatrix} \boldsymbol{\Phi}_1(\mathbf{x}_i^{j,j}) & \dots & \boldsymbol{\Phi}_N(\mathbf{x}_i^{j,j}) \end{bmatrix}, \quad \mathbf{q}^{j,j} \equiv \begin{bmatrix} \mathbf{q}_1^{j,j} \\ \vdots \\ \mathbf{q}_N^{j,j} \end{bmatrix}$$

$$[\boldsymbol{\Psi}_i] \equiv \begin{bmatrix} \boldsymbol{\psi}_1(\mathbf{x}_i^{j,j}) & \dots & \boldsymbol{\psi}_M(\mathbf{x}_i^{j,j}) \end{bmatrix}, \quad \boldsymbol{\eta}^{j,j} \equiv \begin{bmatrix} \eta_1^{j,j} \\ \vdots \\ \eta_M^{j,j} \end{bmatrix} \tag{8.3}$$

Again, it is demanded that there is zero elastic deformation at the location of the floating frame. By taking the variation of (8.2) and evaluating the Craig-Bampton modes at the location of the floating frame P_j, a modified form of the constraint (3.7) is obtained:

$$\delta\mathbf{q}_j^{j,j} = [\boldsymbol{\Phi}_{CB}]\delta\mathbf{q}^{j,j} + [\boldsymbol{\Psi}_{CB}]\delta\boldsymbol{\eta}^{j,j} = \mathbf{0} \tag{8.4}$$

where $[\boldsymbol{\Psi}_{CB}]$ is used to denote the $(6 \times M)$ matrix of internal Craig-Bampton modes evaluated at the floating frame P_j.

In comparison with (3.7), the term $[\boldsymbol{\Psi}_{CB}]\delta\boldsymbol{\eta}^{j,j}$ is added to the constraint, because the internal modes may also cause a deformation at P_j. At this point, recall the kinematic relation (3.15) that expresses the variation of the local interface coordinates in terms of the variation of the absolute interface coordinates and the variation of the absolute floating frame coordinates:

$$\delta\mathbf{q}^{j,j} = [\bar{\mathbf{R}}_O^j]\delta\mathbf{q}^{O,O} - [\boldsymbol{\Phi}_{rig}][\mathbf{R}_O^j]\delta\mathbf{q}_j^{O,O} \qquad (8.5)$$

By substituting (8.5) in (8.4), the rigid body motions can be eliminated from the Craig-Bampton modes and the variation of the absolute floating frame coordinates can be expressed in terms of the variation of the local interface coordinates and the variation of the natural coordinates of the internal modes:

$$\delta\mathbf{q}_j^{O,O} = [\mathbf{R}_j^O]\big([\boldsymbol{\Phi}_{CB}][\boldsymbol{\Phi}_{rig}]\big)^{-1}\big([\boldsymbol{\Phi}_{CB}][\bar{\mathbf{R}}_O^j]\delta\mathbf{q}^{O,O} + [\boldsymbol{\Psi}_{CB}]\delta\boldsymbol{\eta}^{j,j}\big) \qquad (8.6)$$

In compact form this can be written as:

$$\delta\mathbf{q}_j^{O,O} = [\mathbf{R}_j^O]\big([\mathbf{Z}][\bar{\mathbf{R}}_O^j]\delta\mathbf{q}^{O,O} + [\mathbf{Z}_2]\delta\boldsymbol{\eta}^{j,j}\big),$$
$$[\mathbf{Z}_2] \equiv \big([\boldsymbol{\Phi}_{CB}][\boldsymbol{\Phi}_{rig}]\big)^{-1}[\boldsymbol{\Psi}_{CB}] \qquad (8.7)$$

It can be seen that the relation between $\delta\mathbf{q}_j^{O,O}$ and $\delta\mathbf{q}^{O,O}$ is the same as in Eq. (3.17) and that the relation between $\delta\mathbf{q}_j^{O,O}$ and $\delta\boldsymbol{\eta}^{j,j}$ is accounted for simply by an additional transformation matrix $[\mathbf{Z}_2]$. By back substitution of (8.7) in (8.5), it is possible to express the variation of the local interface coordinates in terms of the variation of the global interface coordinates and the variation of the natural coordinates of the internal modes:

$$\delta\mathbf{q}^{j,j} = [\mathbf{T}][\bar{\mathbf{R}}_O^j]\delta\mathbf{q}^{O,O} + [\mathbf{T}_2]\delta\boldsymbol{\eta}^{j,j}, \qquad [\mathbf{T}_2] \equiv -[\boldsymbol{\Phi}_{rig}][\mathbf{Z}_2] \qquad (8.8)$$

For the sake of completeness, it is mentioned that when the transformation matrices are determined based on the body's undeformed configuration, $[\mathbf{\Phi}_{CB}][\mathbf{\Phi}_{rig}] = \mathbf{1}$. With this simplification, $[\mathbf{Z}_2] \approx [\mathbf{\Psi}_{CB}]$ and $[\mathbf{T}_2] \approx -[\mathbf{\Phi}_{rig}][\mathbf{\Psi}_{CB}]$, similarly as described in Chapter 3. In the floating frame formulation, the equation of motion is expressed in terms of the absolute floating frame coordinates, local interface coordinates and local natural coordinates. Using (8.7) and (8.8), the following coordinate transformation can be established:

$$
\begin{bmatrix} \delta\mathbf{q}_j^{O,O} \\ \delta\mathbf{q}^{j,j} \\ \delta\mathbf{\eta}^{j,j} \end{bmatrix} = \begin{bmatrix} [\mathbf{R}_j^O][\mathbf{Z}][\bar{\mathbf{R}}_O^j] & [\mathbf{R}_j^O][\mathbf{Z}_2] \\ [\mathbf{T}][\bar{\mathbf{R}}_O^j] & [\mathbf{T}_2] \\ \mathbf{0} & \mathbf{1} \end{bmatrix} \begin{bmatrix} \delta\mathbf{q}^{O,O} \\ \delta\mathbf{\eta}^{j,j} \end{bmatrix} \tag{8.9}
$$

This coordinate transformation can now be applied to the equation of motion, following the same procedure as described in Chapter 4. Note that the transformed equation of motion is now also expressed in terms of the natural coordinates $\mathbf{\eta}^{j,j}$. Because these natural coordinates correspond to deformation modes that are zero at the interface points, they will not be present in any kinematic constraint equation. Hence, the constraint equations can still be satisfied directly, without the use of Lagrange multipliers, also when the internal Craig-Bampton modes are taken into account.

8.2 Including a general set of deformation modes

Consider the general case in which a body's elastic deformation is described locally with an arbitrary set of M deformation shapes. In this section it is explained how even for this general case, the presented method for creating superelements can still be applied. However, the deformation shapes should be able to describe rigid body motions. If this is not the case, the rigid body modes need to be added to the deformation shapes. The resulting formulation depends on the dimension $m \leq M$ of the subspace spanned by the deformation shapes on the $6N$ interface coordinates. The strategy depends on whether m is larger than, equal to or smaller than $6N$. These different cases will be elaborated on after the general formulation is introduced.

The variation in the position of an arbitrary point P_i on the flexible body can be expressed in the same way as before:

$$\delta \mathbf{q}_i^{j,j} = [\bar{\boldsymbol{\Phi}}_i] \delta \boldsymbol{\zeta}^{j,j} \tag{8.10}$$

where $[\bar{\boldsymbol{\Phi}}_i]$ now denotes the $(6 \times M)$ matrix of arbitrary deformation shapes evaluated at P_i and $\delta \boldsymbol{\zeta}^{j,j}$ is the variation of the corresponding generalized coordinates. The constraint that there is no deformation at the location of the floating frame P_j can be expressed as:

$$\delta \mathbf{q}_j^{j,j} = [\bar{\boldsymbol{\Phi}}_j] \delta \boldsymbol{\zeta}^{j,j} = \mathbf{0} \tag{8.11}$$

To create a superelement based on the floating frame formulation, again a relation is required between the absolute floating frame coordinates, local generalized coordinates corresponding to the deformation modes and absolute interface coordinates. From the method presented in this work, it is known how to establish this relation if the local interface coordinates are used to describe the body's deformation.

For this reason, the variations in the interface points $\delta \mathbf{q}^{j,j}$ are first expressed in terms of the variations of the generalized coordinates $\delta \boldsymbol{\zeta}^{j,j}$, by evaluating (8.10) at every interface point:

$$\delta \mathbf{q}^{j,j} = [\bar{\boldsymbol{\Phi}}_{IP}]\delta \boldsymbol{\zeta}^{j,j}, \qquad [\bar{\boldsymbol{\Phi}}_{IP}] \equiv \begin{bmatrix} \bar{\boldsymbol{\Phi}}_1 \\ \vdots \\ \bar{\boldsymbol{\Phi}}_N \end{bmatrix} \qquad (8.12)$$

where $[\bar{\boldsymbol{\Phi}}_{IP}]$ is the $(6N \times M)$ matrix of deformation modes evaluated at the interface points. The local generalized coordinates need to be expressed in terms of the local interface coordinates. Equation (8.12) can be inverted as:

$$\delta \boldsymbol{\zeta}^{j,j} = [\bar{\boldsymbol{\Phi}}_{IP}]^{+}\delta \mathbf{q}^{j,j} \qquad (8.13)$$

Here, in general $[\bar{\boldsymbol{\Phi}}_{IP}]^{+}$ denotes the pseudoinverse of $[\bar{\boldsymbol{\Phi}}_{IP}]$. In general (8.13) is an approximation of the generalized coordinates in the least square sense. Substitution in (8.11) yields a constraint in terms of the local interface coordinates:

$$\left[\bar{\boldsymbol{\Phi}}_j\right][\bar{\boldsymbol{\Phi}}_{IP}]^{+}\delta \mathbf{q}^{j,j} = \mathbf{0} \qquad (8.14)$$

The remaining steps to express the absolute floating frame coordinates in terms of the absolute interface coordinates are the same as before. To this end, equation (8.5) is substituted in (8.14) and rewritten to:

$$\delta \mathbf{q}_j^{O,O} = \left[\mathbf{R}_j^{O}\right][\mathbf{Z}_{gen}][\bar{\mathbf{R}}_O^{j}]\delta \mathbf{q}^{O,O}, \qquad [\mathbf{Z}_{gen}] \equiv \left([\bar{\boldsymbol{\Phi}}_j][\bar{\boldsymbol{\Phi}}_{IP}]^{+}[\boldsymbol{\Phi}_{rig}]\right)^{+}[\bar{\boldsymbol{\Phi}}_j][\bar{\boldsymbol{\Phi}}_{IP}]^{+} \quad (8.15)$$

where $[\mathbf{Z}_{gen}]$ is introduced as the general transformation matrix. Back substitution in (8.5) yields for the local interface coordinates:

$$\delta \mathbf{q}^{j,j} = \left[\mathbf{T}_{gen}\right][\bar{\mathbf{R}}_O^{j}]\delta \mathbf{q}^{O,O}, \qquad [\mathbf{T}_{gen}] \equiv \mathbf{1} - [\boldsymbol{\Phi}_{rig}][\mathbf{Z}_{gen}] \qquad (8.16)$$

Finally, the relation between the local generalized coordinates and the absolute interface coordinates is obtained by back substitution of (8.16) in (8.13):

$$\delta\boldsymbol{\zeta}^{j,j} = [\bar{\boldsymbol{\Phi}}_{IP}]^+[\mathbf{T}_{gen}][\bar{\mathbf{R}}_O^j]\delta\mathbf{q}^{O,O} \qquad (8.17)$$

The equation of motion in the floating frame formulation can be expressed in terms of the absolute interface coordinates as follows:

$$\begin{bmatrix} \delta\mathbf{q}_j^{O,O} \\ \delta\boldsymbol{\zeta}^{j,j} \end{bmatrix} = \begin{bmatrix} [\mathbf{R}_j^O][\mathbf{Z}_{gen}][\bar{\mathbf{R}}_O^j] \\ [\bar{\boldsymbol{\Phi}}_{IP}]^+[\mathbf{T}_{gen}][\bar{\mathbf{R}}_O^j] \end{bmatrix} \delta\mathbf{q}^{O,O} \qquad (8.18)$$

For every numerical increment, the equations of motion can be solved for an increment in the absolute interface coordinates. Then the increment in the floating frame coordinates and local generalized coordinates need to be computed in order to determine the body's elastic deformation.

1. **Craig-Bampton modes: $m = M = 6N$**
Consider the case where the static Craig-Bampton modes are used. Now $m = M = 6N$ and $[\bar{\boldsymbol{\Phi}}_{IP}]$ equals the identity matrix. In this case the above formulation reduces to the standard form discussed in the previous chapters.

2. **Other deformation shapes: $m = 6N$**
Consider the case where $m = 6N$ other deformation shapes are chosen, but with a linear combination of these shapes a unit deformation of each interface point can still be described. In this case, the deformation shapes span the same space on the interface points as the Craig-Bampton modes. However, because other deformation are used, the body may have internal elastic deformations that are different from the Craig-Bampton modes. In this case, the relation between the generalized coordinates $\delta\boldsymbol{\eta}^{j,j}$ and local interface coordinates $\delta\mathbf{q}_j^{j,j}$ (8.11) can uniquely be inverted. Hence, $[\bar{\boldsymbol{\Phi}}_{IP}]^+$ equals $[\bar{\boldsymbol{\Phi}}_{IP}]^{-1}$ and (8.14) is exact.

3. More deformation shapes: $m > 6N$

Consider the case where the partition of deformation shapes on the interface points is larger than the number of interface coordinates: $m > 6N$. In this case the local interface coordinates are not able to uniquely determine the body's deformation. To solve this problem, it is proposed to decompose the space spanned by the deformation shapes into a subspace that is uniquely spanned by the $6N$ local interface coordinates and a subspace of size $M - 6N$ that has zero deformation at the interface points. After this decomposition, the strategy explained in the previous section can be used. For this purpose, the deformation shapes are manipulated such that a form similar to (8.2) is obtained. Substitution of (8.10) and (8.12) in the variation of (8.2) yields:

$$\delta\mathbf{q}_i^{j,j} = [\bar{\mathbf{\Phi}}_i]\delta\boldsymbol{\zeta}^{j,j} = [\mathbf{\Phi}_i][\bar{\mathbf{\Phi}}_{IP}]\delta\boldsymbol{\zeta}^{j,j} + [\mathbf{\Psi}_i]\delta\boldsymbol{\eta}^{j,j} \qquad (8.19)$$

where $[\mathbf{\Psi}_i]$ is a $\big(6 \times (M - 6N)\big)$ matrix of yet unknown internal deformation shapes. This can be rewritten as:

$$[\mathbf{\Psi}_i]\delta\boldsymbol{\eta}^{j,j} = ([\bar{\mathbf{\Phi}}_i] - [\mathbf{\Phi}_i][\bar{\mathbf{\Phi}}_{IP}])\delta\boldsymbol{\zeta}^{j,j} \qquad (8.20)$$

The $(6 \times M)$ matrix $[\bar{\mathbf{\Phi}}_i] - [\mathbf{\Phi}_i][\bar{\mathbf{\Phi}}_{IP}]$ has a nullspace with size $6N$. Using a singular value decomposition, $M - 6N$ linearly independent columns can be obtained. These columns form $[\mathbf{\Psi}_i]$. Hence, when $M > 6N$, the internal deformation shapes $[\mathbf{\Psi}_i]$ are obtained from the singular value decomposition of $[\bar{\mathbf{\Phi}}_i] - [\mathbf{\Phi}_i][\bar{\mathbf{\Phi}}_{IP}]$ and after that treated similarly as internal Craig-Bampton modes.

4. Less deformation shapes: $m < 6N$

Consider the case where the partition of deformation shapes on the interface points is smaller than the number of interface coordinates: $m < 6N$. This means that the body has less freedom to deform than interface coordinates. Hence, the interface coordinates are not all independent, but are somehow constrained by the limited number of deformation shapes. This means that the expression that relates the generalized coordinates to the interface coordinates (8.13) should be augmented with additional constraints that are posed on the interface coordinates. In this case, it

should be determined which subspace of the interface coordinates is not spanned by the chosen deformation shapes. Then, the local interface coordinates should be constrained such that this subspace is suppressed. In this way it would be possible to for instance suppress axial deformation of a beam and include only its bending and torsion.

From the above discussion it should be understood that the method of creating superelements as presented in this work cannot be applied only when static Craig-Bampton modes are used, but also for an arbitrary set of deformation shapes. This set of deformation shapes must be able to describe rigid body motion or augmented with rigid body modes. Depending on the interface space spanned by this (augmented) set, a different strategy is used to manipulate the deformation shapes such that the same superelement formulation can be applied.

8.3   Including local geometric nonlinearities

Consider problems in which large deformations occur within a body. For these cases a geometrical nonlinear formulation is also required locally. It is considered that in these cases a nonlinear finite element model of a body is available. Unfortunately, linear model order reduction techniques cannot be applied to these geometrical nonlinear problems. To account for geometric nonlinearities, the linear reduction basis can be augmented with modal derivatives [31], which can be interpreted as a second order enhancement. This method has been used for many problems before and the author has applied it in earlier work for the study of large stroke flexure mechanisms [28, 32].

In [33], Wu et al. have explained how modal derivatives can be applied to augment a linear reduction basis of Craig-Bampton modes by their modal derivatives. This method was applied successfully to reduce several structural dynamics problems. Since the new superelement formulation presented in this work uses Craig-Bampton modes to describe a body's local elastic behavior, it is suggested to apply the method in [33] to create a model order reduction method suitable for flexible multibody systems in which each body may be subjected to large deformations. In order to include these modal derivatives in the formulation, the strategy explained in Section 8.2 can be used.

Consider a flexible body of which its linear elastic behavior is described with sufficient accuracy by the Craig-Bampton modes. These may be both the static interface modes and the internal vibration modes, but without loss of generality only the static Craig-Bampton modes are considered here.

The modal derivative $\boldsymbol{\theta}_{ij}$ denotes the sensitivity of Craig-Bampton mode $\boldsymbol{\phi}_i$ with respect to an elastic deformation in Craig-Bampton degree of freedom q_j. The modal derivatives are computed as [32, 33]:

$$\boldsymbol{\theta}_{ij} = -\mathbf{K}^{-1}\frac{\partial \mathbf{K}}{\partial q_j}\boldsymbol{\phi}_i \qquad (8.21)$$

where $\mathbf{K} = \mathbf{K}(\mathbf{q})$ should be interpreted as the nonlinear finite element model's stiffness matrix of the body with all interface coordinates fixed, except for all coordinates of the interface point of which q_i is a generalized coordinate. As an example, consider a two-dimensional beam. Figure 8.1 shows the Craig-Bampton modes related to the bending deformation of the right interface point (ϕ_1, ϕ_2) and the three corresponding modal derivatives $(\theta_{11}, \theta_{12}, \theta_{22})$. Note that the Craig-Bampton modes describe a deformation in the transverse direction $v(x)$, whereas the modal derivatives describe a deformation in the axial direction $u(x)$. Hence, the modal derivatives describe the shortening of the beam that occurs when it is subjected to bending. From Figure 8.1, θ_{11} should be interpreted as the shortening of the beam, when the beam is subjected to a transverse displacement according to ϕ_1. Similarly, θ_{22} is the shortening of the beam when the beam is subjected to a transverse displacement according to ϕ_2.
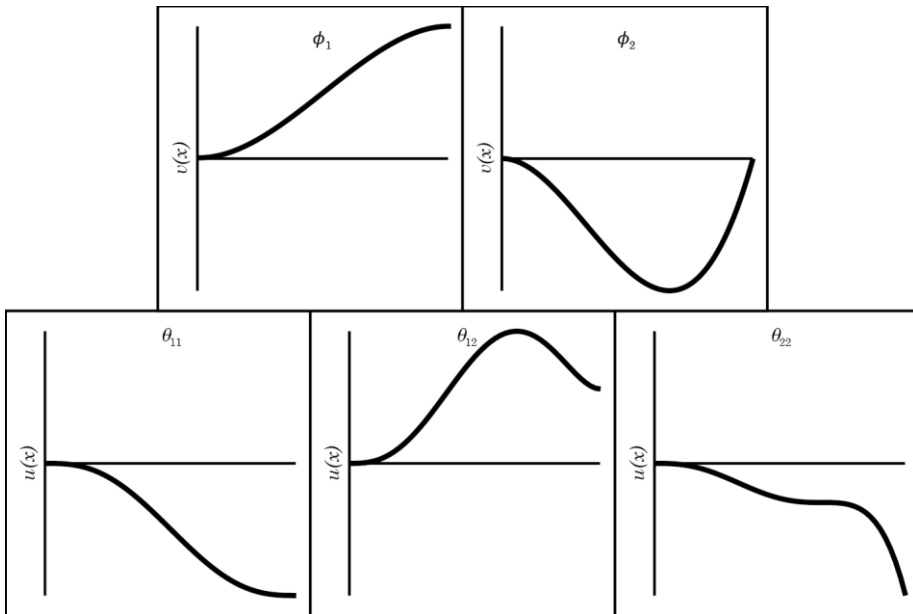

Fig. 8.1   Craig-Bampton modes and modal derivatives related to a 2D beam's right interface point.

It is important to mention that the modal derivatives have a nonzero deflection at the interface points. Consequently, motion of the interface points causes excitation of both the local interface coordinates corresponding to the Craig-Bampton modes and the generalized coordinates corresponding to the modal derivatives. However, it is possible to modify the basis of the modal derivatives by subtracting the component that is already present in the static Craig-Bampton modes. It is interesting to note that this is in fact the same procedure as discussed in Section 8.2 for the case that $M > 6N$. Because the modified reduction basis is obtained by elementary column operations, they span the same reduced space. This strategy was also proposed in [33].

Let $\mathbf{q}$ denote all generalized coordinates corresponding to the local finite element model of the body. It can be partitioned in the boundary nodes $\mathbf{q}^b$ at the body's interface points and internal nodes $\mathbf{q}^i$. The proposed local reduction is as follows:

$$\mathbf{q} = \begin{bmatrix} \mathbf{q}^b \\ \mathbf{q}^i \end{bmatrix} = \begin{bmatrix} \mathbf{1} & \mathbf{0} \\ \mathbf{\Phi} & \mathbf{\Theta} \end{bmatrix} \begin{bmatrix} \mathbf{q}^{j,j} \\ \mathbf{\zeta}^{j,j} \end{bmatrix} \tag{8.22}$$

where $\mathbf{\Phi}$ is the set of Craig-Bampton modes, $\mathbf{\Theta}$ is the set of all modified modal derivatives and here $\mathbf{\zeta}^{j,j}$ denote their generalized coordinates. If the internal Craig-Bampton modes are also taken into account, the local reduction basis can be written as:

$$\mathbf{q} = \begin{bmatrix} \mathbf{q}^b \\ \mathbf{q}^i \end{bmatrix} = \begin{bmatrix} \mathbf{1} & \mathbf{0} & \mathbf{0} \\ \mathbf{\Phi} & \mathbf{\Psi} & \mathbf{\Theta} \end{bmatrix} \begin{bmatrix} \mathbf{q}^{j,j} \\ \mathbf{\eta}^{j,j} \\ \mathbf{\zeta}^{j,j} \end{bmatrix} \tag{8.23}$$

In this way, an efficient description of a body's local deformation is obtained. The strategy for establishing the coordinate transformation from local interface coordinates to absolute interface coordinates is the same as before. However, it should be anticipated that as a consequence of the geometric nonlinearities, the calculation of the elastic forces may require additional Newton-Raphson iterations in the solution procedure.

As a first validation of this solution strategy, an equilibrium analysis is performed on several flexure mechanisms in [28], since flexure elements are typically subjected to deformations outside the linear range. Figure 8.2 shows the equilibrium configuration of a cross flexure mechanism that is subjected to a bending moment. Both flexures are modelled using 10 elements. It can be seen that when each flexure is reduced using 2 Craig-Bampton modes and 3 corresponding modal derivatives, the simulation results are still very close to the unreduced model and the results obtained by the nonlinear finite element analysis of Ansys. It can be seen that the proposed reduction basis produces slightly stiffer than exact results, as one should expect from model order reduction.
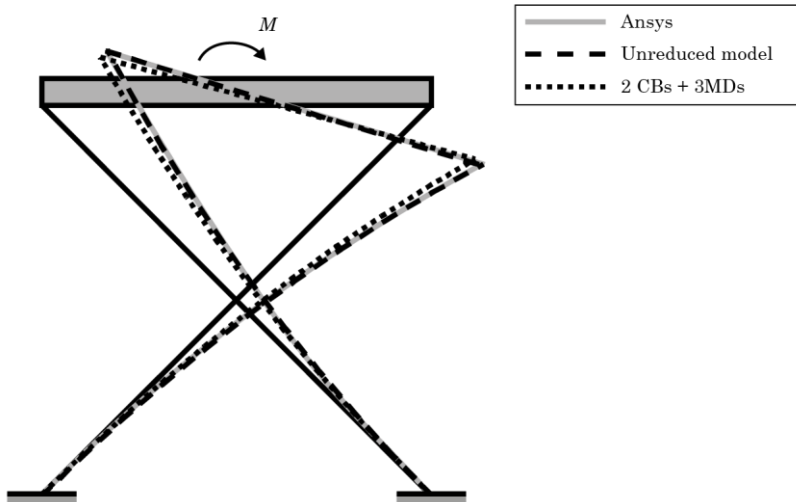

Fig. 8.2   Equilibrium analysis of a cross flexure mechanism subjected to a bending moment

8.4   Bodies with more than two interface points

The new superelement formulation can be applied to bodies that consist of an arbitrary number of interface points. However, in this work only validation problems have been presented that use beams. In [29], the author has contributed to the validation of the new method for plates. In this section, a preliminary static result is presented that is reused from [29]. This example merely serves to demonstrate that it is possible to implement bodies with more than two interface points in the method. However, in order to fully demonstrate the validity of the method for plates, additional benchmark problems should be studied. In particular, examples in which beam theory does not hold anymore would be of interest.

Consider a cantilever plate that is subjected to two equal forces on its two tip nodes that remain vertical at all times. The cantilever has length 10 m, width 1 m and thickness 0.1 m. The Young's modulus is 12 GPa and the Poisson ratio is 0.3. Figure 8.3 shows the deformed shape of the cantilever for several values of the applied load. In the new superelement formulation, 10 bodies are used for which each body includes all 24 Craig-Bampton modes. The results are compared with simulations obtained with the inertial frame formulation of Ansys where 10 standard 4 node shell181 elements are used, the corotational formulation in Spacar where 10 beam elements are used and the new superelement formulation where 10 beams are used to model the bodies. Figure 8.4 shows the normalized transverse (w/L) and axial ($-u/L$) displacements. It can be seen that there is a close resemblance in the simulation results obtained with the four different formulations.
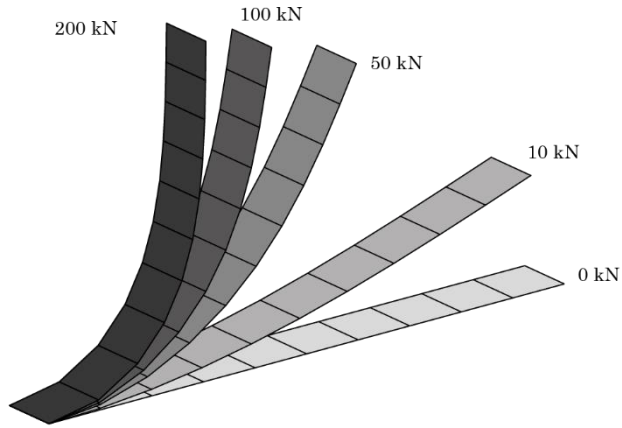
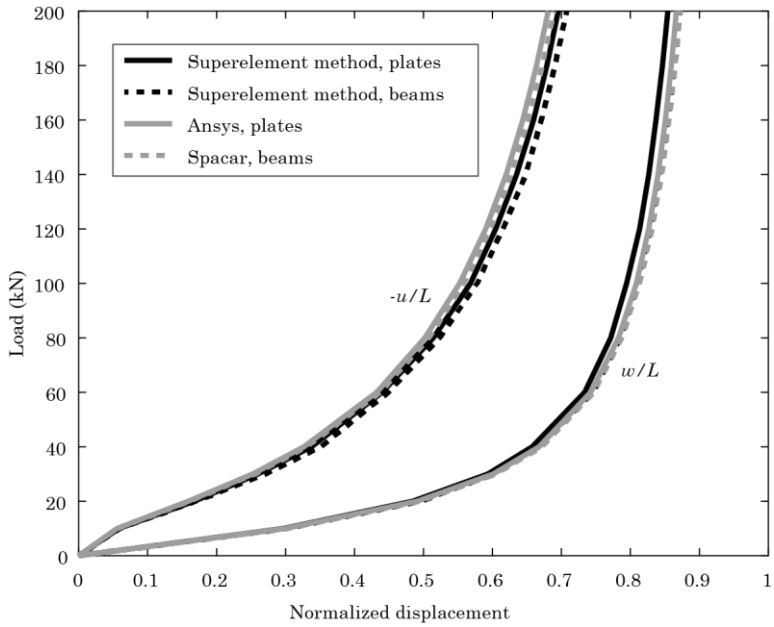**Fig. 8.3** Deflected shape of the cantilever plate for different loads.

Fig. 8.4 Displacement components of the cantilever plate.

8.5   Superelement formulation in terms of screw theory

The method presented in this work was developed entirely in terms of conventional engineering coordinates. However, in some areas of dynamics, it is common to formulate both the kinematics and kinetics using screw theory. In this notation, the location and orientation of a coordinate frame are conveniently combined in a homogenous transformation matrix and its time derivative is defined by the twist vector. Standard works about screw theory can be found for instance in [34, 35, 36]. For purposes in multibody dynamics, efforts have been made to formulate certain often-used elements, such as (geometrically exact) beams, in terms of screw theory [37]. Due to the compact notation of screw theory, it is also applied in fields closely related to multibody dynamics, for example robotics and mechanism design.

For this reason, the author has developed the new superelement formulation in terms of screw theory. A journal paper entitled "An absolute interface coordinates floating frame of reference formulation using screw theory" is being prepared [30]. A summary is presented here.

Consider a flexible body with floating frame $\{P_j, E_j\}$ and an arbitrary material point $\{P_i, E_i\}$. The position vector $\mathbf{r}_j^{0,O}$ and rotation matrix $\mathbf{R}_j^O$ can be conveniently combined to form the (4×4) matrix $\mathbf{H}_j^O$, which is defined as:

$$\mathbf{H}_j^O \equiv \begin{bmatrix} \mathbf{R}_j^O & \mathbf{r}_j^{0,O} \\ \mathbf{0} & 1 \end{bmatrix} \tag{8.24}$$

In screw theory, the matrix $\mathbf{H}_j^O$ is commonly known as the homogenous transformation matrix from P_j to P_O. It can be used to write the translation and rotation of a vector in a single operation. To show this, the absolute position of P_i as introduced in Eq. (2.18) can be written in the following form:

$$\begin{bmatrix} \mathbf{r}_i^{0,O} \\ 1 \end{bmatrix} = \begin{bmatrix} \mathbf{R}_j^O & \mathbf{r}_j^{0,O} \\ \mathbf{0} & 1 \end{bmatrix} \begin{bmatrix} \mathbf{r}_i^{j,j} \\ 1 \end{bmatrix} \tag{8.25}$$

In this way, the homogenous transformation matrix $\mathbf{H}_j^O$ can be recognized as the matrix that transforms the position of P_i relative to P_j to the position of P_i relative to P_O. Figure 8.5 shows a graphical representation of the global position of P_i using the floating frame P_j in terms of the coordinate transformations discussed above.
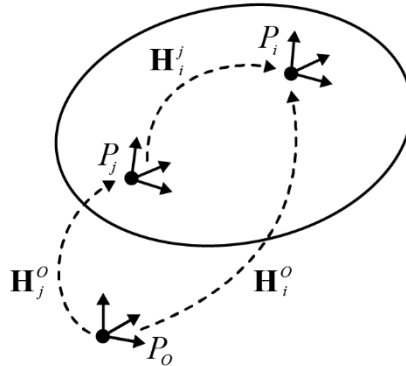

Fig. 8.5 Graphical representation of the absolute position of arbitrary point P_k on a flexible body expressed as the superposition of the absolute position of the floating frame P_j and the position of P_k relative to P_j. The figure shows the relevant position vectors **r** and homogenous transformation matrices **H**.

Equation (8.25) can be written in short as:

$$\mathbf{p}_i^{O,O} = \mathbf{H}_j^O \mathbf{p}_i^{j,j} \tag{8.26}$$

where $\mathbf{p}_i^{O,O}$ and $\mathbf{p}_i^{j,j}$ are now used to denote the (4×1) vectors that consist of the actual position vectors $\mathbf{r}_i^{O,O}$ and $\mathbf{r}_i^{j,j}$ augmented with a 1. An important advantage of using the homogenous transformation matrices is that they can be used to denote a transformation of position and orientation in a single convenient operation. By direct multiplication of the matrices, it can be checked that the following compact notation holds:

$$\mathbf{H}_i^O = \mathbf{H}_j^O \mathbf{H}_i^j \tag{8.27}$$

The time derivative of the homogenous transformation matrix $\mathbf{H}_j^O$ can be found by differentiating (8.24):

$$\dot{\mathbf{H}}_j^O = \begin{bmatrix} \widetilde{\boldsymbol{\omega}}_j^{O,O} \mathbf{R}_j^O & \dot{\mathbf{r}}_j^{O,O} \\ \mathbf{0} & 1 \end{bmatrix} \tag{8.28}$$

It can be shown that the time derivative of a homogenous transformation matrix can be written as a matrix times the homogenous transformation matrix itself:

$$\dot{\mathbf{H}}_j^O = \widetilde{\boldsymbol{\xi}}_j^{O,O} \mathbf{H}_j^O \tag{8.29}$$

Using the fact that $\mathbf{H}_j^O$ denotes the inverse transformation of $\mathbf{H}_O^j$, the expression for $\widetilde{\boldsymbol{\xi}}_j^{O,O}$ can be computed by post-multiplying (8.29) by $\mathbf{H}_O^j$. The result can be written as:

$$\widetilde{\boldsymbol{\xi}}_j^{O,O} = \dot{\mathbf{H}}_j^O \mathbf{H}_O^j = \begin{bmatrix} \widetilde{\boldsymbol{\omega}}_j^{O,O} & \dot{\mathbf{r}}_j^{O,O} + \widetilde{\mathbf{r}}_j^{O,O} \boldsymbol{\omega}_j^{O,O} \\ \mathbf{0} & 0 \end{bmatrix} \tag{8.30}$$

It can be seen that the elements of the (4×4) matrix $\widetilde{\boldsymbol{\xi}}_j^{O,O}$ can be constructed from the (6×1) vector $\boldsymbol{\xi}_j^{O,O}$ known as the twist, which is defined as:

$$\boldsymbol{\xi}_j^{O,O} \equiv \begin{bmatrix} \boldsymbol{\omega}_j^{O,O} \\ \dot{\mathbf{r}}_j^{O,O} + \widetilde{\mathbf{r}}_j^{O,O} \boldsymbol{\omega}_j^{O,O} \end{bmatrix} \tag{8.31}$$

The twist can be interpreted as a velocity vector in which the linear velocity of P_j is replaced by the linear velocity of the point that is instantaneously coinciding with P_O. This means that for a rigid body, the twist is independent of the location of the floating frame, which is convenient. However, for the flexible bodies under consideration in the present work, this is no longer the case.

The global twist of an arbitrary point on the flexible body P_k can be expressed in terms of the global twist of the floating frame P_j and the local twist of P_k relative to P_j.

This is done by differentiating (8.27) with respect to time. By rewriting the result, the relation is expressed in the following form:

$$\boldsymbol{\xi}_k^{O,O} = \boldsymbol{\xi}_j^{O,O} + \mathbf{A}_j^O \boldsymbol{\xi}_k^{j,j}, \qquad \mathbf{A}_j^O \equiv \begin{bmatrix} \mathbf{R}_j^O & \mathbf{0} \\ \tilde{\mathbf{r}}_j^{O,O}\mathbf{R}_j^O & \mathbf{R}_j^O \end{bmatrix} \qquad (8.32)$$

Here the (6×6) matrix $\mathbf{A}_j^O$ is introduced as the matrix that transforms the local twist $\boldsymbol{\xi}_k^{j,j}$ to the global frame. In this transformation, $\mathbf{A}_j^O$ is similar to the rotation matrix $\mathbf{R}_j^O$ transforming a position vector and to the homogenous transformation matrix $\mathbf{H}_j^O$ transforming an augmented position vector. Because $\mathbf{A}_j^O$ is constructed from elements already in $\mathbf{H}_j^O$, it is known as the adjoint transformation matrix of $\mathbf{H}_j^O$ or simply the adjoint of $\mathbf{H}_j^O$. In literature it is also commonly denoted as $\mathbf{Ad}_j^O$, $Ad_{\mathbf{H}_j^O}$ or $Ad(\mathbf{H}_j^O)$. The notation used here is chosen for its compactness. It is interesting to note the following relations between the velocity vector $\dot{\mathbf{q}}_j^{O,O}$ and the twist $\boldsymbol{\xi}_j^{O,O}$:

$$\dot{\mathbf{q}}_j^{O,O} = \left[-\tilde{\mathbf{r}}_j^{O,O}\right]\boldsymbol{\xi}_j^{O,O} \quad \leftrightarrow \quad \boldsymbol{\xi}_j^{O,O} = \left[\tilde{\mathbf{r}}_j^{O,O}\right]\dot{\mathbf{q}}_j^{O,O} \qquad (8.33)$$

Consider that the static Craig-Bampton modes are used to describe the body's deformation. Following a similar strategy as presented in Chapter 3, it is possible to express the local twist $\boldsymbol{\xi}_i^{j,j}$ of an arbitrary point on a flexible body in terms of the local twist of the interface points $\boldsymbol{\xi}^{j,j}$:

$$\boldsymbol{\xi}_i^{j,j} = \left[\tilde{\mathbf{r}}_i^{j,j}\right][\boldsymbol{\Phi}_i]\left[-\tilde{\mathbf{r}}^{j,j}\right]\boldsymbol{\xi}^{j,j}, \qquad \left[-\tilde{\mathbf{r}}^{j,j}\right] \equiv \begin{bmatrix} \left[-\tilde{\mathbf{r}}_1^{j,j}\right] & & \\ & \ddots & \\ & & \left[-\tilde{\mathbf{r}}_N^{j,j}\right] \end{bmatrix} \qquad (8.34)$$

By rewriting (8.32), the local twist of the interface points can be expressed in the difference between the global twist of the interface points and the twist of the floating frame. By demanding zero elastic deformation at the location of the floating frame, the floating frame's twist can be expressed in terms of the global interface twists:

$$\boldsymbol{\xi}_j^{0,0} = \mathbf{A}_j^O [\mathbf{Z}][-\tilde{\mathbf{r}}^{j,j}]\big[\mathbf{A}_O^j\big]\boldsymbol{\xi}^{0,0}, \qquad \big[\mathbf{A}_O^j\big] \equiv \begin{bmatrix} \mathbf{A}_O^j & & \\ & \ddots & \\ & & \mathbf{A}_O^j \end{bmatrix} \qquad (8.35)$$

With this relation, it also becomes possible to express the local interface velocities in terms of the global interface twists:

$$\dot{\mathbf{q}}^{j,j} = [\mathbf{T}][-\tilde{\mathbf{r}}^{j,j}]\big[\mathbf{A}_O^j\big]\boldsymbol{\xi}^{0,0} \qquad (8.36)$$

In (8.35) and (8.36), the transformation matrices $[\mathbf{Z}]$ and $[\mathbf{T}]$ are defined the same as in Eq. (3.17) and (3.18). At this point, it is possible to transform the equations of motion of a flexible body from the floating frame formulation to a superelement formulation in terms of the global twists of the interface points. Alternatively, the equations of motion can be derived directly from the principle of virtual work. In this way, the equation of motion in the floating frame formulation is not required first. A full derivation of this procedure is presented in [30] and is beyond the scope of this section. The resulting equations of motion take a similar form as derived in Chapter 4:

$$\bar{\mathbf{M}}\dot{\boldsymbol{\xi}}^{0,0} + \bar{\mathbf{C}}\boldsymbol{\xi}^{0,0} + \bar{\mathbf{K}}\mathbf{q}^{j,j} = \mathbf{w}^{0,0} \qquad (8.37)$$

in which $\bar{\mathbf{M}}$, $\bar{\mathbf{C}}$ and $\bar{\mathbf{K}}$ are the generalized mass matrix, fictitious force matrix and stiffness matrix, respectively. $\mathbf{w}^{0,0}$ is the absolute vector of externally applied wrenches on the interface points. Note that, in the same way as in Chapter 4, the elastic forces are still expressed in the local interface coordinates, as no closed form of the transformation exists on the position level.

References

[1] T.M. Wasfy, A.K. Noor. Computational strategies for flexible multibody systems. Applied Mechanics Reviews, 56 (6), 553-613 (2003)

[2] R. de Borst, M.A. Crisfield, J.J.C. Remmers, C.V. Verhoosel. Non-linear Finite Element Analysis of Solids and Structures, 2nd edition. John Wiley & Sons (2012)

[3] I.S. Sokolnikoff. Mathemathical Theory of Elasticity. McGraw-Hill (1956)

[4] S. Timoshenko, J.N. Goodier. Theory of Elasticity. McGraw-Hill (1934)

[5] E.J. Haug. Computer Aided Kinematics and Dynamics of Mechanical Systems: Basic Methods. Prentice Hall (1989)

[6] A.A. Shabana. Dynamics of Multibody Systems. Cambridge, Cambridge University Press (1998)

[7] A. Cardona, M. Géradin. Modeling of superelements in mechanism analysis. International Journal for Numerical Methods in Engineering, Vol 32, 1565-1593 (1991)

[8] A. Cardona, M. Géradin. A superelement formulation for mechanism analysis. Computer Methods in Applied Mechanics and Engineering, Vol 100, 1-29 (1992)

[9] A. Cardona. Superelements Modelling in Flexible Multibody Dynamics. Multibody System Dynamics, Vol 4, 245-266 (2000)

[10] M.H.M. Ellenbroek, J.P. Schilder. On the use of absolute interface coordinates in the floating frame of reference formulation for flexible multibody dynamics. Multibody System Dynamics, 43 (3), 193-208 (2018)

[11] J.P. Schilder, M.H.M. Ellenbroek, A. de Boer. Superelements in a minimal coordinates floating frame of reference formulation. IMSD, Lisbon, Portugal, 2018.

[12] J.P. Schilder, M.H.M. Ellenbroek. Superelements in a screw theory based floating frame of reference formulation. WCCM, New York, United States, 2018.

[13] R.R. Craig, M.C.C. Bampton. Coupling of substructures for dynamic analysis. AIAA Journal, 6 (7), 1313-1319 (1968)

[14] R.R. Craig: Coupling of substructures for dynamic analyses: an overview. Structures, Structural Dynamics and Material Conference, 41st AIAA/ASME/ASCE/AHS/ASC, Atlanta, AIAA-2000-1573 (2000)

[15] M. Géradin, D.J. Rixen. Mechanical Vibrations. Wiley (2015)

[16] M.A. Crisfield. A consistent co-rotational formulation for non-linear, three-dimensional, beam elements. Computer Methods in Applied Mechanics and Engineering, Vol 81, 131-150 (1990)

[17] G.F. Moita, M.A. Crisfield. A finite element formulation for 3-D continua using the co-rotational technique. Internal Journal for Numerical Methods in Engineering, Vol 39, 3775-3792 (1996)

[18] M.H.M. Ellenbroek. On the fast simulation of the multibody dynamics of flexible space structures. PhD thesis. University of Twente (1994)

[19] J.P. Schilder. Dynamics 3. Reader. University of Twente (2016)

[20] J.P. Schilder, K.S. Dwarshuis, M.H.M. Ellenbroek, A. de Boer. Geometric interpretation of a floating frame of reference based superelement formulation for flexible multibody systems. Submitted to Multibody System Dynamics on 31-07-2018.

[21] J.P. Schilder, K.S. Dwarshuis, M.H.M. Ellenbroek, A. de Boer. The tangent stiffness matrix for an absolute interface coordinates floating frame of reference formularion. Submitted to Multibody System Dynamics on 08-02-2018.

[22] J.B. Jonker, J.P. Meijaard. A geometrically non-linear formulation of a three-dimensional beam element for solving large deflection multibody system problems. International Journal of Non-Linear Mechanics, vol 53, 63-74 (2013)

[23] J.B. Jonker. Dynamics of Spatial Mechanisms with Flexible Links. PhD thesis. Technical University of Delft (1988)

[24] S.E. Boer, R.G.K.M. Aarts, J.P. Meijaard, D.M. Brouwer, J.B. Jonker. A nonlinear two-node superelement for use in flexible multibody systems. Multibody System Dynamics, 31 (4), 405-431, (2014)

[25] S.E. Boer, R.G.K.M. Aarts, J.P. Meijaard, D.M. Brouwer, J.B. Jonker. A nonlinear two-node superelement with deformable-interface surfaces for use in flexible multibody systems. Multibody System Dynamics, 34 (1), 53-79, (2015)

[26] J.B. Jonker, J.P. Meijaard. SPACAR – Computer program for dynamic analysis of flexible spatial mechanisms and manipulators. Multibody Systems Handbook, 123-143, (1990)

[27] IFToMM Technical Committee for Mutlibody Dynamics: Library of Computational Benchmark Problems. Consulted on 14-09-2017 www.iftomm-multibody.org/benchmark

[28] J.P. Schilder, F.M. Segeth, M.H.M. Ellenbroek, M. van den Belt, A. de Boer. Model order reduction of large stroke flexure hinges using modal derivatives. ISMA, Leuven, Belgium (2018)

[29] M. van den Belt, J.P. Schilder, D.M. Brouwer. An absolute interface coordinates floating frame of reference formulation for plates. ISMA, Leuven, Belgium, (2018)

[30] J.P. Schilder, M.H.M. Ellenbroek. A new superelement formulation for flexible multibody systems using screw theory. To be submitted.

[31] S. R. Idelsohn, A. Cardona. A reduction method for nonlinear structural dynamic analysis. Computer Methods in Applied Mechanics and Engineering, 49, 253-279 (1985)

[32] M. van den Belt, J.P. Schilder. The use of modal derivatives in determining stroke-dependent frequencies of large stroke flexure hinges. ECCOMAS thematic conference on multibody dynamics, Prague, Czech Republic, (2017)

[33] L. Wu, P. Tiso, F. van Keulen. A modal derivatives enhanced Craig-Bampton method for geometrically nonlinear structural dynamics. ISMA, Leuven, Belgium, (2016)

[34] R.S. Ball. A Treatise on the Theory of Screws, Cambridge, Cambridge University Press (1998)

[35] J. Phillips. Freedom in Machinery, Volume 1: Introducing Screw Theory. Cambridge, Cambridge University Press (1984)

[36] J. Phillips. Freedom in Machinery, Volume 2: Screw Theory Exemplified. Cambridge, Cambridge University Press (1990)

[37] V. Sonneville, A. Cardona, O. Brüls. Geometrically exact beam finite element formulated on the special Euclidean group $SE(3)$. Comput. Methods Appl. Mech. Engrg., 268, 451-474, (2014)

Publications

Journal papers

1. M.H.M. Ellenbroek and J.P. Schilder. On the use of absolute interface coordinates in the floating frame of reference formulation for flexible multibody dynamics. Multibody System Dynamics, 14-12-2017. https://doi.org/10.1007/s11044-017-9606-3

2. J.P. Schilder, K.S. Dwarshuis, M.H.M. Ellenbroek and A. de Boer. The tangent stiffness matrix for an absolute interface coordinates floating frame of reference formularion. Submitted to Multibody System Dynamics on 08-02-2018.

3. J.P. Schilder, K.S. Dwarshuis, M.H.M. Ellenbroek and A. de Boer. Geometric interpretation of a floating frame of reference based superelement formulation for flexible multibody systems. Submitted to Multibody System Dynamics on 31-07-2018.

4. J.P. Schilder and M.H.M. Ellenbroek. A new superelement formulation for flexible multibody systems using screw theory. To be submitted.

Conference papers

1. J.P. Schilder, M.H.M. Ellenbroek, R. Hagmeijer and A. de Boer. Hydro-elasticity in flexible multibody dynamics. ISMA, Leuven, Belgium, 2016.

2. J.P. Schilder, M.H.M. Ellenbroek and A. de Boer. Recursive solution procedures for flexible multibody systems: comparing condensation and transfer matrix methods. ECCOMAS thematic conference on multibody dynamics, Prague, Czech Republic, 2017.

3. M. van den Belt and J.P. Schilder. The use of modal derivatives in determining stroke-dependent frequencies of large stroke flexure hinges. ECCOMAS thematic conference on multibody dynamics, Prague, Czech Republic, 2017.

4. J.P. Schilder, M.H.M. Ellenbroek and A. de Boer. Recursive thoughts on the simulation of flexible multibody dynamics of slender offshore structures. COTech 2017, Stavanger, Norway, 2017.

5. J.P. Schilder, M.H.M. Ellenbroek and A. de Boer. Superelements in a minimal coordinates floating frame of reference formulation. IMSD, Lisbon, Portugal, 2018.

6. J.P. Schilder, R. Baptist and M.W.G. Maris. Roller coaster train dynamics: the effect of the zero-car location. IMSD, Lisbon, Portugal, 2018.

7. J.P. Schilder and M.H.M. Ellenbroek. Superelements in a screw theory based floating frame of reference formulation. WCCM, New York, United States, 2018.

8. J.P. Schilder, F.M. Segeth, M.H.M. Ellenbroek, M. van den Belt and A. de Boer. Model order reduction of large stroke flexure hinges using modal derivatives. ISMA, Leuven, Belgium 2018.

9. M. van den Belt, J.P. Schilder and D.M. Brouwer. An absolute interface coordinates floating frame of reference formulation for plates. ISMA, Leuven, Belgium, 2018.

10. J.P. Schilder, M.H.M. Ellenbroek, M. van den Belt and A. de Boer. On the efficient simulation of the flexible multibody dynamics of flexure based precision mechanisms using superelements. ASPE, Las Vegas, United States, 2018.

11. M. van den Belt, J.P. Schilder and D.M. Brouwer. Efficient modelling of short and wide leaf springs using a superelement formulation. ASPE, Las Vegas, United States, 2018.

Presentations

1. J.P. Schilder. Multiphysics and coupled problems. Engineering Mechanics Symposium, Papendal, The Netherlands, 2016.

2. J.P. Schilder. A new floating frame of reference formulation for flexible multibody dynamics. Engineering Mechanics Symposium, Papendal, The Netherlands, 2017.

Dissemination

1. Hogere cijfers door zijn formule.
   NOS op 3, 11-06-2016.
   https://www.youtube.com/watch?v=smU18yxzjMg

2. Wat is de beste plek in de achtbaan?
   Galileo, RTL5, 17-06-2016.
   https://www.youtube.com/watch?v=7Lb78ZUPpg4

3. Hoe maak je de allertofste achtbaan ter wereld?
   Universiteit van Nederland, 29-05-2017.
   https://www.youtube.com/watch?v=JTpeNjYuiWE

4. Hoe kan een kleine trilling een complete brug slopen?
   Universiteit van Nederland, 02-06-2017.
   https://www.youtube.com/watch?v=bd8Rtmy_E-w

5. Met je laptop in de collegezaal? Dan haal je lagere cijfers.
   Nieuwsuur, NPO2, 26-09-2017.
   https://nos.nl/nieuwsuur/artikel/2194882-met-je-laptop-
   in-de-collegezaal-dan-haal-je-lagere-cijfers.html

6. Hoe pak je je koffer perfect in?
   Het LAB, 10-11-2017.
   https://www.youtube.com/watch?v=o2im02x-fzE

7. Waarom overleef je een perfect ronde looping niet?
   Het LAB, 15-12-2017.
   https://www.youtube.com/watch?v=5VWOUwRtXI8

8. G-krachten temmen in de achtbaan.
   NEMO Kennislink, 18-04-2018.
   https://www.nemokennislink.nl/publicaties/
   g-krachten-temmen-in-de-achtbaan

Awards

1. Isaac Newton's Education Award: Best teacher in Mechanical Engineering, 2013.

2. University of Twente's Central Education Award: Teacher of the year, 2014.

3. Isaac Newton's Education Award: Best teacher in Mechanical Engineering, 2017.

Honorary positions

1. Member of the Young Academy at the University of Twente, 2014 – present.

Dankwoord

Dit dankwoord was werkelijk het laatste stukje tekst dat ik aan mijn thesis toevoegde. Ik vond het een moeilijke, maar ook mooie taak, die ik voor een groot deel midden in de nacht heb volbracht. Het gaf me de gelegenheid terug te blikken op de zes jaar van mijn promotieonderzoek, maar ook op alle tijd daarvoor. Hoewel misschien een beetje cliché, kwam ik tot de conclusie ik dit werk nooit had kunnen volbrengen zonder de steun van familie, vrienden, collega's en andere mensen die grote invloed hebben gehad op mijn leven. Ik ben jullie veel dank verschuldigd!

Allereerst wil ik mijn ouders bedanken voor jullie inspanningen mij op te voeden. Ik denk niet dat ik dat zelf beter had kunnen doen. Ik ben heel gelukkig dat ik door jullie grote steun en liefde onbezorgd heb kunnen studeren en heb kunnen werken aan mijn onderzoek. Het is fijn om te weten dat ik altijd op jullie kan rekenen. Ook wil ik mijn zusje Milou erg bedanken. Niet voor iets in het bijzonder, maar gewoon omdat je het leukste, liefste en grappigste zusje bent dat ik me kan voorstellen. Ik hou heel erg van jullie!

Natuurlijk verdienen álle collega's van Technische Mechanica mijn dank voor het zijn van hele fijne collega's. Jullie hebben ervoor gezorgd dat ik met plezier aan het werk ging. In het bijzonder wil ik mijn kantoorgenoten bedanken: Arjan, Pieter, Alexandre, Derek, Marieke, Erwin, het was me een groot genoegen om lange tijd met jullie een kantoor te delen. Anne en Erwin wil ik vooral bedanken voor jullie hulp in mijn eerste jaren van mijn PhD. Jullie waren een goed voorbeeld. Axel, ik wil jou erg bedanken voor al je hulp bij mijn demonstraties en bij metingen onder -voor jou- extreme omstandigheden. De geweldige ondersteuning van Debbie en Belinda kan ik ook niet onbenoemd laten. Ik kan me niet voorstellen hoe de Noordring zou functioneren zonder jullie.

Door zelf les te geven, ben ik er achter gekomen dat je als gemotiveerde docent echt het verschil kunt maken voor je studenten. In mijn tijd op het Zuyderzee College en aan de Universiteit Twente heb ik van veel goede docenten les gehad. Daarom lijkt het me gepast om de vijf docenten die mij blijvend wisten te inspireren hier te noemen. Ik wil mevrouw Brons, mevrouw Vermeulen en meneer Takens enorm bedanken voor jullie bevlogenheid voor en het plezier waarmee jullie me naar school lieten gaan. Ik wil Rob Hagmeijer bedanken voor zijn geweldige colleges. Ik weet nog dat ik na het eerste college stromingsleer dacht "Wow, zo moet dat dus." Je bent de docent die ik altijd wilde zijn. Tenslotte wil ik Peter van der Hoogt bedanken voor het enthousiasme voor Dynamica dat hij me heeft gegeven. Zeer droevig was zijn overlijden kort na mijn afstuderen. Elles, Maja, Bert, Rob, Peter, ik voel me een zeer bevoorrecht mens van jullie les te hebben gehad!

In de afgelopen zes jaar heb ik veel afstudeerders begeleid en van hen heb ik veel geleerd. Naast goede afstudeerders waren jullie vaak ook hele goede studentassistenten die me van veel werkdruk hebben verlicht. Koen en Mieke, jullie werk is enorm zinnig gebleken voor mijn onderzoek en ik ben heel blij dat we samen verschillende artikelen hebben kunnen schrijven. Mieke, ik kijk met veel plezier terug op je aanwezigheid in onze villa in Praag. Ik wil jou in het bijzonder bedanken voor de grote inspanning die je hebt verricht om alle figuren in dit boekje er een beetje fatsoenlijk uit te laten zien. Zonder jou was het lelijk geworden.

Ik prijs me gelukkig in alle fasen van mijn tijd als scholier, student en PhD-er goede vrienden nabij te hebben gehad:

Astrid en Mirjam, ik kijk met ontzettend veel plezier terug op onze gezamenlijke periode op het gymnasium. Hoewel de romereis van toen leuk was, vond ik onze eigen romereis, 10 jaar later, eigenlijk veel specialer. Ik zie uit naar alle food & drinks trips die nog gaan komen.

Klaas-Jan, ik wil jou enorm bedanken voor onze gedeelde studietijd, waarin we veel projecten en vakken samen hebben gedaan. In het bijzonder denk ik terug aan de sommensets van Fluid Mechanics 2, die eindeloos leken. Ik vond het fijn dat met jou te kunnen doen. Meer nog wil

ik je bedanken voor het zijn van een goede vriend toen we allebei klaar waren met onze studie. Alle avonden die we vulden met uiteenlopende bordspellen en goede lange gesprekken over de zin van het leven zijn me zeer dierbaar. Hoewel dat er de komende twee jaar iets minder zullen zijn, reken ik erop dat we dat daarna kunnen inhalen.

Chris, in welk pretpark we elkaar voor het eerst hebben ontmoet, kan ik me niet meer herinneren. Maar ik ben heel gelukkig dat we na zo veel jaar, en zo veel afgelegde kilometers achtbaantrack nog steeds niet zijn uitgekeken op onze gezamenlijke hobby. De tijd waarin we de internetfora domineerden is dan misschien geweest, maar ik ben nog altijd erg blij met jou als reisgenoot en als goede vriend.

Voor het delen van mysterieuze weekenddagen wil ik alle bewoners van het Spookhuis; Boukje, Femke, Laura, Erik, Friso, zeer bedanken. Jullie zijn allemaal schitterende mensen, maar toch het allerbest als volledig gezelschap. Ik ga er van uit dat ook wanneer de laatste negen cases ooit zijn opgelost, we genoeg andere redenen kunnen verzinnen om nog meer weekenden samen door te brengen.

Een aantal mensen verdient mijn grote dank, omdat zij mijn leven op een unieke manier hebben veranderd. Ik denk dat ik dankzij de volgende mensen een veel rijker mens ben geworden:

Chao, I would like to thank you very much for that one day you invited me to a game of badminton. It must have been more than 8 years ago since I did some serious sports and that is something you really changed. For that I am very grateful. Our endless series of tiresome singles on this particular Saturday I will never forget.

Het team van Studium Generale, maar in het bijzonder Peter en Hiska, ik ben jullie enorm dankbaar voor het moment dat ik in een praktisch lege theaterzaal naar opera heb kunnen kijken. Het was een overweldigende ervaring van hele grote schoonheid. De vele avonden dat ik hierna heb kunnen genieten van met name dans en ballet zijn erg waardevol voor me geweest. Voor mijn kennismaking met de kunsten verdienen jullie veel lof.

Het is enorm bijzonder hoe één iemand op zo veel verschillende gebieden precies het juiste voorbeeld kan zijn. Boukje, ik ben heel gelukkig dat ik je heb leren kennen. Veel uitgebreider dan dat ik hier kan doen, schreef ik je al eens hoe blij ik ben met jouw inspiratie op het sportveld, in de keuken, in het theater en in de collegezaal. Eerder dacht ik dat er wel aspecten zouden zijn waarop je misschien een minder goed voorbeeld bent, maar inmiddels sluit ik niet uit dat paaldansen enorm verlichtend zou kunnen zijn. Ik overweeg het. Je bent een goede muze en een nog veel betere vriendin.

Tenslotte schieten woorden te kort om te beschrijven hoe groot mijn grensoverschrijdende dank is voor de twee geweldige personen zonder wie mijn promotie absoluut niet mogelijk was geweest.

Marcel, je bent een fantastische begeleider! Ik kijk echt met heel veel plezier terug onze tijd samen. Je had altijd leuke ideeën, goede vragen en interessante theorieën die ik niet altijd direct begreep. Zo herinner ik me een ochtend waarop ik je vertelde dat ik eindelijk begreep wat je me een jaar eerder had gevraagd. Die vraag had ik toen wel diezelfde ochtend nog beantwoord. Inmiddels denk ik dat ik je bijna altijd snap. Ik denk dat je zo'n goede begeleider was, omdat het je is gelukt om jouw enthousiasme op mij over te brengen. Dat werkt zeer aanstekelijk.

André, je bent een fantastische promotor! Ik wil je ontzettend bedanken voor je grote vertrouwen in mij. Vanaf het moment dat ik studentassistent was bij stijfheid en sterkte ben je een hele goede leermeester geweest. Je hebt me veel vrijheid gegeven in mijn onderzoek en je had altijd goed advies. In de meeste gevallen had je gelijk. De bovenmenselijke inspanningen die je hebt geleverd om mijn docentschap mogelijk te maken en om me op de UT te kunnen laten blijven, ontroeren me zeer. Ik hoop dat ik ook tijdens je welverdiende pensioen af en toe een beroep kan doen op je wijze raad.

Ten diepste zijn jullie allemaal hele lieve schatjes, dank jullie wel!